

CENTRE OF TOXICOLOGY

THE SCHOOL OF PHARMACY

UNIVERSITY OF LONDON



**The Mechanism of 2,3,5,6-tetramethyl-*p*-
phenylenediamine Myotoxicity in the Rat:**

An In Vivo and In Vitro Study

A Thesis submitted by

Jeannette Ann Blair

to the University of London

for examination for the degree of

Doctor of Philosophy

2001



ProQuest Number: 10104792

All rights reserved

INFORMATION TO ALL USERS

The quality of this reproduction is dependent upon the quality of the copy submitted.

In the unlikely event that the author did not send a complete manuscript and there are missing pages, these will be noted. Also, if material had to be removed, a note will indicate the deletion.



ProQuest 10104792

Published by ProQuest LLC(2016). Copyright of the Dissertation is held by the Author.

All rights reserved.

This work is protected against unauthorized copying under Title 17, United States Code.
Microform Edition © ProQuest LLC.

ProQuest LLC
789 East Eisenhower Parkway
P.O. Box 1346
Ann Arbor, MI 48106-1346

ABSTRACT

2,3,5,6-TMPD, a derivative of *p*-phenylene diamine causes necrosis of skeletal muscle in a highly specific manner when administered to rats. The mechanism of TMPD toxicity *in vivo* is not fully understood.

Previous research has revealed that the initiation site of TMPD toxicity is the mitochondrial respiratory chain protein, cytochrome *c* oxidase (complex IV), which catalyses the oxidation of the amine. Re-reduction of the di-imine metabolite by DT-diaphorase (NAD(P)H:quinone oxidoreductase) may facilitate a futile redox cycling reaction with concomitant depletion of reduced glutathione (GSH) and pyridine nucleotides.

A single dose of TMPD ($60 \mu\text{mol kg}^{-1}$) caused a reduction in glutathione (GSH) and ATP levels in the diaphragm. The effect was less pronounced in quadriceps muscle. These biochemical changes were accompanied by increases in serum transaminases and the skeletal muscle isoform of creatine kinase (CK-MM). Electron microscopy revealed gross damage to the mitochondria and sarcotubular elements of both diaphragm and quadriceps muscle. Oxidative fibres appeared to be more vulnerable to the toxic effects of TMPD than glycolytic fibres. This may reflect the metabolic differences and/or numbers of mitochondria that these muscles possess.

Glutathione-*S*-transferase (GST) activity was increased in a dose-dependant manner, although glutathione reductase activity was inhibited by TMPD treatment. Superoxide dismutase (SOD) activity showed little change following exposure to the amine and correlated with evidence to suggest that oxidation of TMPD is not accompanied by significant oxygen activation.

Cytotoxicity is believed to occur as a result of GSH depletion and the formation of mixed disulphides. Redox cycling of TMPD within the mitochondrion almost certainly contributes to the decrease in respiratory control and ADP:O ratios. This loss of function strongly correlates with the depletion of the mitochondrial GSH pool. Loss of the tripeptide would leave the thiol groups of the cell vulnerable to oxidative modification, which may explain the decrease in activity of the respiratory chain proteins, complex I, and complex II-III.

ACNOWLEDGEMENTS

I would like to thank my 3 supervisors, Dr. John Turton, Dr. Cathy Waterfield and Ann Rowlands for all their sound advice, support and encouragement over the course of the project. Fond thanks to Dr. Tim Bates, not only for his excellent teachings in all things mitochondrial, but also for his kindness and friendship over the last 4 years (not to mention a few great ‘working’ lunches – Italian-style!).

To all those staff (past and present) at SoP without whom day-to-day PhD life would have been much more difficult, Adrian, Dan, Dave McCarthy, Steve, Donna and Dave, thank you!

I would also like to mention all those at GlaxoSmithKline who have been extremely helpful over the past few years, be it in the preparation of histological slides (Jenny), teaching me the art of immunostaining (Helen), processing numerous batches of serum samples (Malcolm York’s group), or in helping me to produce some stunning EM work (thank you, Paul!).

I am indebted to GlaxoSmithKline and BBSRC for financial support.

Special thanks must be given to my friends, Tanya, Jane, Mita, Matthew and Laura for their friendship (tea and sympathy etc), particularly during my last year of study, which was somewhat of a challenge! Also to my wonderful family, Mum, Dad, Anita, Pat, Janine and Rebecca, who always loved me even when I seemed very hard to live with! To my best friend Sam, for all the fun in the early days (remember that red dress) and for providing a willing ear to bash towards the end!

Finally, a very special mention for my two lovely little girls, Alexandra and Georgiana. This thesis is for both of you.

CONTENTS

	Page
ABSTRACT	ii
ACKNOWLEDGEMENTS	iii
CONTENTS	iv
TABLES	ix
FIGURES	x
ABBREVIATIONS	xiii
CHAPTER 1	1
INTRODUCTION	1
1.1 SKELETAL MUSCLE PATHOLOGY	1
1.1.1 Muscle fibre histology	1
1.1.2 Myofibril and myofilament histology	2
1.1.3 Myofibre contraction	3
1.1.4 Skeletal muscle fibre typing	4
1.2 SKELETAL MUSCLE TOXICITY	7
1.2.1 Biochemical and cellular mechanisms of toxicity	7
1.2.1.1 Neurogenic toxicity	7
1.2.1.2 Localised toxicity	7
1.2.1.3 Impaired cell membrane function	8
1.2.1.4 Mitochondrial myopathies	8
1.2.1.5 Microtubule disruption	9
1.2.1.6 Lysosomal myopathies	9
1.2.1.7 Altered protein turnover	9
1.2.2 Assessment of skeletal muscle damage	11
1.2.2.1 Microscopy	11
1.2.2.2 Biochemical evaluation	11
1.2.2.3 Electrophysiological evaluation	12
1.2.2.4 Skeletal muscle cell culture	12
1.3 TETRAMETHYL-<i>p</i>-PHENYLENEDIAMINE (TMPD) AND THE PHENYLENEDIAMINES	14
1.3.1 Physical and chemical properties	14
1.3.2 Applications	15
1.3.3 Metabolism of <i>p</i> -PD and its derivatives	15
1.3.3.1 Absorption, distribution, metabolism and excretion (ADME) studies of <i>p</i> -phenylenediamine	16
1.3.3.2 Metabolism of TMPD	16
a) <i>N,N,N',N'</i> -tetramethyl- <i>p</i> -phenylenediamine	17
b) 2,3,5,6-tetramethyl- <i>p</i> -phenylene diamine	19
1.3.4 Toxicity of TMPD and <i>p</i> -phenylenediamine derivatives	20

1.3.4.1 Acute and chronic toxicity	20
1.3.4.2 Mutagenicity and carcinogenicity of <i>p</i> -phenylene diamine and its derivatives	22
1.3.4.3 Teratogenicity	23
1.3.4.4 <i>In vitro</i> studies	24
1.4 FREE RADICAL DAMAGE AND CELL DEATH	27
1.4.1 Necrosis	28
1.4.1.1 Morphological changes evident in necrosis	28
1.4.1.2 Mechanisms involved in necrotic cell death	29
1.5 PROTECTIVE PATHWAYS OF MAMMALIAN CELLS	31
1.5.1 Glutathione	31
1.5.2 Superoxide dismutase and catalase	33
1.6 MITOCHONDRIA	35
1.6.1 Structure	35
1.6.2 Oxidative phosphorylation	35
1.6.3 Characterisation of mitochondrial function	36
1.6.4 The oxygen electrode	36
1.7 AIMS OF THE RESEARCH PROJECT	38
CHAPTER 2	
MATERIALS AND METHODS	47
2.1 CHEMICALS	47
2.2 <i>IN VIVO</i> STUDIES	48
2.2.1 Animal husbandry	48
2.2.2 Post mortem procedure	48
2.2.3 Serum biochemistry	49
2.2.4 Reduced glutathione determination	50
a) Spectrophotometric method	50
b) Fluorometric method	50
2.2.5 ATP determination	51
2.2.6 Immunohistochemical staining for fast myosin	51
2.2.7 Electron microscopy	52
2.3 <i>IN VITRO</i> STUDIES	53
2.3.1 Isolation of hepatocytes	53
2.3.2 Preparation of newborn rat skeletal muscle cells	55
2.3.3 Glutathione reductase	57
2.3.4 Glutathione peroxidase	57
2.3.5 Glutathione- <i>S</i> -transferase	58
2.3.6 Superoxide dismutase	58
2.3.7 Lactate dehydrogenase	59
2.3.8 Creatine kinase	60
2.3.9 Preparation of rat muscle mitochondria	61
2.3.10 Preparation of rat heart mitochondria	62
2.3.11 Preparation of rat liver mitochondria	62
2.3.12 Bio-Rad DC protein assay	62
2.3.13 Measuring respiratory control	63
2.3.14 Measuring ATP synthesis	63
2.3.15 Mitochondrial Complex I assay	64

2.3.16 Mitochondrial Complex II-III assay	64
2.3.17 Statistical analysis	65

CHAPTER 3

THE MORPHOLOGICAL AND BIOCHEMICAL EFFECTS OF A SINGLE DOSE OF TMPD *IN VIVO* 66

3.1 INTRODUCTION	66
3.2 MATERIALS AND METHODS	69
3.2.1 Animals and compound administration	69
3.2.2 Fast myosin histochemistry	69
3.2.3 Electron microscopy	69
3.2.4 Experimental design	70
Study 1: Investigation of skeletal muscle lesion development following a single dose of TMPD at 20 – 60 $\mu\text{mol kg}^{-1}$	70
Study 2: Investigation in rats treated with TMPD to assess biochemical changes occurring prior to lesion development at 24 hours	71
3.2.5 Statistical analysis	72
3.3 RESULTS	73
3.3.1 Study 1: Investigation of skeletal muscle lesion development following a single dose of TMPD at 20 – 60 $\mu\text{mol kg}^{-1}$	73
i) Clinical effects following TMPD treatment	73
ii) Serum biochemistry	73
iii) Light microscopy	73
iv) Fast myosin histochemistry	74
3.3.2 Study 2: Investigation in rats treated with TMPD to assess biochemical changes occurring prior to lesion development at 24 hours	75
i) Serum biochemistry	75
ii) Light microscopy	76
iii) Electron microscopy	76
iv) Tissue glutathione	77
v) Tissue ATP	77
3.4 DISCUSSION	78

CHAPTER 4

THE EFFECT OF TMPD ON LIVER AND SKELETAL MUSCLE ANTIOXIDANT ENZYME ACTIVITIES *IN VITRO* AND *IN VIVO* 98

4.1 INTRODUCTION	98
4.2 MATERIALS AND METHODS	100
4.2.1 Study 1: The effect of TMPD on antioxidant enzyme levels in isolated rat hepatocytes and cultured myocytes <i>in vitro</i>	100
4.2.1.1 Measurement of TMPD toxicity	100
4.2.1.2 Measurement of cell antioxidant enzyme activities	100

4.2.2	Study 2: TMPD toxicity and antioxidant enzyme activities of liver and skeletal muscle <i>in vivo</i> : effect of the NAC	101
4.2.2.1	Animal husbandry	101
4.2.2.2	Experimental design	101
4.3	RESULTS	102
4.3.1	Study 1: The effect of TMPD on antioxidant enzyme levels in isolated rat hepatocytes and cultured myocytes <i>in vitro</i>	102
4.3.1.1	Assessment of TMPD toxicity	102
4.3.1.2	Measurement of cell antioxidant enzyme activities	102
4.3.2	Study 2: TMPD toxicity and antioxidant enzyme activities of liver and skeletal muscle <i>in vivo</i> : effect of NAC	103
4.3.2.1	Skeletal muscle and liver antioxidant enzyme Activities	103
4.4	DISCUSSION	105

CHAPTER 5

AN INVESTIGATION OF THE *IN VITRO* TOXICITY OF TMPD USING ISOLATED MITOCHONDRIA 116

5.1	INTRODUCTION	116
5.2	MATERIALS AND METHODS	117
5.2.1	Animal husbandry	117
5.2.2	Isolation of mitochondria	117
5.2.3	The effect of TMPD on <i>in vitro</i> mitochondrial respiration	117
5.2.4	The effect of TMPD on <i>in vitro</i> mitochondrial ATP synthesis	118
5.2.5	The effect of TMPD on <i>in vitro</i> mitochondrial GSH concentration	118
5.2.6	The effect of TMPD on <i>in vitro</i> mitochondrial complex activities	118
5.3	RESULTS	119
5.3.1	The effect of TMPD on <i>in vitro</i> mitochondrial respiration	119
5.3.2	The effect of TMPD on <i>in vitro</i> mitochondrial ATP synthesis	119
5.3.3	The effect of TMPD on <i>in vitro</i> mitochondrial GSH concentration	119
5.3.4	The effect of TMPD on <i>in vitro</i> mitochondrial complex activities	120
5.4	DISCUSSION	121

CHAPTER 6

	FINAL DISCUSSION	130
6.1	THE ROLE OF THE MITOCHONDRION IN TMPD TOXICITY	130
6.2	THE ROLE OF THE GLUTATHIONE SYSTEM IN TMPD TOXICITY	132
6.3	GENERAL CONCLUSIONS	136

REFERENCES	138
APPENDICES	152
PUBLICATIONS	165

LIST OF TABLES

Table 1.1	Properties of mammalian skeletal muscle fibre types based on the classification system of Landon (1992)
Table 1.2	Drugs and toxins known to induce skeletal muscle injury
Table 1.3	A biochemical profile of serum enzymes/parameters used to assess organ injury
Table 1.4	GSH and GSSG contents in different organs of 60-day male Wistar rats
Table 3.1	Muscle lesion scoring system
Table 3.2	Study 1; Serum biochemistry parameters in rats given a single dose of TMPD and sampled at 24 hours
Table 3.3	Study 1; Muscle lesion scores of rats given a single dose of TMPD and sampled at 24 hours
Table 3.4	Study 2; Lesion type versus fibre type at the ultrastructural level
Table 3.5	Study 2; Serum biochemistry parameters in rats given a single dose of TMPD ($60 \mu\text{mol kg}^{-1}$) and sampled at 0-24 hours
Table 4.1	The effect of TMPD on the antioxidant enzyme activities of cultured myocytes and isolated hepatocytes
Table 4.2	The effect of co-administration of NAC on the antioxidant enzyme activities of skeletal muscle and liver in TMPD-treated animals
Table 4.3	Effect of the administration of NAC (4 mmol kg^{-1}), TMPD ($60 \mu\text{mol kg}^{-1}$), and NAC + TMPD on serum enzyme levels in rats, with sampling at 24 hours post dosing
Table 5.1	The effect of TMPD ($0.1\text{-}0.5 \text{ mM}$) on <i>in vitro</i> mitochondrial respiration of skeletal muscle, heart, and liver

LIST OF FIGURES

- Figure 1.1 Structure of skeletal muscle.
- Figure 1.2 Normal muscle. Transverse section of normal skeletal muscle.
- Figure 1.3 Photomicrograph of rat skeletal muscle showing the transverse (cross) striations of the muscle fibres cut longitudinally.
- Figure 1.4 Myofibril structure.
- Figure 1.5 Electron micrograph of a longitudinal section of a rat myofibre.
- Figure 1.6 Diagrammatic representation of the sarcotubular system, showing the close association between the T tubules and the sarcoplasmic reticulum.
- Figure 1.7 Electron micrograph of a longitudinal section of rat skeletal muscle showing the triads of the conducting system.
- Figure 1.8 Transverse section of rat skeletal muscle (gastrocnemius), stained by the immunohistochemical technique for demonstrating fast myosin.
- Figure 1.9 The structural isomers of tetramethyl-*p*-phenylenediamine.
- Figure 1.10 The redox cycle of glutathione.
- Figure 1.11 The mitochondrion.
- Figure 1.12 The electron transport chain.
- Figure 1.13 The oxygen electrode.
- Figure 1.14 Measuring respiratory control in isolated mitochondria.
- Figure 3.1 Electron micrograph of soleus (type I) muscle from a control rat.
- Figure 3.2 Electron micrograph of quadriceps (type II) muscle from a control rat.
- Figure 3.3 Effect of TMPD on body weight.
- Figure 3.4 Effect of TMPD on diet consumption.
- Figure 3.5 Effect of TMPD on water consumption.
- Figure 3.6. (a) Transverse section of normal gastrocnemius muscle.

- Figure 3.6. (b) Transverse section of gastrocnemius muscle taken 24 hours after dosing with TMPD ($60 \mu\text{mol kg}^{-1}$).
- Figure 3.7. (a) Electron micrograph of soleus muscle taken 8 hours after dosing with TMPD ($60 \mu\text{mol kg}^{-1}$) showing slightly swollen mitochondria.
- Figure 3.7. (b) Electron micrograph of soleus muscle taken 8 hours after dosing with TMPD ($60 \mu\text{mol kg}^{-1}$) showing markedly swollen mitochondria.
- Figure 3.8. (a) Electron micrograph of diaphragm muscle taken 8 hours after dosing with TMPD ($60 \mu\text{mol kg}^{-1}$). Marked dilatation of the sarcotubular system is evident.
- Figure 3.8. (b) Electron micrograph of soleus muscle taken 8 hours after dosing with TMPD ($60 \mu\text{mol kg}^{-1}$). Adjacent membranes of the sarcotubular system appear to have fused to yield larger vacuoles.
- Figure 3.9. (a) Transverse section of quadriceps muscle taken from a rat 24 hours after dosing with TMPD ($60 \mu\text{mol kg}^{-1}$). Early signs of degeneration are evident with characteristic rounded, hyaline fibres.
- Figure 3.9. (b) Serial section of quadriceps muscle stained with fast myosin antibody. Early degeneration of some type IIA fibres can be seen.
- Figure 3.10 The time-dependent effect of TMPD on (a) liver, (b) diaphragm, and (c) quadriceps glutathione levels.
- Figure 3.11 The time dependent effect of TMPD on (a) liver, (b) diaphragm, and (c) quadriceps ATP levels.
- Figure 4.1 Intracellular rat myocyte (10 DIV) and hepatocyte (1×10^5 cells) GSH content following 24 hours exposure to TMPD (0-1 mM).
- Figure 4.2 Intracellular rat myocyte (10 DIV) and hepatocyte (1×10^5 cells) ATP content following 24 hours exposure to TMPD (0-1 mM).
- Figure 4.3 Intracellular rat myocyte (10 DIV) CK content following 24 hours exposure to TMPD (0-1 mM).
- Figure 4.4 Extracellular rat myocyte (10 DIV) and hepatocyte (1×10^5 cells) LDH leakage following 24 hours exposure to TMPD (0-1 mM).
- Figure 5.1 The effect of TMPD (0.1-0.5 mM) on ATP synthesis of freshly isolated rat liver, heart and skeletal muscle mitochondria.
- Figure 5.2 The effect of TMPD (0.1-0.5mM) on GSH content of freshly isolated rat liver, heart and skeletal muscle mitochondria.
- Figure 5.3 The effect of TMPD (0.1-0.5 mM) on complex I activity of freshly isolated rat liver, heart and skeletal muscle mitochondria.

Figure 5.4 The effect of TMPD (0.1-0.5 mM) on complex II-III activity of freshly isolated rat liver, heart and skeletal muscle mitochondria.

LIST OF ABBREVIATIONS USED IN TEXT

ADP	Adenosine diphosphate
ALP	Alkaline phosphatase
ALT	Alanine aminotransferase
ANSA	8-anilino-1-naphthalene sulfonic acid
AST	Aspartate aminotransferase
ATP	Adenosine triphosphate
BSA	Bovine serum albumin
BSO	Buthione sulfoximine
CCCP	Carbonyl cyanide m-chlorophenylhydrazone
CDNB	1-chloro-2,4-dinitrobenzene
CK	Creatine kinase
DIV	Days in vitro
DMEM	Dulbecco's modified Eagle's medium
DTNB	Dithionitrobenzene
ETC	Electron transport chain
FCS	Foetal calf serum
γ -GCS	γ -glutamyl cysteine synthetase
GPx	Glutathione peroxidase
GRed	Glutathione reductase
GSH	Glutathione (reduced form)
GSSG	Glutathione (oxidised form)
GST	Glutathione-S-transferase
H&E	Haematoxylin and eosin
ip	intraperitoneal
LDH	Lactate dehydrogenase
NAC	N-acetyl cysteine
NADH	Nicotinamide adenine dinucleotide (reduced form)
NADH-TR	NADH-tetrazolium reductase
NADPH	Nicotinamide adenine dinucleotide phosphate (reduced form)
PBS	Phosphate buffered saline
PTAH	Phosphotungstic acid haematoxylin

RCR	Respiratory control ratio
ROS	Reactive oxygen species
sc	subcutaneous
SOD	Superoxide dismutase
SSA	Sulphosalicylic acid
TCA	Trichloroacetic acid
TEM	Transmission electron microscopy
TNPSH	Total non-protein sulphhydryls
UHQ	Ultra high quality

CHAPTER 1

INTRODUCTION

1.1 SKELETAL MUSCLE PATHOLOGY

1.1.1 Muscle fibre histology

Most skeletal muscle, as the name implies, is attached to bone, and its contraction is responsible for supporting and moving the skeleton. The contraction of skeletal muscle is initiated by impulses in the motor neurons to the muscle, and is under voluntary control.

Skeletal muscle consists of bundles of muscle 'fibres' which are grouped into regular arrangements, bound together by collagenous connective tissue (Landon, 1992). For descriptive purposes, this tissue is usually divided into 3 components (Fig. 1.1): the epimysium; a tough elastic envelope of collagen that separates the muscle from adjacent structures; the perimysium, an invagination of the outermost sheath of collagen which subdivides the enclosed muscle fibres into smaller fascicles; and the endomysium, a fine interlacing network of collagen fibrils that separates the individual muscle fibres from one another (Landon, 1992). Muscle fibres (also known as myofibres) actually consist of multinucleated syncytia, which can measure up to 10cm or more in length, with diameters of 10-100 μ m (Ross et al., 1995). Multinucleation occurs following fusion of embryonic mononucleated myoblasts (muscle stem cells). The myofibre nuclei are generally found around the periphery of the cell (Fig. 1.2), under the cell membrane, also traditionally known as the sarcolemma (Junquiera et al., 1986).

Contrary to belief, skeletal muscle is not a strictly permanent tissue type, as the cells from which it is composed retain some capacity for regeneration. Myoblasts (embryonic muscle cells) arise from satellite cells, a population of resting undifferentiated myogenic cells that reside (and are resistant to many agents that are known to injure mature fibres) between the sarcolemma and the external lamina. Although much less abundant (only 3-5%) in muscles of mature animals than in newborn animals, they serve as stem cells that can be activated in adult life and eventually form mature myofibres (Van Vleet et al., 1991).

1.1.2 Myofibril and myofilament histology

The structural and functional subunit of the muscle fibre is the myofibril (Fig. 1.1). This subcellular component occupies 85-90% of the total volume of the fibre (Landon, 1992). The complete structure of the contractile apparatus of the skeletal myofibre can only be fully visualised under the electron microscope. Each myofibril is composed of serially repeating segments of identical structure. These segments are called sarcomeres and their precise lateral alignment, from one myofibril to the next, gives the fibre its characteristic cross-striations (Fig. 1.3), from which the alternate name, 'striated muscle' is derived (Landon, 1992). An individual sarcomere is composed of a dark central band, of fixed length, (typically 1.5 μm) flanked by two paler bands (Fig. 1.4), the lengths of which will vary according to the contractile state of the myofibre.

The sarcomere pattern described above is mainly due to the presence of 2 types of filaments, thick and thin filaments, arranged in parallel to the long axis of the myofibrils (Fig. 1.4) in a symmetrical pattern (Junquiera et al., 1986). The dense central A (anisotropic) band is composed of myosin molecules, which are present in different isoforms in different types of skeletal muscle (Lightfoot, 1998). This band is crossed at its mid-point by a dark, narrow transverse line, the M band (Fig. 1.5), which is bordered by a paler band of variable width, known as the H band (Landon, 1992). The light I (isotropic) band (predominantly composed of actin molecules but also containing troponin and tropomyosin molecules), present on either side of the

A band, is divided at its mid-point by a narrow dense line called the Z band (Fig. 1.4 and 1.5). The Z band thus marks the longitudinal boundaries of the individual sarcomeres (Lightfoot, 1998; Landon, 1992).

The cytoplasm of the myofibre, the sarcoplasm, forms a thin layer between the plasmalemma (Fig. 1.4) and the external surfaces of the outermost myofibrils (Landon, 1992). The mitochondria, and the membrane systems of the T tubules and sarcoplasmic reticulum (analogous to the endoplasmic reticulum) can be found within the sarcoplasm (Fig. 1.6 and 1.7). The so-called 'sarcotubular system', formed at the junction of the A and I bands (Fig. 1.6) is an important component in the link between nervous impulse and contraction of a muscle (Lightfoot, 1998).

1.1.3 Myofibre contraction

Contraction of a myofibre occurs via shortening of the sarcomere, which is achieved by a sliding movement of the I filaments towards the centre of the A band (Landon, 1992). The sliding-filament theory of muscular contraction (Huxley and Hanson, 1954; Huxley and Niedergerke, 1954) now forms the generally accepted explanation for sarcomere shortening. The increasing overlap of the thick and thin filaments is facilitated by the continual formation and breaking of cross-links between the filaments. Cross-bridge formation/breakdown is an energy-dependent process requiring ATP hydrolysis, catalysed by myosin ATPase (Ross et al., 1995). Activation of the contraction mechanism is induced by a local increase in the calcium ion concentration (Ebashi, 1980). This process occurs, in turn, with the arrival of a nerve impulse at the sarcolemma. The close relationship of the sarcoplasmic reticulum with the T-tubule system enables the depolarization 'instruction' of the T tubule to result in the release of calcium from the sarcoplasmic reticulum into the sarcoplasm (Lightfoot, 1998). The process of muscle contraction is terminated by the recapture of free calcium ions by the sarcoplasmic reticulum (Ross et al., 1995).

1.1.4 Skeletal muscle fibre typing

Skeletal muscle fibres of vertebrates do not form a single homogeneous population (Landon, 1992), and can be divided into a number of sub-classes, which reflect their metabolic function and type of activity (Lightfoot, 1998). One of the earliest visible differences reported, related to their varying degree of red colouration, which Kuhne (1865) showed to be due to an intrinsic pigment, later termed myoglobin. It was discovered that the increased myoglobin content of the so-called 'red' muscles, which thus increased their capacity to attract and hold oxygen (Landon, 1992), was associated with increased activity of the cytochrome oxidase system (Lawrie, 1952). 'White' muscles lacked these properties and were found to be much more efficient in the anaerobic synthesis of energy-rich materials, which are usually stored in the form of glycogen (Lawrie, 1953). Anatomical distribution studies (Dawson and Romanul, 1964; Close, 1972), which identified 'red' and 'white' muscles in a large number of vertebrate species, led to the consensus that 'red' muscles, whose activity is continuously being fuelled by the process of aerobic glycolysis, are responsible for sustained powerful activity, such as that required by postural functions, whereas 'white' muscles, although capable of rapid powerful action, lack stamina because of the exhaustion of their relatively limited stores of energy-rich compounds, hence their preferential employment in vigorous, yet intermittent activity (Landon, 1992).

Some muscles are predominantly one fibre type whereas others are a mixture, particularly in man (Lightfoot, 1998). The recognition that most muscles are composed of fibres which can be shown to possess a range of metabolic activities, and that the 'redness' or 'whiteness' of a muscle reflects the sum of the properties of its constituent fibres, was dependant upon the development of histochemical techniques and their application to frozen-sectioned, fresh or fixed muscle (Nachmias and Padykula, 1958; Dubowitz and Pearse 1960; Engel 1962).

The most widely adopted system of fibre typing (based on the ATPase histochemical reaction) is that of Brooke and Kaiser (1970), which divides muscle fibres into 3 major classes (Table 1.1): type I, type IIA, and type IIB. The major properties of fibre

classification are listed in Table 1.1.

More recently, immunocytochemical studies have shown that at least 6 myosin heavy chains can be consistently detected in developing and mature mammalian skeletal muscle (Smith et al., 1999). The embryonic isoenzyme is successively replaced by neonatal, and either type I, or type II isoforms as these fibres differentiate (Landon, 1992). These myosin heavy-chain isoenzymes are thought to associate with a larger number of different light-chain isoenzymes, to produce a continuum of potential fibre types (Pette and Staron, 1988). Such interactions may explain the metabolic heterogeneity of skeletal muscle fibres and their ability to respond to functional demand by changes in their phenotypic expression (Landon, 1992).

Table 1.1

Properties of mammalian skeletal muscle fibre types based on the classification system of Landon (1992)

FIBRE TYPE	I	HA	IIB
Size	Small	Intermediate	Large
Myoglobin content	High	High	Low
Energy metabolism	Oxidative	Oxidative/glycolytic	Glycolytic
Glycogen content	Low	High	Intermediate
Lipid content	High	Intermediate	Low
Mitochondria	Many	Many	Few
Local capillary density	High	High	Low
Enzyme activities			
ATPase (pH 9.4)	Low	Moderate to high	High
ATPase (pH 4.4-4.6)	High	Low	Intermediate
ATPase below pH 4.3	High	Low	Low
Oxidative SDH^a, NADH-TR^b	High	Intermediate	Low
Phosphorylase	Low	High	High
Physiological characteristics^c			
Speed of contraction	Slow	Intermediate to fast	Fast
Resistance to fatigue	High	Intermediate	Low

^a SDH; succinate dehydrogenase, ^b NADH-TR; nicotinamide adenine dinucleotide-tetrazolium, ^c based on animal experiments.

1.2 SKELETAL MUSCLE TOXICITY

Skeletal muscle is a ubiquitous tissue with a high biochemical activity (Kakulas and Mastaglia, 1992). This activity is attributable to the need for large amounts of energy and a high protein turnover (Daniel, 1977). The specialised metabolic requirements of the tissue mean that skeletal muscle is prone to damage by a variety of drugs, chemicals and toxins (Table 1.2) (Kakulas and Mastaglia, 1992). The resulting damage or dysfunction to the tissue may be induced via both indirect and direct mechanisms (Van Vleet et al., 1991).

1.2.1 Biochemical and cellular mechanisms of toxicity

1.2.1.1 Neurogenic toxicity

Interruption of the peripheral neural supply to muscle results in the development of muscular atrophy, and depending on the site of the lesion, can cause loss of use of the affected limb (Lightfoot, 1998). However, a wide variety of xenobiotics that interfere with the neural supply, commonly do so by interfering with the processes of neuromuscular transmission e.g. many antibiotics, including the aminoglycosides kanamycin, neomycin, streptomycin and gentamycin have both a presynaptic and postsynaptic effect on acetylcholine neurotransmission (Argov and Mastaglia, 1988). Injection of paraoxon in the rat causes a progressive myopathy attributed to excessive concentrations of acetylcholine (Van Vleet et al., 1991). In some cases, xenobiotics (particularly drugs of an addictive nature) have induced skeletal muscle toxicity by dramatically increasing motor neuron activity e.g. heroin and amphetamine (Van Vleet et al., 1991).

1.2.1.2 Localised toxicity

Localised muscle damage can occur following the intramuscular administration of a drug. Focal myopathy caused by intramuscular injection of narcotic analgesics, such as pentazocine (Lightfoot, 1998; Van Vleet et al., 1991) and local anaesthetics such as lignocaine (Steiness et al., 1977) are well known.

1.2.1.3 Impaired cell membrane function

Damage to the cell membrane can induce changes in the electrical properties of a cell e.g. reduced concentrations of potassium, which may occur in patients treated with diuretics such as amphotericin, causes muscle weakness (myotonia). This effect is believed to be a side effect of reduced membrane excitability. In contrast, increased membrane excitability is thought to be the mechanism by which drugs such as salbutamol, clenbuterol and cimetidine cause muscle cramping. Individuals treated with clofibrate may develop myotonia and muscle fibre necrosis. Although the precise mechanism of toxicity is not known, metabolic studies have shown that clofibrate causes an impairment of glucose and fatty acid oxidation (Paul and Abidi, 1979). Other hypocholesterolaemic agents such as pravastatin and lovastatin induce similar effects. Type II fibres are predominantly affected but the mechanism is uncertain (Lightfoot, 1998).

1.2.1.4 Mitochondrial myopathies

The nucleoside analogue, zidovudine, a long-term treatment for patients with AIDS has been reported to produce a distinctive myopathy characterised by large numbers of 'ragged-red' fibres (Dalakas et al., 1990), which at the level of the electron microscope contain grossly enlarged mitochondria with paracrystalline inclusions and abnormal cristae (Panegyres et al., 1990). Zidovudine is postulated to interfere with the homeostasis of mitochondrial DNA (Panegyres, et al., 1990). Clinical effects of the myopathy include myalgia, muscle weakness and elevated serum CK levels (Kakulas and Mastaglia, 1992). There are a number of chemicals that are known to induce mitochondrial myopathy in experimental animals as a consequence of their effects on aerobic metabolism. The uncoupling agent 2,4-dinitrophenol 'uncouples' the process of oxidative phosphorylation from that of electron transport within the mitochondria, effectively blocking the synthesis of ATP (Cooper et al., 1988). The *p*-phenylene diamines, an important group of industrial chemicals, have been shown to elicit mitochondrial changes similar to 2,4,-dinitrophenol (Munday, 1992; Blair et al., 1998), however, the mechanism is not fully understood. A myopathy similar to that induced by zidovudine, has been reportedly induced by germanium (Wu et al., 1992); administration to experimental animals over several weeks significantly reduced both cytochrome *c* oxidase and succinate cytochrome *c* reductase activity.

1.2.1.5 Microtubule disruption

Vincristine and colchicine interfere with the polymerisation of tubulin into microtubules. This causes an axonal peripheral neuropathy, which, in some individuals may be associated with a proximal myopathy. However, recovery occurs promptly upon drug withdrawal.

1.2.1.6 Lysosomal myopathies

The antimalarial drug, chloroquine may induce a proximal myopathy or neuropathy characterised by normal or mildly elevated serum enzyme (e.g. CK) levels (Mastaglia, 1982; Ngaha, et al., 1989). The condition is reversible but recovery is slow. Experiments have demonstrated a marked increase in the activity of lysosomal enzymes, particularly acid proteases, and swelling of the sarcoplasmic reticulum (Mastaglia et al. 1977; Schmalbruch, 1980). It is unclear whether the associated muscle weakness is derived from the phospholipidosis, or as a result of a direct effect on the sarcolemma (Lightfoot, 1998).

1.2.1.7 Altered protein turnover

Changes in the turnover rate of skeletal muscle protein are especially common in patients treated with certain hormones. For example, corticosteroids such as betamethazone and dexamethazone produce muscle weakness and fibre atrophy, toxic effects that are well documented in man and experimental animals. These compounds induce a selective atrophy of type II fibres, believed to be due to a decrease in protein synthesis (Van Vleet et al., 1991), although high doses of the steroids increase degradation of muscle protein (Lightfoot, 1998). In contrast, growth hormone and the β_2 -adrenergic agonists, clenbuterol and salbutamol, produce an increase in muscle fibre mass (hypertrophy). This change is due to increased protein synthesis without cell proliferation (Lightfoot, 1998). Clenbuterol also changes the relative proportions of muscle fibre types, increasing glycolytic type II fibres at the expense of oxidative type I fibres (Reichel et al., 1993). Chronic ethanol exposure has also been postulated to disturb protein synthesis in man and animals (Preedy and Peters, 1990), though the mechanism(s) of its myotoxic effects are poorly understood.

Table 1.2
 Drugs and toxins known to induce skeletal muscle injury

Class/toxic agent	Type of agent
Neurogenic	
Gentamycin, kanamycin and others	Antibiotics
Paraoxon	Organophosphate cholinesterase inhibitor
Local toxicity	
Pentazocine	Narcotic analgaesic
Lignocaine	Local anaesthetic
Impaired membrane function	
Amphotericin	Diuretic agent
Salbutamol, clenbuterol	β -adrenergic agents
Pravastatin, lovastatin	Cholesterol lowering agent
Mitochondrial toxicity	
Zidovudine	Anti-retroviral agent
2,4-dinitrophenol	Oxidative phosphorylation uncoupling agent
<i>p</i> -Phenylene diamines	Industrial chemicals
Microtubule toxicity	
Vincristine	Chemotherapeutic agent
Colchicine	Used in the treatment of gout
Lysosomal toxicity	
Chloroquine	Anti-malarial agent
Altered protein turnover	
Betamethazone, dexamethazone	Corticosteroids

1.2.2 Assessment of skeletal muscle damage

Skeletal muscle is a comparatively rare target organ, in comparison with, for example the liver, kidney, or lung. It is rarely exposed to high concentrations of xenobiotics (unless the compound e.g. a local anaesthetic, is injected into or near the muscle), does not possess specialised re-uptake systems, and is not known to have substantial cytochrome P-450 activity (Crosbie et al., 1997). Perhaps, for these reasons, detailed study of the skeletal musculature generally is not performed in regulatory toxicity studies (drug safety evaluation).

1.2.2.1 Microscopy

It is usually unfeasible to examine more than a small number of muscles at necropsy, although ideally the muscle tissue taken for histology would exhibit the various fibre types. The leg muscles of the rat, which include the soleus, long digitor extensor and gastrocnemius muscles are ideal specimens to examine as they consist of both single and mixed fibre type populations (Lightfoot, 1998). However, the vast majority of toxicological experimental protocols require the examination of only a single, mixed fibre type muscle such as the gastrocnemius. In addition to histological observation, biochemical assays of serum (Table 1.3) are useful in the detection of altered muscle-specific enzyme levels, and indeed any other abnormal parameters found in peripheral blood which may be associated with the toxicity of the compound under evaluation. Special stains to demonstrate cross-striations (PTAH) and lipid vacuoles (Sudan IV) can also be performed. The measurement of certain enzymes such as ATPase and NADH-TR are ideally carried out using frozen sections, although it is possible to evaluate fibre-type populations on fixed skeletal muscle tissue using immunological markers such as fast myosin (Fig. 1.8).

1.2.2.2 Biochemical evaluation

The most sensitive and specific enzyme commonly used as an indicator of myotoxicity is serum creatine kinase (CK). This enzyme is released from muscle cells in a number of myopathies e.g. muscular dystrophy (Smith et al., 1999), or AIDS patients being treated with zidovudine (Panegyres et al., 1990). Three isoforms (MM,

MB and BB) can be detected in peripheral blood (Table 1.3). The MM isoform is predominant in skeletal muscle. However, peak levels of CK can occur very rapidly and may be missed when following a standard protocol with set sampling times. Other enzymes, which often become elevated in serum following skeletal muscle injury, include, aspartate alanine transferase (ALT) and lactate dehydrogenase (LDH, of which 5 isoforms exist). However, they are not specific to skeletal muscle and therefore the ratio of their abundance in serum, relative to certain other enzymes (or isoforms), become important. Urinary myoglobin is also an indicator of skeletal muscle damage, although the protein is unstable unless stored at low temperatures, making it unsuitable as a biomarker of muscle injury in regulatory studies.

1.2.2.3 Electrophysiological evaluation

Electromyography can be used to detect potential muscle abnormalities and involves recording the summated electrical potentials generated when the many fibres within the muscle under observation are stimulated, via an electrode. The procedure can be useful in distinguishing between xenobiotic-induced myopathy and neuropathy (Van Vleet et al., 1991).

1.2.2.4 Skeletal muscle cell culture

Although not routinely used as a method to determine xenobiotic toxicity of novel compounds *in vivo* (Lightfoot, 1998), skeletal muscle cell cultures are widely used in research as a model to evaluate the biochemical effect of xenobiotics on muscle (Kato et al., 1992) and can often provide a valuable insight into the mechanism of toxicity (Harauchi and Hirata, 1993; Blair et al., 1998).

Table 1.3A biochemical profile of serum enzymes/parameters used to assess organ injury^a

Parameter	Abbreviation	Clinical Diagnosis
Alanine amino transferase	ALT	Raised in liver necrosis /injury. Also indicative of kidney damage.
Aspartate amino transferase	AST	↑ with liver necrosis or injury of any cause. Also ↑ after necrosis or trauma to heart or skeletal muscle. AST usually > ALT in these cases.
Alkaline phosphatase	ALP	↑↑ with liver cholestasis. ↓ activity related to reduced food consumption.
Albumin	ALB	↓ following decreased synthesis by the liver in cases of acute/chronic liver injury. ↑ in renal proteinuria.
Total protein	TP	↓ with chronic liver disease due to decreased synthesis. Also ↓ with severe kidney damage.
Urea	BUN	↑ with impaired kidney function.
Creatinine	CRE	↑ following acute/chronic renal function impairment.
Glutamate dehydrogenase	GLDH	↑ in all categories of hepatic and biliary tract diseases.
Lactate dehydrogenase	LDH	↑↑ in cirrhosis, obstructive jaundice and renal diseases of many types. Also in skeletal muscular diseases and congestive heart failure. Isoenzyme pattern used to determine damaged organ(s).
	LDH 1 & 2	↑ LDH 1 particularly following skeletal muscle injury. ↑ LDH 2 indicative of testicular injury and haemolysis of any cause.
	LDH 2, 3 & 4	'Midzone fraction' ↑ following massive platelet destruction and after skeletal muscle injury.
	LDH 5	↑ with skeletal muscle injury, also with many types of liver injury e.g. cirrhosis, hepatitis, congestion.
Creatine kinase	CK	Most increases relate to trauma/diseases of skeletal or heart muscle.
	CK-MM	Main source of this isoenzyme is the heart (20-40% of total activity). ↑ in inflammatory conditions of heart, circulatory shock and myocardial infarction.
	CK-MB	Mainly present in skeletal muscle, but also in heart (4:1 ratio wet tissue weight). ↑ in myopathic disorders and trauma.
	CK-BB	Highest activity found in brain and smooth muscle. ↑ with many forms of cancer, following multisystem insult and in chronic renal failure.

^aBurtis and Ashwood, 1995; Tietz, 1995.

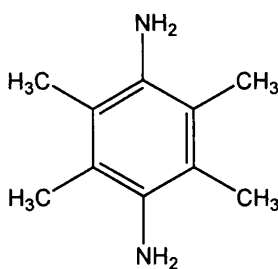
1.3 TETRAMETHYL-*p*-PHENYLENEDIAMINE (TMPD) AND THE PHENYLENEDIAMINES

1.3.1 Physical and chemical properties

Phenylene diamines are aromatic amines with two amino groups attached to benzene. There are three isomeric Phenylene diamines: ortho, meta, and para, or 1,2-; 1,3-; and 1,4-benzenediamine respectively. They are all white solids, which darken upon standing in air and they are completely soluble in hot water (Layer, 1978).

2,3,5,6-tetramethyl-*p*-phenylenediamine (Fig. 1.9a) is a tan-coloured solid, which is sparingly soluble in cold water (readily soluble in ethanol), forming a neutral solution. *N,N,N',N'*-tetramethyl-*p*-phenylene diamine (Fig. 1.9b) is a grey-black solid, dissolving more readily in water than its isomer, forming an intensely violet-coloured solution called Würster's Blue.

a)



b)

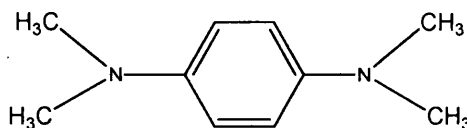


Figure 1.9 The structural isomers of tetramethyl-*p*-phenylene diamine.

The *p*-phenylenediamines are readily oxidised by free radicals, or free radical sources e.g. bromine, chlorine, oxygen or peroxides, to give radical cations called Würster salts. These salts are stable in water-ethanol solutions at pH 3, allowing isolation of the respective hydrochloride. The intensely coloured solutions formed as a result of their ease of oxidation, serves as a test for the type of substitution on the *p*-phenylene diamine (Layer, 1966). The unique reactivity of this family of compounds explains their many uses, both in industry and for analytical research.

1.3.2 Applications

2,3,5,6-TMPD is one of a number of derivatives of the *p*-phenylene diamine family. These derivatives constitute an important group of aromatic compounds, widely used in industry and research.

The first member of the group, the unsubstituted isomer *p*-phenylene diamine, is the primary intermediate in permanent hair dye formulations. Other industrial applications include their use as photographic developers, accelerators in the process of rubber vulcanisation, and as intermediates in the manufacture of azo dyes (Combes and Haveland-Smith, 1982). Perhaps the widest use of *p*-phenylene diamine derivatives in research is for the study of electron transport processes in mitochondria (Burcham and Harman, 1991; Sarti et al., 1994), though they have also been employed as antioxidants in the study of free radical mechanisms (Carbonera and Azzone, 1988).

1.3.3 Metabolism of *p*-PD and its derivatives

Three classes of *p*-phenylene diamine derivatives that cause skeletal muscle toxicity (myotoxicity) are now known; the *N*-methylated compounds, the ring aminated 1,2,4-triaminobenzene, and the ring methylated derivatives. The nature of their metabolism, which is explained in the following paragraphs, is consistent with a role for oxidative processes in the initiation of the pathological changes observed to occur

in skeletal muscle of rats dosed with these compounds (Munday, et al., 1990).

1.3.3.1 Absorption, distribution, metabolism, and excretion (ADME) studies of *p*-phenylene diamine

Very little data regarding the bioavailability, distribution, metabolism and excretion *p*-phenylene diamine exist in the literature, with the exception of a study by Ioannou and Matthews (1985). These authors could find no significant difference in the bioavailability of the unsubstituted compound, either by route, intravenous (iv) vs. oral, or dose, when administered in the dihydrochloride form to rats and mice.

Ioannou and Matthews (1985) reported that with the exception of adipose tissue, distribution of *p*-phenylene diamine was found to be roughly proportional to tissue volume i.e. none of the tissues studied appeared to concentrate the amine. The tissues of female rats (at 3 days following iv injection) contained higher amounts of *p*-PD-derived radioactivity than did those of male rats. In the mouse, males were found to have higher concentrations of the chemical in the liver, whereas females had higher concentrations in muscle tissue.

Several metabolites of the parent compound were reported (Ioannou and Matthews, 1985), their chemical nature and quantity displaying both species and sex-related differences. Clearance of these metabolites was found to be rapid (mainly through urine), with greater than 90% excretion in 24 hours.

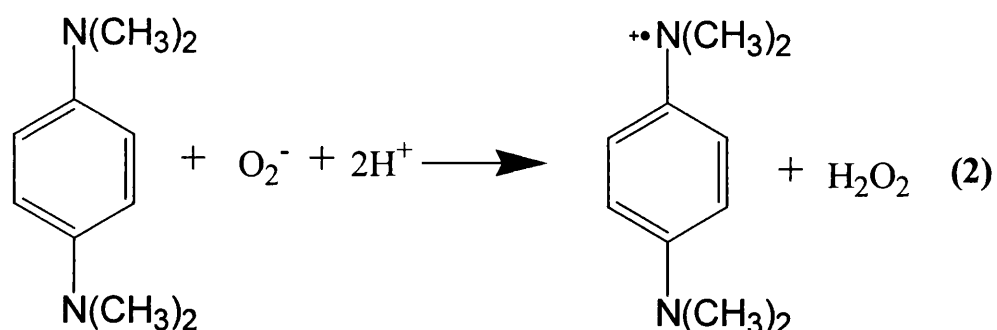
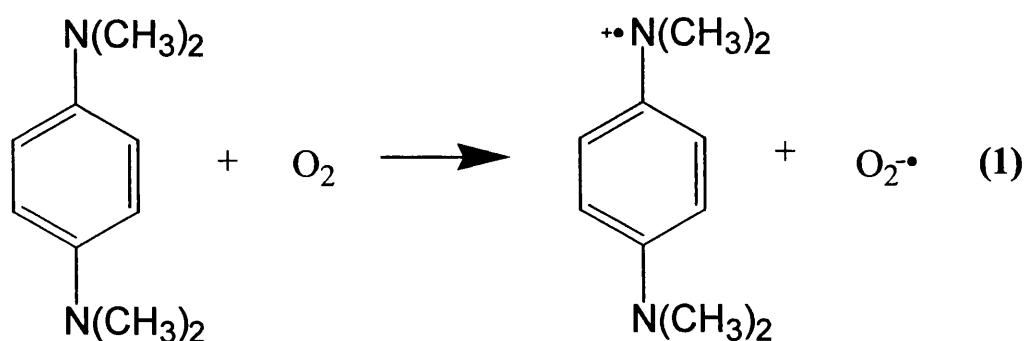
1.3.3.2 Metabolism of TMPD

Many of the *p*-phenylene diamine derivatives autoxidize to the corresponding cation radical, often referred to as Würster salts, which are exceptionally stable (LuValle et al., 1948). However, depending upon the compound and the oxidizing agent, *p*-phenylene diamines may undergo a 1- or 2-electron oxidation.

a) *N,N,N',N'*-tetramethyl-*p*-phenylene diamine (*N,N,N',N'*-TMPD)

Autoxidation of *N,N,N',N'*-TMPD yields only the 1-electron oxidation product, the Würster salt, which in this case is much more stable than the 2-electron oxidation product quinonedi-imine. Molecular oxygen is reduced to hydrogen peroxide, with intermediate formation of superoxide radical.

As is the case with 1,2,4-triaminobenzene (Munday, 1986), it is believed that the autoxidation reaction of *N,N,N',N'*-TMPD is initiated by electron transfer from amine to molecular oxygen (Reaction 1), with further Würster's Blue being formed by reaction of *N,N,N',N'*-TMPD with superoxide radical (Reaction 2).

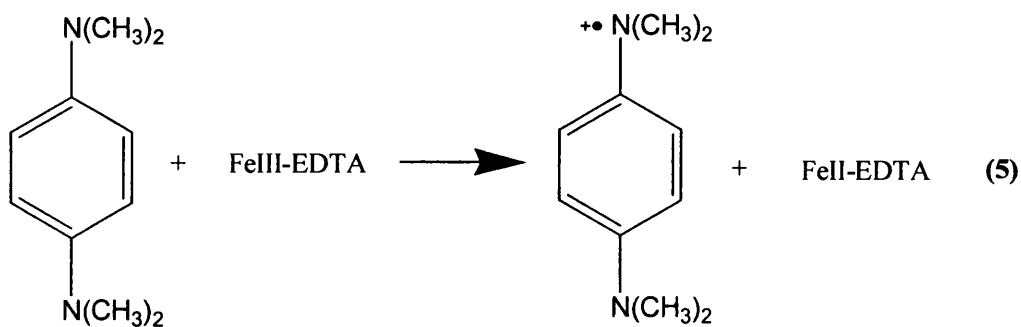


In support of this theory, aromatic amines are known to be readily oxidised by superoxide (Crank and Makin, 1984), and superoxide dismutase decreases the rate of formation of Würster's Blue, thus reflecting inhibition of Reaction 1. When catalase is present, uptake of oxygen during *N,N,N',N'*-TMPD autoxidation is decreased, yet the enzyme has no effect upon formation of Würster's Blue, suggesting that hydrogen peroxide is an end product in the overall reaction (Munday et al., 1989). Both superoxide dismutase and catalase appear to reduce oxygen uptake during *N,N,N',N'*-TMPD autoxidation, due to the return of oxygen to the solution via Reactions 3 and 4.



Ionic copper and the copper-containing enzyme, caeruloplasmin, catalyse oxidation of the N-methylated product. Despite the fact that haematin (the hydroxide of haem) is an effective catalyst, ionic iron only increases the rate of TMPD oxidation when complexes with EDTA. In contrast however, the catalytic activity of copper is abolished by such metal chelating agents, and may be a consequence of different reaction mechanisms (Munday et al., 1989).

Hydroxyl radical is also formed during the autoxidation of TMPD catalysed by iron-EDTA. This complex has been shown to be an effective promoter of hydroxyl radical formation in reactions in which ferrous iron is oxidised by hydrogen peroxide and then recycled by either superoxide radical or an organic reductant. The catalytic cycle between Fe(III) EDTA and superoxide radical is better known as the iron-catalysed Haber-Weiss reaction. However, Munday et al. (1989) reported that superoxide dismutase did not affect hydroxyl radical formation, and therefore this mechanism cannot apply in this case. It is considered more likely that the species is generated from TMPD via the sum of Reactions 5 and 6, in a manner similar to the radicals derived from other redox cycling compounds e.g. doxorubicin and paraquat (Timbrell, 1992).

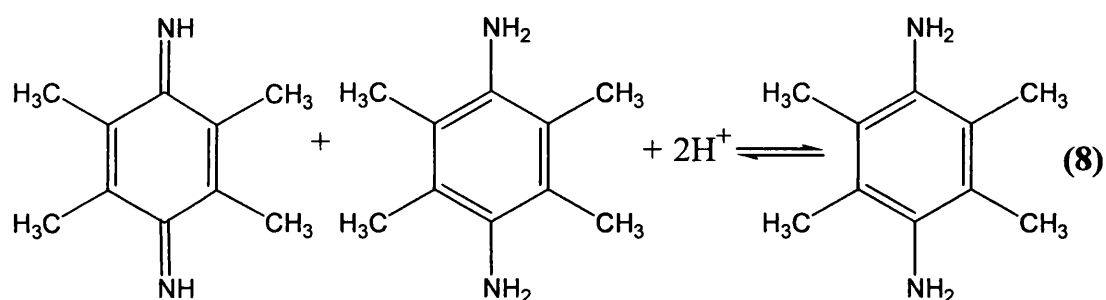
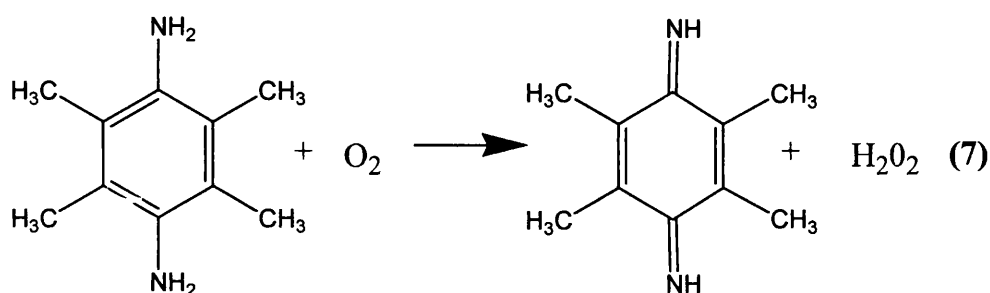


b) 2,3,5,6-tetramethyl-*p*-phenylenediamine (2,3,5,6-TMPD)

Both the Würster salt and the quinonedi-imine derived from the ring methylated isomer are comparatively stable, and investigations by Munday et al. (1990) have shown that both these compounds are produced upon autoxidation of 2,3,5,6-TMPD. Free superoxide could not be detected during 2,3,5,6-TMPD autoxidation, as superoxide dismutase was without effect on either the rate of product formation or oxygen consumption (Munday et al. 1990). As with the *N*-methylated isomer, catalase inhibited oxygen uptake during 2,3,5,6-TMPD autoxidation, providing evidence for hydrogen peroxide generation in the reaction. The final product of oxidation is tetramethyl-*p*-benzoquinone, following hydrolysis of the quinonedi-imine (LuValle et al., 1948). Similar to the behaviour of *N,N,N',N'*-TMPD, autoxidation of 2,3,5,6-TMPD was stimulated by metal ions (Munday et al., 1990). However, chelating agents failed to influence the rate of autoxidation, proving that metal catalysis is not obligatory.

When glutathione, NADH or NADPH were present, the accumulation of the quinonedi-imine and Würster compound, during 2,3,5,6-TMPD autoxidation was inhibited (Munday et al., 1990). Similar results have been recorded for another

autoxidizable compound, triaminobenzene (Munday, 1987), which is also known to cause skeletal muscle toxicity (Munday, 1987; Walker, 1970). These data are consistent with the establishment of a redox cycle between the amine and its oxidation products (Reaction 7 and 8).



1.3.4 Toxicity of TMPD and *p*-phenylene diamine derivatives

1.3.4.1 Acute and chronic toxicity

One of the earliest and most extensive studies of *p*-phenylene diamine toxicity was carried out by Jasmin (1961). Although earlier acute studies had been reported in the rabbit (Tainter and Hanzlik, 1924), and cat and dog (Davis, 1946), few data had been compiled on the target organs of this family of chemicals, making it difficult at that time to do little more than speculate on their mode of action.

In 1961, Jasmin undertook a series of experiments to investigate the toxicity (acute and chronic) of the *p*-phenylene diamines in the rat. Acute lethal convulsions were observed following a single intraperitoneal (ip) or subcutaneous (sc) injection of 4-mg. Chronic toxicity of *p*-PD could be induced by administering a twice-daily dose of 2mg, which was found to be sufficiently well tolerated (over a 4-10 day period), and produced notable pathological changes in the brain, lymphatic organs, skeletal and cardiac muscles, gastric mucosa, pancreas and ovaries.

p-Phenylene diamine has been reported to provoke an inflammatory response in a number of laboratory animals (Kalish and Wood 1995; Liden and Boman 1988). Indeed, at the site of sc injection, an acute inflammatory response (typified by a massive influx of polymorphs) rapidly ensues (Jasmin, 1961). It is probably with this effect in mind that the sc route is generally the preferred method of dosing with *p*-phenylene diamine derivatives, as it is considered the 'safest' in terms of initial response. However, disagreement exists regarding the causal agent of the inflammatory response. Some authors attribute the effect of the chemical *in vivo* to the para- position of its amine groups (Rajka, 1952); others consider the change to be due to the intermediary metabolites of the parent compound, notably the quinonediimine (Mayer, 1954). With the aim of establishing a correlation between the activity of each family member of the *p*-phenylene diamine group with its chemical structure, Jasmin (1961) carried out a number of experiments with several *p*-PD derivatives and compared their toxic action(s) by employing acute versus chronic dosing regimes.

Jasmin (1961) determined that the convulsive nature of the *p*-phenylene diamine derivatives was found to be directly proportional to their degree of methylation, and that this characteristically toxic action could not be reproduced by other non-methyl containing derivatives. Moreover, it was consistently shown that only the methylated derivatives induced muscle injury (myopathy) when administered chronically. The severest muscle lesions were observed when using the free compound. This trend, relating the degree of methylation with the extent of toxicity produced (particularly with regard to muscle damage) was also observed by Munday et al. (1989) using *N*-methylated *p*-phenylene diamine and ring methylated *p*-phenylene diamine (Munday et al., 1990), as reflected by elevated plasma levels of muscle-related enzymes, and histological evidence.

Despite the similar pathological changes evoked in skeletal muscle, the two types of compound (*N*-methylated and ring-methylated) have equivocal effects on the heart (cardiac muscle). Munday et al. (1989) reported moderate degrees of necrosis in skeletal muscle following administration of *N,N,N',N'*-TMPD, which were comparable to the intensity of skeletal muscle damage seen in animals dosed with *N*-methylated compounds. However, with the exception of a small amount of necrosis in animals receiving the high dose of 2-methyl *p*-phenylene diamine, no heart lesions were recorded with ring-methylated compounds, even when severe damage to skeletal muscle was evident. This finding was supported by Draper et al. (1994), who, when using an identical dose regime (25, 50 or 75 $\mu\text{mol kg}^{-1} \text{ day}^{-1}$ TMPD) found no evidence of any cardiac lesions, except at the highest dose of TMPD. However, these last workers made the interesting observation that very selective damage to stage 14 testicular tubules was apparent in animals dosed with 75 $\mu\text{mol TMPD kg}^{-1} \text{ day}^{-1}$.

The reason for this observed difference between the *N*-methylated and ring-methylated compounds in their effects upon cardiac muscle, is unknown. The answer may lie in their different oxidation pathways: *N*-methylated *p*-phenylene diamines oxidise by a 1-electron process, yielding hydrogen peroxide with immediate formation of superoxide radical (Munday, 1988). In contrast, ring-methylated *p*-Phenylene diamines are oxidised to quinonedi-imines, and although hydrogen peroxide is produced in this reaction, no evidence for superoxide formation was found (Munday et al., 1990).

1.3.4.2 Mutagenicity and carcinogenicity of *p*-phenylene diamine and its derivatives

The amine of *p*-phenylene diamine is one of several classes of chemicals thought to contribute to the increased incidence of bladder cancer reported among dye manufacturing industry workers (Wynder et al., 1963; Anthony and Thomas, 1970), however the data on the carcinogenicity of *p*-phenylene diamine are equivocal. Despite several investigators using the *Salmonella typhi* mutagenicity test, results vary from one laboratory to another. Ames et al. (1975), and Venitt and Searle (1976), have reported that *p*-phenylene diamine is not mutagenic, or only weakly

mutagenic. More recently, Rojanapo et al. (1986) confirmed the findings of Ames et al. (1975) in that *p*-phenylene diamine was only weakly mutagenic when tested with *S. typhi* in the presence of rat liver S-9 fraction. However Rajanapo et al. (1986) were interested in the activity of the oxidation product of *p*-phenylene diamine (produced upon the reaction of the parent compound with H₂O₂), which they found to be strongly mutagenic. This mutagenic behaviour has also been observed by Watanabe et al. (1990), who found that H₂O₂-oxidised *p*-phenylene diamine was a potent mutagen. This is an interesting finding as the reaction described in this last report is similar to that occurring in the hair dyeing process. Further experiments by Rojanapo et al. (1986) revealed that the oxidation product of *p*-phenylene diamine is carcinogenic to Wistar rats, particularly the female, both by sc injection and skin painting; tumours of the mammary gland and uterus were induced, respectively.

It seems that the carcinogenic potential of these compounds is dependent upon the location of the amine groups on the benzene ring. Substituted phenylene diamines appear to be least active when the amino groups are para to one another. Activity increases when the para position is occupied by a non-amino substituent, or the two amino groups become ortho to the substituted group (Sontag, 1981).

1.3.4.3 Teratogenicity

Following a heightened interest in the safety of hair-colouring ingredients, DiNardo et al. (1985) tested the teratogenic potential of a number of oxidative hair dyes, including *N,N*-dimethyl-*p*-phenylene diamine, in the rat. This compound was administered throughout gestation (at a dose which exceeded a 100-fold exaggeration of human exposure) and its effects were compared with the well known positive control in such teratogenic studies, vitamin A. Except for a slight reduction in weight gain of the dams during pregnancy, which may be indicative of a certain degree of maternal toxicity, *N,N*-dimethyl-*p*-phenylene diamine did not produce teratogenic effects in the offspring.

The teratogenic potential of *p*-phenylene diamine and several other compounds typically found in oxidative hair-colouring formulations was investigated by Burnett and Goldenthal (1988). In agreement with the findings of DiNardo et al. (1985) topical application of hair dyes had no adverse effect on the fertility of either males or females, or on gestation, lactation and weaning indices. The average number weaned per litter and the mean body weights of the weanlings were comparable among the *p*-phenylene diamine-treated and control groups.

1.3.4.4 *In vitro* studies

Concurrent with the aforementioned *in vivo* studies, *in vitro* experiments conducted by Munday et al. (1989, 1990) investigated the autoxidation of *N*-methylated and ring-methylated *p*-phenylene diamine derivatives and their effects on isolated erythrocytes. As a general rule, autoxidation rate, severity of oxidative damage in erythrocytes *in vitro* (as determined by glutathione depletion and methaemaglobinaemia), and myotoxic activity *in vivo*, were all proportional to the degree of methylation of each derivative under investigation. This data suggests that free-radical species generated through intracellular oxidation, may be involved in the initiation of toxic effects *in vivo*.

The oxidation of *p*-phenylene diamine is mediated by a number of endogenous enzymes, including caeruloplasmin (Frieden and Hsieh, 1976), myeloperoxidase (Pember et al., 1983), and prostaglandin synthase (Van der Ouderaa et al., 1977). Despite this, it seems unlikely that these enzymes are involved in the myotoxicity of these compounds since one would expect the greatest toxicity to be seen in those tissues possessing the highest activity of these enzymes e.g. thyroid, kidney and liver (O'Brien, 1988; Subrahmanyam and O'Brien, 1985), rather than skeletal muscle. However, *p*-phenylene diamine oxidation is also mediated by the cytochrome *c*/oxidase system (Keilen and Hartree, 1938; Packer and Mustafa, 1966). These compounds have been used for over 50 years in the study of terminal oxidases in the respiratory chain, and *N,N,N',N'*-TMPD and its 1-electron oxidation product, Würster's Blue are used as artificial electron carriers in the study of mitochondrial metabolism (Jacobs, 1960; Alexandre and Lehninger, 1984). Thus a large amount of data exists regarding the biochemical effects of certain *p*-phenylene diamine

derivatives in mitochondria, yet the possibility that the same reactions might elicit a toxic response *in vivo* has not been addressed.

Further to initial investigations involving administration of several *p*-phenylene diamine derivatives to experimental animals (Munday et al., 1989; 1990), Munday (1992) tested the hypothesis that mitochondrial metabolism may be involved in the initiation of the harmful effects of these derivatives upon muscle *in vivo*. The mitochondria of skeletal muscle (a tissue which contains large numbers of this organelle to support its high energy requirements) were found to be particularly effective in promoting *p*-phenylene diamine oxidation *in vitro*. Moreover, the magnitude of the mitochondrial effects produced by each compound in the series correlated well with their previously reported ability to cause muscle necrosis *in vivo*.

It has been shown that the locus of *p*-phenylene diamine oxidation in the mitochondrion is the cytochrome *c*/oxidase system (Keilen and Hartree, 1938; Packer and Mustafa, 1966), as shown by the inhibitory effect of the cytochrome oxidase inhibitors cyanide and sulphide. Thus it would follow that the rate of TMPD oxidation should increase with increasing concentrations of cytochrome *c*/oxidase. Indeed, studies have shown that mitochondrial cytochrome *c*/oxidase concentration differ widely between different tissues (Williams et al., 1968; Williams and Thorp, 1969); the order published by these workers put skeletal muscle at the top of the list, several places ahead of liver.

These findings suggest that the high mitochondrial content of muscle may account for the toxicity of *p*-phenylene diamine to this tissue. This hypothesis seems plausible in view of the literature that highlights the important role of the cytochrome *c*/oxidase system in *p*-phenylene diamine oxidation, and the much lower levels of these enzymes in the liver, as compared to skeletal muscle.

Primary cultures of rat skeletal muscle cells have also been employed to study the adverse effects of *p*-phenylene diamine (Harauchi and Hirata, 1993). When cultured in the presence of TMPD (0.3 mM), atrophy and/or swelling of the cells was observed. At the highest concentration (1.0 mM) muscle cell viability was drastically reduced. The authors also used the muscle-specific enzyme creatine kinase (CK) as a

marker of cell injury. However, it was determined that once released, CK is inactivated quickly in the extracellular medium, and thus established that it is preferable to measure cellular CK as a more reliable indicator of cell damage.

In agreement with *in vivo* findings (Jasmin, 1961; Munday et al. 1989, 1990), *p*-phenylene diamine analogues damaged myofibres in primary culture in the same 'structure-activity' order; that is, damage increased *in vitro* with increasing methylation of the molecule. This effect is believed to be related to the ease with which the compounds in the series can form free radicals (Munday, 1988).

1.4 FREE RADICAL DAMAGE AND CELL DEATH

The electronic structure of molecular oxygen in the ground state is unusual in that despite being a radical species, it is only sparingly reactive with the majority of organic molecules. For aerobic life to be possible, O₂ must accept electrons one at a time from another radical e.g. a transition metal such as iron or copper. These types of 2/4 electron reductions *in vivo*, rely on co-ordinated, serial enzyme-catalysed one-electron reactions.

The ‘trade-off’ for the cell in terms of being able to make use of oxygen in this way is the generation of superoxide and hydrogen peroxide, respectively. In the presence of free transition metal ions, superoxide and H₂O₂ together, generate the extremely reactive hydroxyl radical, which is ultimately thought to be the species responsible for initiating the destruction of biomolecules. All of these species are involved in the toxicity of O₂ and are collectively referred to as oxidants, or reactive oxygen species (ROS).

ROS can be generated from a number of sources e.g. via the electron transport chain (ETC), as a result of peroxisomal fatty acid metabolism, and also as a consequence of innate immunity during phagocytosis.

The mitochondrial enzyme, cytochrome *c* oxidase is responsible not only for the activation of oxygen for reduction, but must also ensure that none of the potentially harmful intermediates i.e. superoxide or hydrogen peroxide ‘escape’ from the active site into solution, and that the final product is indeed water. This function of cytochrome *c* oxidase is achieved by its possession of 2 copper complexes which each donate an electron simultaneously, therefore avoiding the one electron addition product, superoxide.

Conversely, many other enzyme systems are themselves responsible for the generation of ROS. The cytochromes P-450 are a number of isoenzymes that metabolise a wide variety of endogenous and xenobiotic compounds, typically to render them more water-soluble and therefore more easily excreted in urine. Certain substrates accept a single electron from cytochrome P-450 and transfer them to O₂. This generates superoxide and simultaneously regenerates the substrate allowing further cycles to take place. Quinones or bipyridyls e.g. paraquat will undergo this type of reaction.

There are obviously many enzyme systems capable of generating oxidants, sometimes in a tissue or cell specific manner e.g. the deamination of dopamine by monoamine oxidase generates H₂O₂ in some neurones and has been implicated in the cause of Parkinson's disease. The extent of damage that an oxidant attack can induce largely depends on the biological nature of the target in question.

1.4.1 Necrosis

Cellular necrosis is the result of an acute injury of intrinsic or extrinsic origin leading to the irreversible damage and death of the cell. Apoptosis or programmed cell death was originally distinguished from necrosis on the basis of ultrastructure (Kerr, 1971; 1972). Although electron microscopy provides a reliable method for recognising the two processes, in most cases, they can be identified confidently by light microscopy alone.

1.4.1.1 Morphological changes evident in necrosis

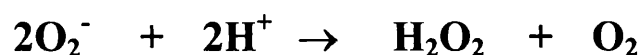
The characteristic light microscopic changes of skeletal muscle necrosis form a continuum, the final stage of which is the complete removal of the contents of the muscle fibre by phagocytic cells (myophagia). Examination of early stage necrosis reveals so-called hyaline (opaque, dark) fibres, which are excessively rounded in transverse section and (at high power) show loss of detail of individual myofibrils. Such fibres stain more darkly than normal muscle fibres in sections stained with

haematoxylin and eosin (Ferry and Cullen, 1991). Furthermore, necrosis is usually accompanied by an acute inflammatory response with exudation of neutrophil leukocytes and monocytes. Another type of change that has been noted in certain metabolic myopathies (Ferry and Cullen, 1991), and has been demonstrated in the present investigations, consists of a microvesicular appearance of damaged myofibres, due to dilatation of the sarcotubular systems.

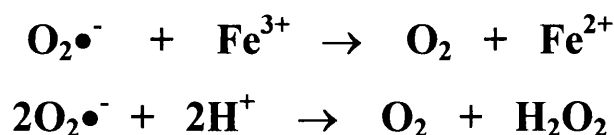
1.4.1.2 Mechanisms involved in necrotic cell death

Unsaturated phospholipids, glycolipids and cholesterol are the major components of biological cell membranes, and are prominent targets of oxidant attack. Uncontrolled generation of ROS can result in lipid peroxidation, a degenerative process that perturbs membrane structure and/or function, often with pathological consequences for the cell.

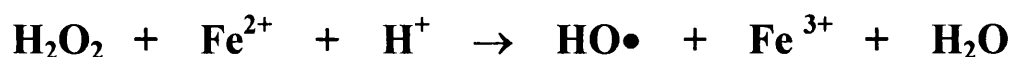
As established above, the activation of molecular O₂ carries with it the inherent risk of yielding superoxide. This may be metabolised to hydrogen peroxide by superoxide dismutase, and then to water or protonated to the hydroperoxy radical, HOO•.



The presence of transition metals, such as iron or copper, can lead to the formation of hydroxyl radicals; these are thought to be one of the most reactive and toxic free radicals found in biological systems. The generation of the hydroxyl radical can occur via the Haber-Weiss reaction:



or the Fenton reaction:



A number of detoxification mechanisms exist within biological systems to deal with free radical production. However, if large amounts of a radical-generating toxin is present, or if it cannot be cleared, these mechanisms may become overwhelmed, rendering the cell vulnerable to further rounds of oxidant attack, and the possible formation of hydroxyl radicals and singlet oxygen. This condition is termed oxidative stress, and as well as causing propagative lipid peroxidation, will also cause damage to cellular proteins and DNA (Timbrell, 1992).

1.5 PROTECTIVE PATHWAYS OF MAMMALIAN CELLS

In order to prevent an overload in free radicals and peroxides, mammals possess a sophisticated defence system capable of providing protection both in the intra- and extracellular aqueous phases, and in membranes (Chaudière, 1994).

1.5.1 Glutathione

Glutathione is a linear tripeptide composed of the α -amino acids, glutamate, cysteine and glycine. It is the most important nonprotein thiol in living systems, and is widely distributed in animal tissues, plants and microorganisms. It exists in thiol-reduced (GSH) and disulphide-oxidised (GSSG) forms.

GSH, which in many cells accounts for more than 90% of the total nonprotein sulphur, is known to function directly or indirectly in many biological processes. These processes include the synthesis of proteins and DNA, the transport of amino acids, as a co-factor of several enzymes and, perhaps most importantly, the metabolism and protection of cells (Meister and Anderson, 1983). GSH exists in millimolar concentrations in most tissues (Kosower and Kosower, 1978). The liver, however, is the organ with by far the highest concentration of GSH, normally having levels of $7\mu\text{mol g}^{-1}$ wet weight (Kretzschmar and Klinger, 1990; Table 1.4).

GSH, and the oxidised form of glutathione, GSSG, are the major thiol redox systems of the cell. The regulation of these redox systems is of great importance for the viability of the cell (Kretzschmar and Klinger, 1990). The glutathione status of normal cells is maintained in the reduced state, being controlled by the glutathione peroxidase and reductase system and connected with the $\text{NADP}^+/\text{NADPH}$ redox pair (Reed, 1986; Fig. 1.x). Depending on the availability of NADPH (the main source is the pentose-phosphate pathway), GSSG is reduced back to GSH by the NADPH-

dependant enzyme, GSSG-reductase (Fig. 1.10). The hepatoprotective role of this enzyme has been elucidated in studies using 1,3-bis(2-chloroethyl)-1-nitrosourea (BCNU) (Eklöw et al. 1984), a potent GSSG-reductase inhibitor.

Table 1.4

GSH and GSSG contents in different organs of 60 day male Wistar rats^a

	GSH	GSSG
	($\mu\text{mol g}^{-1}$ wet weight)	
Liver	7.30 ± 0.24	0.41 ± 0.03
Lung	2.90 ± 0.12	0.38 ± 0.04
Heart	2.39 ± 0.04	0.22 ± 0.02
Kidney	4.00 ± 0.14	0.32 ± 0.02
Brain	1.51 ± 0.04	0.1 ± 0.01

^aTaken from Kretzschmar and Klinger (1990)

Compounds with an electrophilic centre conjugate readily with glutathione. This may be via a simple chemical reaction, whereby GSH acts as an electron donor via GS⁻. Alternatively, interaction of glutathione with many types of compounds is catalysed by GSH-S-transferases. Direct interaction of peroxides and free radicals with biological structures can sometimes play a central role in cell and tissue dysfunction, therefore the maintenance of the glutathione-redox cycle is crucial if cellular injury by xenobiotics is to be avoided.

Approximately 10% of cellular glutathione is mitochondrial (Meredith and Reed, 1982), the major GSH portion being found in the cytosol. GSH synthesis occurs primarily, if not exclusively, in the cytoplasmic compartment in cells, and must be transported into mitochondria via an active transport mechanism through the mitochondrial membranes (Kretzschmar and Klinger, 1990). The half-times for loss of cytoplasmic and mitochondrial (hepatic) GSH were reported to be 2 and 30 hours, respectively (Meredith and Reed, 1982). This would suggest that the net transport of GSH from mitochondria to cytoplasm proceeds with a $t_{1/2}$ of at least 30 hours. Such a transport mechanism presumably functions to conserve mitochondrial GSH during periods of cytoplasmic GSH depletion. However, while some tissues have relatively high cytosolic pools of GSH and rapid turnover rates (liver and kidney $t_{1/2}$ 1-5 h), others have much smaller cytosolic pools and less rapid turnover (heart, skeletal

muscle $t_{1/2}$ 70-116 h) (Potter and Tran, 1993). Since GSH plays an important role in maintaining integrity, variations in GSH content and turnover in different tissues may have significant implications in the susceptibility of that tissue to toxicity.

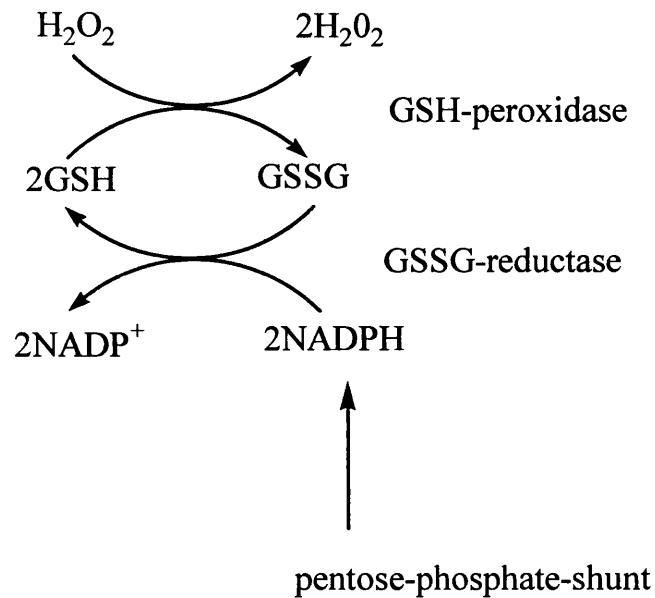
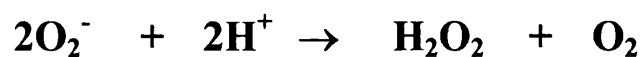


Figure 1.10. The redox cycle of glutathione (Kretzschmar and Klinger, 1990)

1.5.2 Superoxide dismutase and catalase

The superoxide dismutases (SOD) are a ubiquitous family of enzymes that play a central role in accelerating the spontaneous one-electron dismutation of superoxide (McCord and Fridovich, 1969; Fridovich, 1986). Cu/Zn-SOD is found in the cytosol and in mitochondria, whereas Mn-SOD is only present within mitochondria. Dismutation of superoxide yields oxygen and hydrogen peroxide:



Therefore, the subsequent degradation of hydrogen peroxide is required if protection by SOD is to be completely achieved. This is the function of a second dismutase enzyme named catalase, which catalyses the 2-electron dismutation of H_2O_2 into oxygen and water (Chance, 1947):



However, in many cells, such as hepatocytes, endothelial cells, and skeletal muscle myocytes, catalase concentration is very low, the majority being compartmentalised within peroxisomes (De Duve and Baudhuin, 1966). In many cells, however, glutathione peroxidase insures the degradation of hydroperoxides, thus having overlapping functions with catalase. The enzyme has also been found to be present in small amounts in the mitochondrial matrix (Nohl and Jordan, 1980), but the function of mitochondrial catalase is unclear.

1.6 MITOCHONDRIA

1.6.1 Structure

Mitochondria are small oval-shaped intracellular organelles present in the cytoplasm of aerobic cells. Despite a large variation in shape and size (a typical mitochondrion is about $2\mu\text{m}$ in length and $0.5\mu\text{m}$ in diameter) (Wolfe, 1972), electron microscopic studies by Palade and Sjöstrand revealed that all mitochondria have 2 membrane systems: an outer membrane and an extensively folded inner membrane (Figure 1.11). The outer membrane encapsulates the organelle and is essentially porous to low molecular weight compounds, such as metabolites, but not to proteins. The inner membrane is folded into a series of ridges called cristae, and in contrast to the outer membrane, is impermeable to cations such as H^+ , K^+ or Ca^{2+} . This property allows the organelle to establish a stable gradient of ions across the membrane and is essential for the process of ATP synthesis to occur (Darley-Usmar et al., 1994). Thus, there are 2 compartments in the mitochondrion: the intermembrane space between the outer and inner membranes, and the matrix, which is bounded by the inner membrane. Oxidative phosphorylation takes place in the inner mitochondrial membrane (Stryer, 1988).

1.6.2 Oxidative phosphorylation

Most of the energy requirements of aerobic cells are achieved by a series of sequential reactions that take place within the inner mitochondrial membrane. These reactions are collectively referred to as the process of oxidative phosphorylation. In oxidative phosphorylation, electron transfer reactions are coupled with the synthesis of adenosine triphosphate (ATP). Electrons flow from centres that have a low (negative) redox potential (e.g. NADH) to those with a high (positive) redox potential, ultimately molecular oxygen (Darley-Usmar et al., 1994). The electrons are transferred from NADH to oxygen through a chain of 3 large protein complexes, which lie within the inner mitochondrial membrane (Figure 1.12), NADH-Q reductase

(complex I), cytochrome reductase (complex III) and cytochrome oxidase (complex IV) (Stryer, 1988). These 'redox-centres' are arranged in order of redox potential, therefore the spontaneous, and free-energy rich, transfer of electrons through this chain leads to the pumping of protons from the matrix to the other side of the inner mitochondrial membrane. The proton concentration becomes higher on the cytosolic side and an electric potential is generated (Darley-Usmar et al., 1994; Stryer, 1988). This proton-motive force is postulated to drive the synthesis of ATP by ATPase (complex V) (Mitchell, 1979).

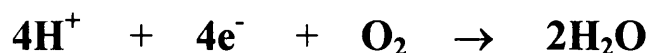
1.6.3 Characterization of mitochondrial function

The mitochondrion's ability to conserve the energy of electron transfer in the form of a proton gradient is critically dependant on the inner membrane being impermeable to protons. In mitochondria with an intact inner membrane, electron transfer can only proceed if the proton gradient is continuously dissipated by the flow back into the mitochondrion via ATP synthase (complex V). Thus, in intact mitochondria electron transfer which can be measured by oxygen consumption, can only occur if ADP is also present. This phenomenon is described as 'coupling' (Rickwood et al., 1987). The extent of coupling in a mitochondrial preparation is easily measured as the respiratory control ratio (RCR). This is a rapid and effective method, commonly used to determine mitochondrial functional integrity. Oxygen consumption in the presence of substrate and ADP (state 3 respiration) is measured and compared with the rate of respiration after the ADP has been consumed (state 4 respiration) (Figure 1.13). Mitochondria that show no difference in state 3 and state 4 respiration are 'uncoupled' (Figure 1.13). This state can be induced by some reagents (e.g. CCCP, or dinitrophenol), appropriately termed 'uncouplers' (Rickwood et al., 1987).

1.6.4 The oxygen electrode

Mitochondrial respiration can be easily measured using a Clarke-type oxygen electrode (Figure 1.14). It contains a silver/silver chloride reference anode surrounding a platinum cathode. These electrodes are immersed in saturated

potassium chloride solution and are separated from the reaction vessel by a thin Teflon membrane. The membrane is freely permeable to oxygen but serves to prevent electrode poisoning. The electrodes are polarised at a voltage of 0.6V. At the platinum cathode electrons reduce oxygen molecules to water:



The chloride anions migrate to the anode and release electrons:



The resulting transfer of electrons from the cathode to the anode causes a current to flow between the two electrodes that can be measured externally. The current is proportional to the partial pressure of oxygen in the sample. Thus, the effects of xenobiotics, respiratory chain inhibitors or uncoupling agents on mitochondrial respiration can be studied.

The oxygen electrode that was used to investigate the effects of TMPD on mitochondrial respiratory function, was specially designed by Dr Tim Bates (Institute of Neurology). The reaction chamber has a much smaller volume (250 μ L) than that of most standard electrodes (typically 3mL). This design feature greatly increases the number of experimental runs possible when using smaller yields of mitochondria.

1.7 AIMS OF THE RESEARCH PROJECT

Limited experimental investigations (Munday et al., 1989,1990; Draper et al., 1994) thus far have shown that several methylated derivatives of *p*-phenylene diamine cause significant skeletal muscle necrosis in the rat, and also induce some possible effects on cardiac muscle and testis. These compounds are unstable in solution and readily undergo autoxidation, generating ROS (the reaction pathway involved, and the ROS produced, depending on the arrangement of methyl groups around the benzene ring). Furthermore a number of workers have correlated the degree of methylation of these compounds with their myotoxicity *in vivo* (Jasmin, 1961; Munday et al., 1989, 1990) and *in vitro* (Harauchi and Hirata, 1993).

Therefore, using previously reported work as a starting point, the aim of the present project was to undertake a more in depth study of the cellular and biochemical mechanisms of TMPD-induced skeletal muscle injury in the rat, and to attempt to identify the basis of the highly selective toxicity of this agent towards skeletal muscle tissue. Initial studies in the present project evaluated the distribution and morphological effects of TMPD on a range of organs when given at several dose levels in the male and female Wistar rat. Serum biochemistry was also carried out to help identify the target sites of lesions, and to define the time scale of lesion development.

In the light of the previously suggested role of intracellular oxidation as the initiating factor in the toxicity of *p*-phenylene diamine, tissue samples removed at post mortem were analysed for early biochemical changes. Levels of reduced glutathione (GSH) were assessed as a measure of oxidative stress in skeletal muscle, as GSH and other antioxidant factors have been shown to be low in this tissue (Malaisse et al., 1982; Grankvist et al., 1981). The liver is the primary site of GSH synthesis and contains considerably higher levels of this protective peptide (6-8mM). Therefore, in addition, in the present investigations the antioxidant capacity of both liver and skeletal muscle

was assessed *in vivo* and *in vitro*, by measuring glutathione reductase, glutathione peroxidase, glutathione-S-transferase and superoxide dismutase activities. These particular studies were undertaken to determine how effectively skeletal muscle and liver could be expected to minimize the damaging effects associated with a redox cycling agent such as 2,3,5,6-TMPD.

The work of Munday (1992), on mitochondrial involvement in TMPD toxicity has been extended to include a number of assays to investigate the effect of TMPD on mitochondrial GSH concentration, ATP synthesizing capacity and its effects on the activities of the individual mitochondrial proteins that make up the electron transport chain.

Thus, a variety of *in vivo*, *ex vivo* and *in vitro* techniques were developed and employed with the aim of being able to more accurately determine the specific myotoxic mechanism of this ring-methylated derivative.

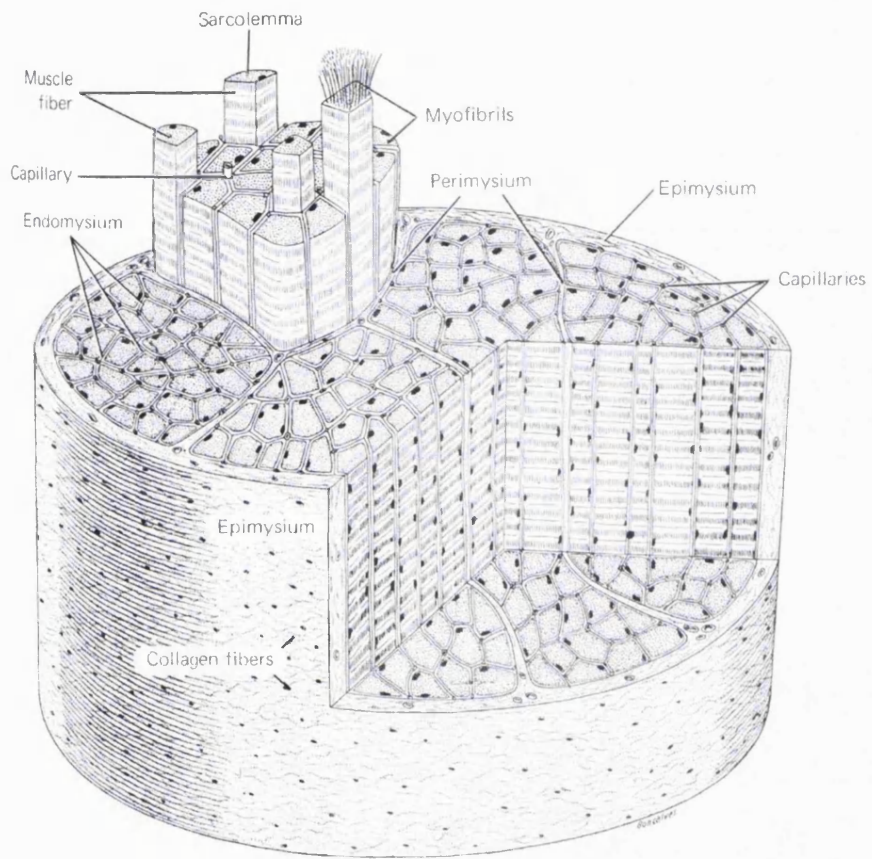


Figure 1.1 Structure of skeletal muscle (Junquiera et al., 1986).

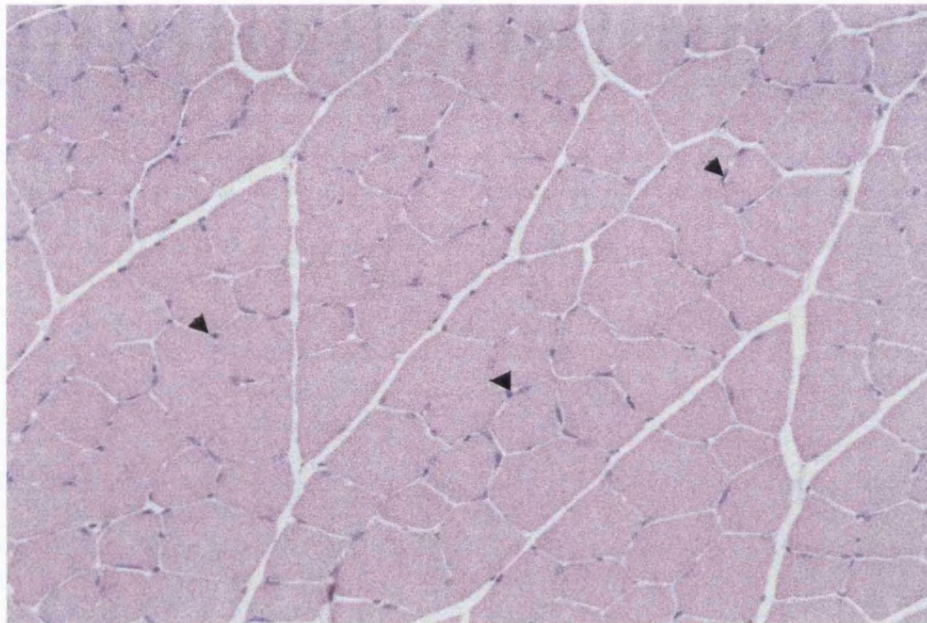


Figure 1.2 Normal muscle. Transverse section of normal skeletal muscle showing polygonal fibres. The nuclei are usually found at the periphery of the cell under the cell membrane (arrowheads). H&E x 200.

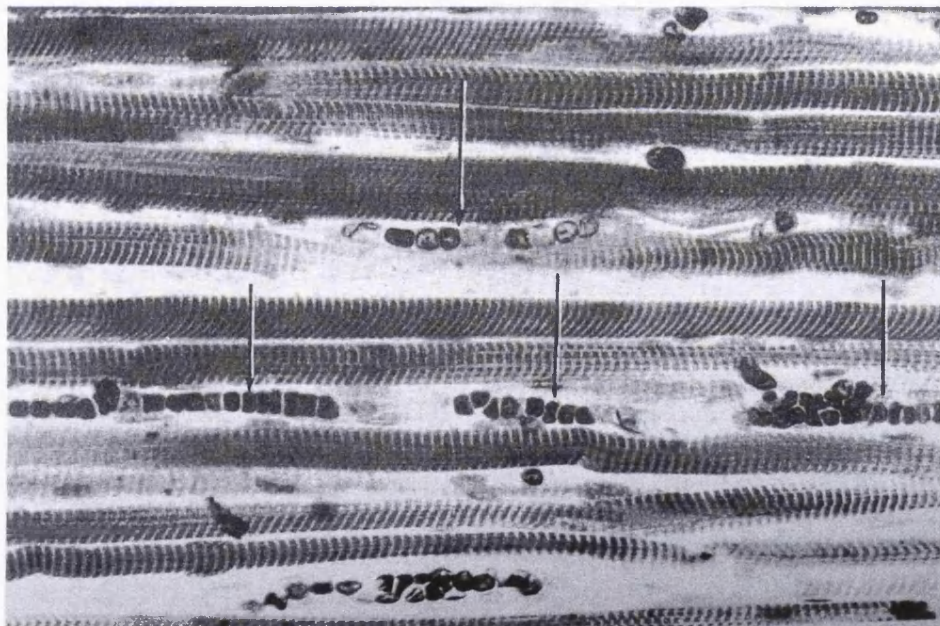


Figure 1.3 Photomicrograph of rat skeletal muscle showing the transverse (cross) striations of the muscle fibres cut longitudinally. The arrows depict red blood cells present within adjacent capillaries. x 700 (Ross et al., 1995).

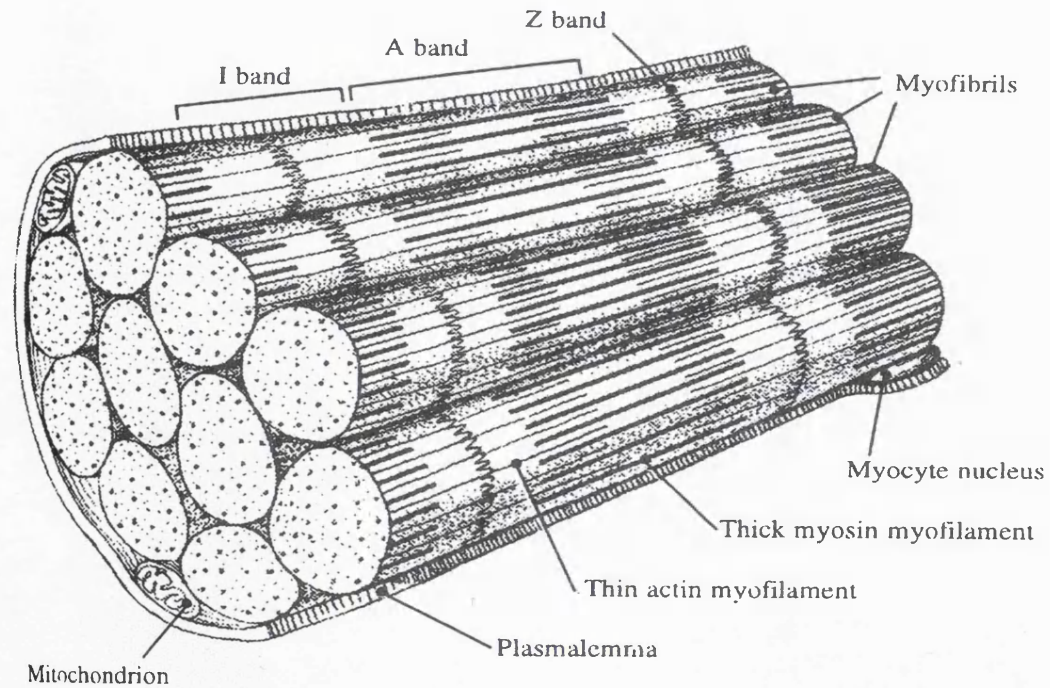


Figure 1.4 Myofibril structure. The diagram represents the internal structure of a myofibre. Each myofibril is composed of serially repeating segments called sarcomeres. Arrangement of the bundles of thick and thin filaments which constitute individual myofibres, Z lines and A and I bands are shown (Lightfoot, 1998).

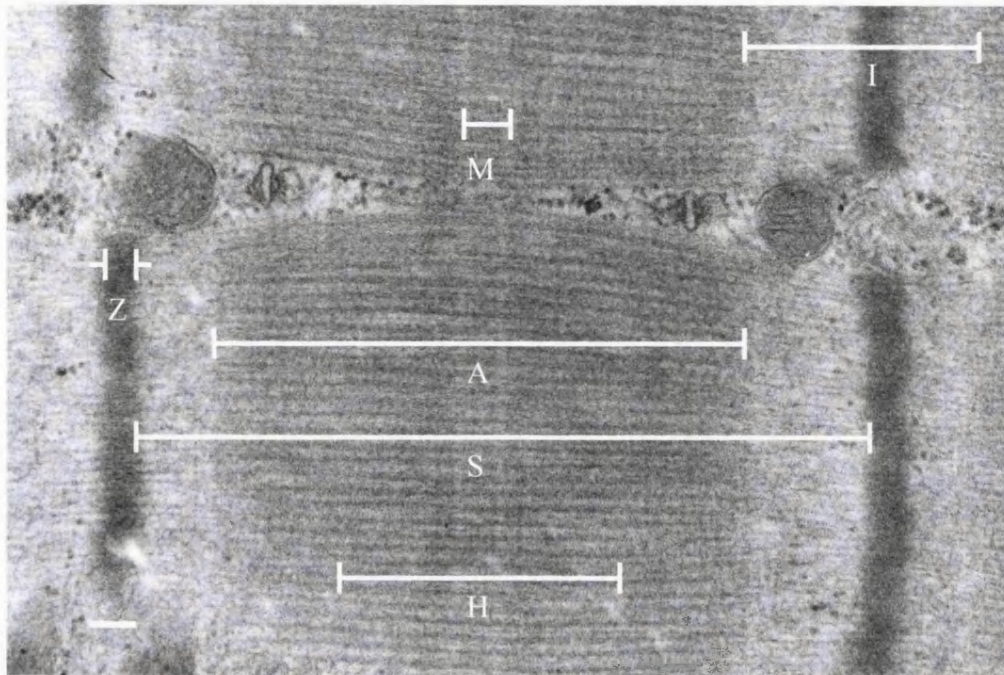


Figure 1.5. Electron micrograph of a longitudinal section of a rat myofibril. A, A band; H, H band; I, I band; M, M band; S, sarcomere; Z, Z band. Bar = 0.1 μm .

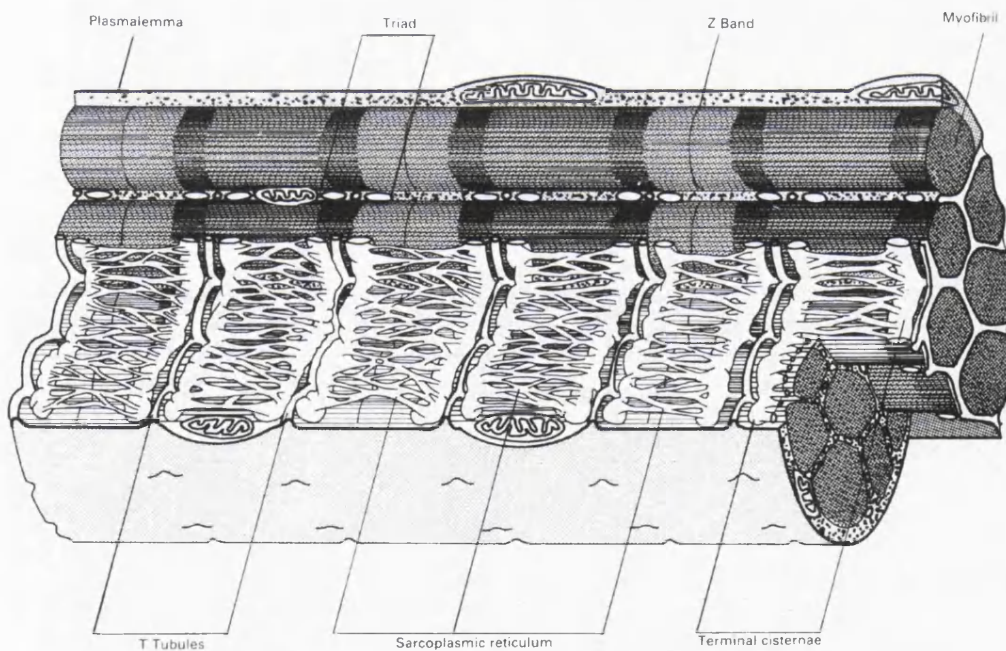


Figure 1.6. Diagrammatic representation of the sarcotubular system, showing the close association between the T tubules and the sarcoplasmic reticulum. Excitation of the plasmalemma is rapidly transmitted via the T tubule system. This promotes the release of Ca^{2+} ions from the sarcoplasmic reticulum and activates the sliding filament mechanism of contraction.

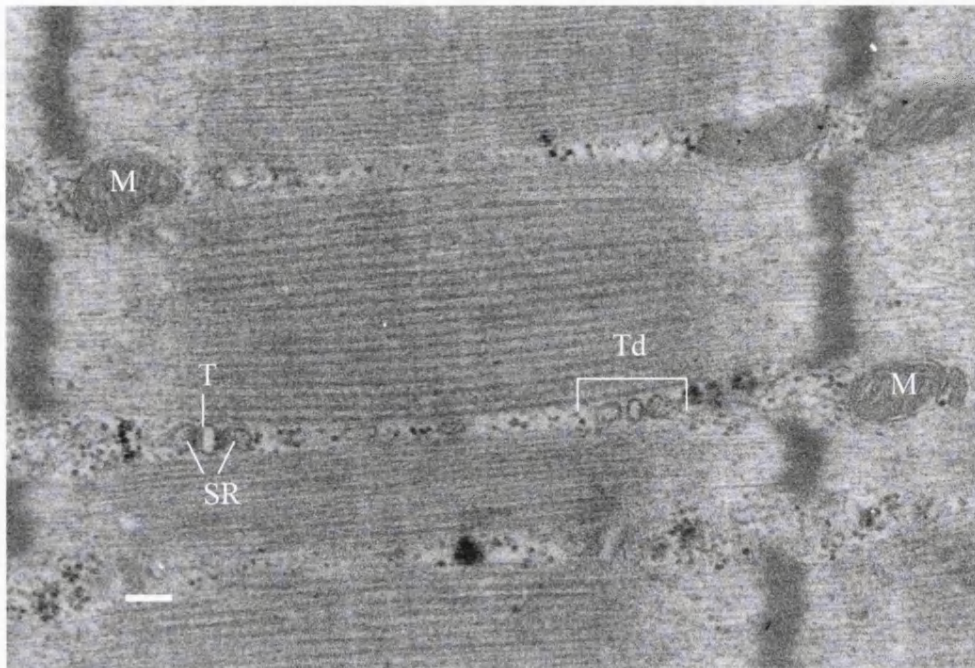


Figure 1.7. Electron micrograph of a longitudinal section of rat skeletal muscle showing the triads (Td) of the conducting system. Each comprises of a T tubule (T) and a pair terminal cisternae of the sarcoplasmic reticulum (SR). The mitochondria (M) provide a rich energy source for muscular contraction. Bar = 0.1 μ m.

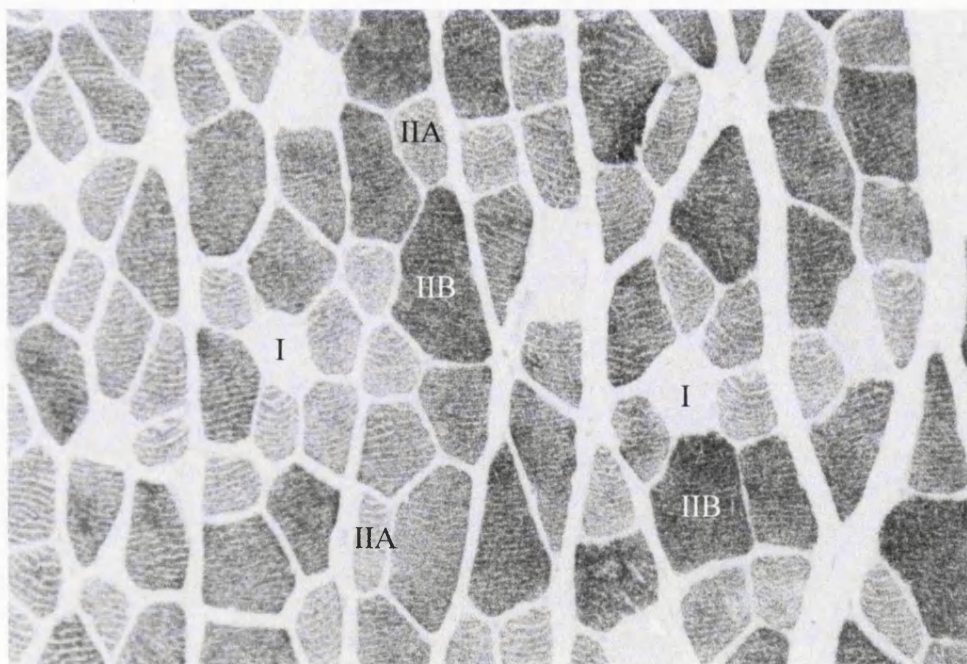


Figure 1.8. Transverse section of rat skeletal muscle (gastrocnemius), stained by the immunohistochemical technique for demonstrating fast myosin, showing 3 types of fibres in the muscle. Type I fibres (I) are seen as pale areas in the section, type IIA (IIA) fibres are small and appear grey, and type IIB fibres (IIB) are large and dark-staining (high fast myosin content). x 400.

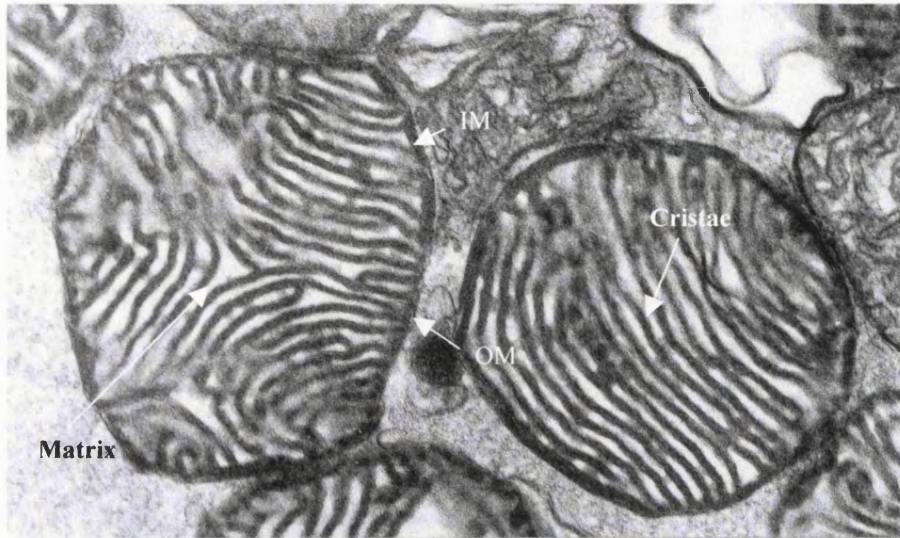


Figure 1.11 Electron micrograph of isolated rat heart mitochondria. The principle structural features are identified. IM = inner membrane, OM = outer membrane. x 38,750.

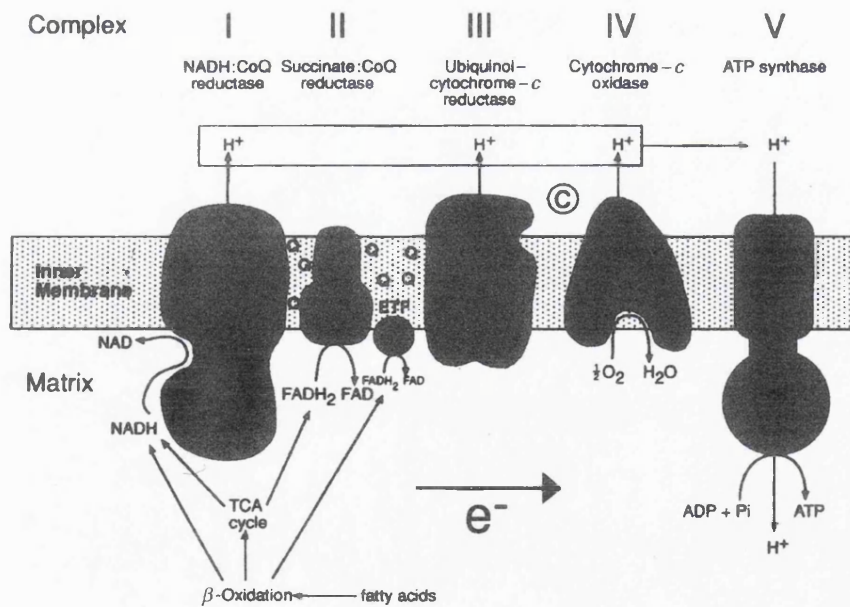


Figure 1.12 The electron transport chain.

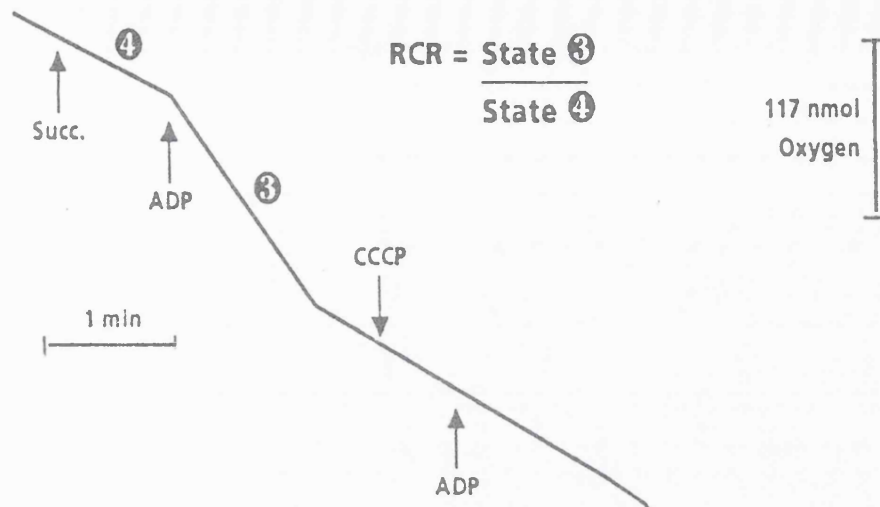


Figure 1.13 Respiratory control in rat skeletal muscle mitochondria. Mitochondria (10 μL) are added to 240 μL of respiration medium in the oxygen electrode followed by substrate (2.5 μL) e.g. succinate. Record O_2 uptake for a few minutes then add 3 μL of ADP (25 mM). State 3 and State 4 respiration are shown as is the amount of O_2 consumed in state 3 respiration for the calculation of the P/O ratio.

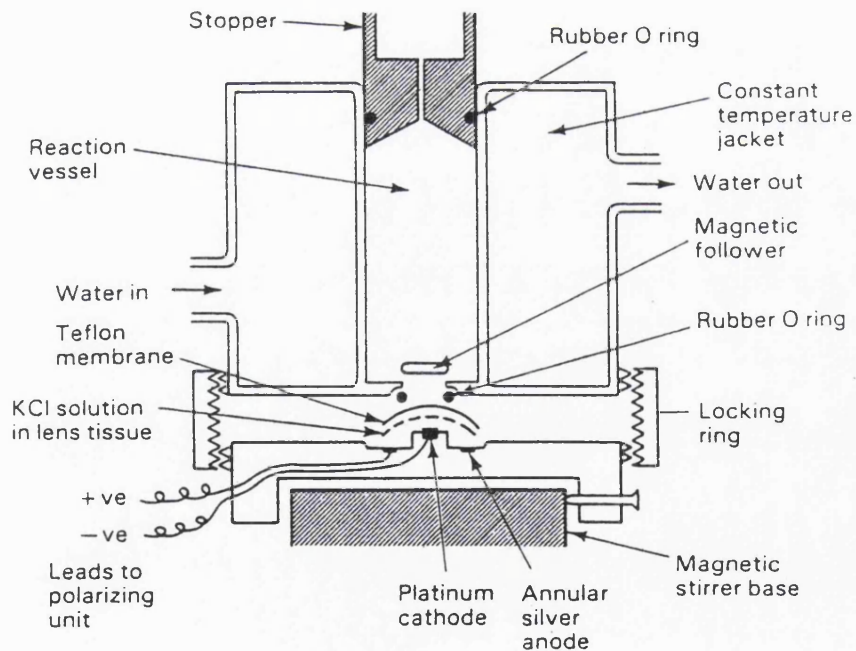


Figure 1.14 A Clark-type (Rank) oxygen electrode.

CHAPTER 2

MATERIALS AND METHODS

2.1 CHEMICALS

Adenosine 5'-triphosphate (disodium salt), albumin (bovine fraction V), 1-chloro-2,4-dinitrobenzene (CDNB), collagenase (from *Clostridium histolyticum*, type I), creatine kinase diagnostic kit (47-10), cytochrome *c* (from horse heart), 5,5'-dithiobis-(2-nitrobenzene) (DTNB), firefly lantern extract, glutaraldehyde (25%), glutathione (oxidised form), glutathione (reduced form), glutathione reductase (stock 250units/mL), HEPES, hydrogen peroxide, NADH (yeast grade III, disodium salt), NADPH (tetrasodium salt), *o*-phthaldialdehyde, pyruvic acid (sodium salt, type II crystalline), sodium arsenite, sodium dithionite, sucrose, 2,3,5,6-tetramethyl *p*-phenylene diamine, TRIS (Trizma base), xanthine, xanthine oxidase (from buttermilk), were obtained from Sigma Chemical Company (Poole, Dorset, UK).

Calcium chloride, sulphosalicylic acid, trichloroacetic acid, magnesium sulphate, mannitol, potassium phosphate, potassium chloride, sodium chloride, sodium hydroxide and sodium hydrogencarbonate were obtained from BDH Ltd. (Poole, Dorset, UK). Coomassie Blue Reagent was supplied by Biorad. Formaldehyde (10.5%) was purchased from Pioneer Research Chemicals Ltd. Methanol (HPLC) grade was obtained from Rathburn Chemicals Ltd. (Walkerburn, Scotland, UK). Foetal calf serum, Dulbecco's modified Eagle's medium (Glutamax I) (DMEM), William's Medium E (Glutamax I), phosphate-buffered saline (PBS), dispase (from *Bacillus polymyxa*), HEPES buffer solution, (1M), trypsin-EDTA, gentamycin (10 mg/mL) and chick embryo extract (lyophilised) were supplied by Life Technologies, Paisley, Scotland. All other compounds were supplied by Sigma or BDH.

2.2 IN VIVO STUDIES

2.2.1 Animal husbandry

Rats of the Han Wistar stock (GlaxoSmithKline, 200-350 g) were used throughout. Animals were allowed to acclimatise (10-14 days) in communal cages after arrival, and allowed food (Rat and Mouse Maintenance Cube Diet; Special Diet Services Ltd., Witham, Essex) and mains drinking water *ad libitum*. Animals were kept in a temperature-controlled room ($21^{\circ}\text{C} \pm 2^{\circ}\text{C}$) with a regular 12-hour light/dark cycle (lights on at 0700h). When on study, animals were housed either in individual metabolism cages or in communal cages, in accordance with the study design. During treatment, bodyweight, diet consumption and water intake of individual animals/groups were monitored daily.

Animals were dosed between 9:30 and 10:30 hours, (with the exception of time-course investigations) following a 2-3 day acclimatization period in the cages. Dosing was by the subcutaneous (sc) route, with the exception of N-acetyl cysteine (NAC), which was given intraperitoneally (ip).

2.2.2 Post mortem procedure

In order to minimise diurnal variation, animals were sacrificed between 9:30 and 12:30 hours where possible, taking one animal from each treatment group in turn. Animals were anaesthetised by an ip injection in the abdominal region, using a mixture of hypnorm/hypnovel (Vet Drug Company, Falkirk, Scotland) in water, in the ratio 1:1:2, respectively at a dose level of 3.33 mL kg^{-1} , and exanguinated from the abdominal aorta, using a 0.8 x 40mm (23G) needle. The blood was immediately transferred to microtainer tubes (Becton Dickenson and Co., Rutherford, N.J., USA) for the separation of serum.

The liver, tissues and other organs, were excised and weighed. Approximately 0.5-1.0 g of liver (taken from the median lobe) and 0.2-0.5 g of muscle tissue (including heart) was dissected free, immediately frozen (in liquid nitrogen) and stored at -80°C for future ATP, total non-protein sulphhydryl (TNPSH), and antioxidant enzyme analysis. A further liver slice (1cm thick) and remaining portions of heart and diaphragm were fixed (for at least 1 week) in 10.5% (v/v) phosphate buffered formalin (pH 7.2) for histological processing. Paired skeletal muscles were taken in their entirety from the other hind limb, stapled securely onto a piece of card to minimize contraction during fixation, and processed in an identical manner to that described above. Small amounts of liver, heart, diaphragm, soleus and quadriceps muscles were cut into cubes, approximately 1mm², and placed in 1% glutaraldehyde buffer (Appendix V) for processing and subsequent examination under the electron microscope.

2.2.3 Serum biochemistry

Blood taken from the abdominal aorta was expelled into serum microtainers. Samples were left to clot at room temperature (45 minutes), centrifuged (13,000 rpm, 1 minute, 20°C) and frozen at -80°C until analysed.

A standard range of clinical biochemical assays of serum were carried out (including special analysis to detect isoforms of those enzymes diagnostic for skeletal muscle damage), at GlaxoSmithKline Research and Development, Ware. These analyses included; alanine transaminase, aspartate transaminase, alkaline phosphatase, lactate dehydrogenase (and isoforms), creatine kinase (and isoforms), albumin, total bilirubin, cholesterol, total protein, glucose, blood urea nitrogen, creatinine, triglycerides, calcium, and phosphate.

Samples were measured at 37°C using the appropriate kits (Boehringer Mannheim, Lewes, E. Sussex UK) on an automatic centrifugal analyser (Hitachi 917 Random Discrete Analyser, Boehringer Mannheim). Isoenzymes of creatine kinase (CK) and lactate dehydrogenase (LDH) were separated using electrophoresis and quantified by scanning densitometry using the REP automated electrophoresis system (Helen

Laboratories UK).

2.2.4 Reduced glutathione determination

a) Spectrophotometric method

The assay method (Ellman et al., 1959) is based on the reaction between 5,5'-dithiobis-(2-nitrobenzene) (DTNB) and the sulphhydryl (-SH) groups on the GSH molecule. GSH comprises >95% of the TNPSH pool in the rat liver (De Master and Redfern, 1987). Furthermore, this method is sensitive to approximately 0.1 mM [-SH], and thus is suitable for sensitively assaying tissues such as the liver (normal GSH concentration is >7 mM). Sample preparation is outlined in Appendix I.

Phosphate buffer (0.25 mL, 0.1 mM, pH 7.4) was added to an equal volume of acid supernatant and mixed. This was followed by further addition of phosphate buffer (4.5 mL, 0.1 M, pH 8.0). DTNB (50 μ L, 39.6 mg in 10 mL buffer, pH 7.4) was then added, the tubes vortexed immediately, and allowed to stand at room temperature for 15 minutes. Absorbance was read at 412 nm. TNPSH concentration of each sample was calculated using a GSH standard curve (0-1 mM in a final volume of 0.25 mL SSA), and expressed as μ mol/g wet weight.

b) Fluorometric method

This method was designed to measure low levels of GSH (0-3.75 nmoles) in isolated hepatocytes (Hissen and Hilf, 1976). The underlying principle of the assay is based on the work of Ellman (1959), and measures TNPSH tissue levels as described above, however in this case the assay relies on the conjugation of *o*-Phthaldialdehyde (OPT) with GSH, to yield a highly fluorescent product, thus greatly enhancing the sensitivity of the assay method. It was used for GSH determination in all tissues (and cells, including hepatocytes) other than liver, due to their significantly lower (particularly skeletal muscle) levels of the tripeptide. Solution and sample preparation is outlined in Appendix II.

An aliquot of acid supernatant (75 μ L) was added to phosphate buffer (2.775 mL, 0.1 M, pH 8.0). *o*-Phthaldialdehyde (150 μ L, 1 mg/mL methanol) was then added, the tubes vortexed and allowed to stand at room temperature for 25 minutes. Fluorescence was read at 350 nm excitation, 420 nm emission. GSH content was determined using a standard curve (0-750 ng in a final volume of 75 μ L) and expressed as μ mol/g wet weight.

2.2.5 ATP determination

Tissue ATP levels were measured as an indicator of cytotoxicity and possibly oxidative stress. The assay (originally designed to measure ATP levels of isolated hepatocytes; Stanley and Williams, 1969) is based on the detection of luciferase-linked bioluminescence using firefly lantern extract, in the presence of ATP. Light emission is proportional to the amount of ATP present. Sample preparation is outlined in Appendix III.

Acid supernatant or standard (10 μ L) was added to buffer (2 mL, see Appendix III) and vortexed to ensure uniform mixing. Firefly lantern extract (luciferase, 100 μ L) was added to initiate the reaction, the mixture vortexed for 2-3 seconds before placing it in the cell holder of the air-cooled photomultiplier (-25°C). After a total time lapse of 15 seconds after the start of the reaction, the photon count was initiated. ATP content of the samples was directly calculated using an ATP standard curve (0-40 μ M ATP in 10% TCA) and expressed as nmol/g of tissue or nmol/mg protein.

2.2.6 Immunohistochemical staining for fast myosin

Untreated tissue sections, serial to those cut and stained for conventional H&E histopathology, were thoroughly dewaxed (minimum of 1 hour) and rehydrated. Slides were washed with PBS buffer (pH 7.4) for 7 minutes, placed in a humidity chamber and covered with 2 changes of PBS (5 minutes each). A little distilled water was placed in the chamber to create a humid atmosphere. To block non-specific

binding, sections were incubated with normal goat serum (5%) for 20 minutes. They were then incubated overnight at 4°C in the cold room with an optimal dilution (1:600; determined previously, using a range of dilutions) of the fast myosin antibody, using 5% goat serum as a diluent. For a negative control, the primary antibody was omitted. Next morning the slides were washed with PBS buffer (7 minutes), and incubated (20°C) with appropriately diluted gold-labelled secondary antibody (60 minutes). The sections were washed once with PBS (7 minutes) and once with distilled water (7 minutes). Slides were returned to the humidity chamber, and excess water removed from the sections with a tissue. Silver enhancement reagent (Dako Ltd., Ely, UK) was prepared by mixing equal amounts of solutions A and B in a glass vial. Mixing of the solutions was performed immediately prior to the silver enhancement step, as the mixture is only stable for a limited period. The silver enhancement reagent (200 µL) was pipetted over the sample area of each slide and the process monitored under a microscope. An incubation time of 20 minutes (20°C) gave sufficient enhancement. The slides were washed with 2 changes of distilled water (5 minutes each), counterstained in Mayer's haematoxylin (10-20 seconds) and rinsed with tap water for 5 minutes to 'blue'. Fibres positive for fast myosin stained dark brown to deep black.

2.2.7 Electron microscopy

Samples of liver, and skeletal muscle of the quadriceps, soleus and diaphragm were fixed in 4% formaldehyde/ 1% glutaraldehyde (Appendix IV) and were sent to GlaxoSmithKline for processing. To select suitable areas for electron microscopy, survey sections (1 µm), stained with toluidine blue, were prepared and examined by light microscopy. One suitable specimen was selected for ultramicrotomy from each tissue and the resulting ultrathin sections were stained with uranyl acetate and lead citrate, and examined in a Philips CM10 transmission electron microscope.

2.3 IN VITRO STUDIES

2.3.1 Isolation of hepatocytes

a) Principle

Hepatocytes were isolated essentially as described by Moldeus et al. (1978). The procedure involves perfusion of the liver *in situ* with 2 balanced salt solutions (Appendix V). The first is Ca²⁺ free and also contains the chelating agent EGTA that serves to disrupt the normal calcium-dependant cell-cell interactions. The second solution contains collagenase to dissolve intercellular collagen, allowing the individual hepatocytes to separate from one another.

b) Animals

Male Han Wistar rats (GlaxoSmithKline, 200-250 g) were allowed to acclimatise for at least one week following arrival. Animal husbandry was as previously described.

c) Isolation procedure

Rats were anaesthetised using a solution of hypnorm/hypnovel as previously described, and the abdominal cavity opened by a v-shaped transverse incision. The viscera were displaced to the right to expose the hepatic portal vein. A small incision into the vein was made to allow insertion of the cannula, which was secured by means of a ligature. The cannula clip was then opened and the liver cleared of blood. To facilitate this procedure, the liver was allowed to swell briefly before the hepatic artery and vein were severed.

A good preparation will blanch rapidly and evenly. The flow rate of the perfusate can then be reduced to a slow trickle and the liver dissected free from the surrounding

connective tissue. Perfusion with Hanks I (Appendix V) was continued for a further 5 minutes. The liver was then transferred to a beaker containing collagenase (50 mg) and 100 mL of Hanks II (this contains Ca^{2+} but no albumin) and perfused until soft (10-15 minutes). The liver was cut from the cannula and transferred into K + H/Alb buffer (50 mL, see Appendix V) in a shallow dish. The capsule was broken and the cells dispersed by gentle 'combing' with a plastic fork. The crude hepatocyte suspension was filtered through a polyamide tea strainer into a 100 mL conical flask.

The cells were centrifuged in 2 x 50 mL centrifuge tubes and spun (1 minute, 4°C, 250 rpm), the supernatant was aspirated off and the tubes filled with Krebs-Henseleit (K+ H, no albumin) buffer and rocked gently to wash the cells. These were spun again, re-suspended and washed once more. The final cell pellet was made up to a final known volume and the viability and cell yield estimated using trypan blue.

d) Trypan blue exclusion

The initial viability of the isolated hepatocytes was measured using the inability of damaged cells to exclude the dye, trypan blue (0.4%).

An aliquot (50 μL) of cell suspension was mixed with trypan blue (450 μL) to estimate initial cell density and viability. Cells were counted in an Improved Neubauer haemocytometer. Cell counts were made in the central gridded area on both sides of the cytometer (0.1 mm^3).

$$\text{Density} = \text{viable cells} \times 10^5 \text{ cells mL}^{-1} \text{ of suspension}$$

$$\text{Yield} = \text{Density} \times \text{total suspension volume}$$

At least 2 separate slides were prepared and counted. Only preparations showing greater than 85% viability by this method were used.

e) Culture of hepatocytes

The isolated hepatocytes were cultured in modified Williams' medium E (see Appendix VI). Cells were plated onto collagen-coated 24-well plates at a density of 1×10^5 /well. After 2 hours, the culture medium was renewed (to remove any non-adherent cells damaged by the isolation procedure). The cultures were allowed to recover overnight before treatment the following day.

2.3.2 Preparation of newborn rat muscle cells

a) Collection of material

Skeletal muscle cells (myocytes) were isolated essentially as described by Harper et al. (1987). 6-10 day old rats were decapitated, rinsed in ethanol (70%) and put into a large sterile beaker of HEPES-DMEM (20 mM) on ice.

One at a time, each rat was placed on an ethanol-washed foil-covered board and using sterile instruments the skin and underlying connective tissue was aseptically removed from each hind limb, to reveal the muscle tissue. All muscle from the dorsal hind limbs was carefully dissected free and placed in a petri-dish containing 2-3 mL HEPES-DMEM. Tissue from individual pups was pooled.

b) Tissue digestion

The total muscle tissue was minced aseptically in a sterile culture dish lid in a small volume of HEPES-DMEM. For optimal digestion the tissue was reduced to 1-2 mm cubes where possible. The resulting mince was transferred to a sterile pot containing 12.5 mL dispase (4mg/mL) in DMEM using a wide bore Pasteur pipette. The remaining enzyme solution was kept on ice and a further 12.5 mL was added after 1-hour digestion. The digestion mixture was incubated at 37°C (5% CO₂) and agitated at regular intervals (15 minutes). Trituration every 30-45 minutes helped dissociate the tissue further. Digestion was normally complete within 2-2.5 hours,

depending on the amount of muscle isolated.

To remove remaining debris, the digest was filtered through a coarse nylon mesh (250 μm). The filtrate was then passed through a fine nylon mesh (20 μm). Retained material was washed with 10 mL 10% FCS DMEM (to maximise final yield and to inhibit further collagenase activity), and the final filtrate diluted with an equal volume of 10% FCS DMEM. The cell suspension was spun at 4°C, 1800 rpm for 20-30 minutes to form a pellet. This was re-suspended in 25 mL 10% FCS DMEM, and spun as before. The final pellet was re-suspended in 10 mL of complete Growth medium (Appendix VI), and a small sample was taken aseptically to determine cell number.

Cells were seeded in collagen-coated 100 mm dishes (Greiner Labortechnik Ltd., Stonehouse, UK), 10^7 cells/dish in complete Growth medium (20 mL) and incubated overnight (37°C, 5% CO_2). Next morning the cells were washed with PBS (Mg^{2+} and Ca^{2+} free), trypsinized and seeded onto new 100 mm plates at a density of 10^4 cells/ cm^2 . After 2 days growth a selective plating procedure was performed.

c) Selective plating

This procedure (described by Polinger, 1970) was carried out to ensure that all subsequent cultures were > 80% myogenic.

The cells were trypsinized from each 100 mm dish by rinsing (15-20 seconds) with 6 mL 0.25% trypsin-EDTA then incubating for 5 minutes at 37°C. Plates were checked for adequate detachment of their cell monolayers and the pellets re-suspended in 10% FCS DMEM (10 mL/100 mm plate). The total cell population was split between twice the number of plates (not collagen-coated) required prior to this procedure, and incubated for 20-30 minutes. Plates were carefully removed from the incubator and the medium (which is now predominantly myogenic) swirled gently. The myocyte-enriched medium was removed into a sterile tube and centrifuged for 5 minutes (1000 rpm). The pellet was re-suspended in complete Growth medium, the cells counted, and plated at a density of 10^4 cells/ cm^2 . After 5

days growth the cells were cultured in Differentiation medium (Appendix VI), to encourage the formation of myotubes.

2.3.3 Glutathione reductase

Glutathione reductase [EC 1.6.4.2] activity was measured using the method of Carlberg and Mannervik (1985). The enzyme catalyses the NADPH-dependent reduction of glutathione disulphide (GSSG) to glutathione. The oxidation of NADPH is followed spectrophotometrically at 340 nm.

The reaction mixture (total 300 μ L) containing the enzyme sample (50 μ L), substrate (30 μ L GSSG, 1 mM), phosphate buffer (0.2 M K_3PO_4 , 2 mM EDTA, pH 7.0) and UHQ water (90 μ L) was equilibrated to 30°C prior to the initiation of the reaction by the addition of 2 mM NADPH (30 μ L) (Appendix VII). The decrease in absorbance due to the conversion of NADPH to NADP was monitored at 340 nm for 5 minutes.

A unit of glutathione reductase activity is defined as the amount of enzyme that catalyses the reduction of 1 μ mol of NADPH per minute. Values were expressed as units per milligram of protein.

2.3.4 Glutathione peroxidase

Glutathione peroxidase [EC 1.11.1.9] activity was measured using the method of Flohé and Gûnzler (1984) and involves the continuous measurement of GSSG formation. The GSSG formed during the glutathione peroxidase reaction is instantly, and continuously, reduced by an excess of glutathione reductase activity, thus providing a constant level of GSH. The concomitant oxidation of NADPH is monitored photometrically.

The reaction mixture (total volume 1 mL) containing phosphate buffer (200 μ L, 0.1 M, pH 7.0), enzyme sample (100 μ L), glutathione reductase (100 μ L, 0.24 u), and

GSH (100 μ L, 10 mM) was pre-incubated for 10 minutes at 37°C. The reaction was started by the addition of 100 μ L of pre-warmed hydroperoxide solution (H_2O_2 , 1.5 mM) and NADPH (100 μ L, 1.5 mM) and the decrease in absorption at 340 nm was monitored for 5 minutes. The non-enzymatic rate was assessed, by replacing the enzyme sample with buffer. Catalase activity was blocked by the addition of sodium azide (100 μ L, 1 mM) (Appendix VIII). Values were expressed as μ mol NADPH/min/mg protein.

2.3.5 Glutathione-S-transferase

The glutathione transferases [EC 2.5.1.18] are a group of related enzymes that catalyse the conjugation of glutathione with a variety of hydrophobic compounds bearing an electrophilic centre. Several isoforms exist, however, only total activity was measured. Enzyme activity was determined photometrically at 340 nm by measuring the formation of the conjugate of glutathione (GSH) and 1-chloro, 2,4-dinitrobenzene (CDNB) according to the method of Warholm et al. (1985).

The reaction mixture (total volume 1 mL) containing glutathione (50 μ L, 20 mM), CDNB (50 μ L, 20 mM in 95% ethanol) and phosphate buffer was equilibrated at 30°C before the initiation of the reaction by the addition of enzyme sample (50 μ L) (Appendix IX). The increase in absorbance at 340 nm was monitored for 3 minutes. A correction for the spontaneous rate was made by measuring, and subtracting, the rate in the absence of the enzyme sample. A unit of enzyme activity is defined as the amount of enzyme that catalyses the formation of 1 μ mol of S-2, 4-dinitrophenylglutathione per minute at 30°C using 1 mM concentrations of GSH and CDNB. Specific activity was expressed as units per mg protein.

2.3.6 Superoxide dismutase

Superoxide dismutase [EC 1.15.1.1] activity was measured using the method of Flohé and Ötting (1984). The term superoxide dismutase is used for a variety of

metalloproteins that scavenge superoxide ($O_2^{\bullet-}$). The free radical nature of the substrate requires that it be generated enzymatically or non-enzymatically *in situ* within the test medium, which also contains an easily measurable indicator reacting with $O_2^{\bullet-}$. This method monitors the reduction rate of cytochrome *c* at 550nm, using the xanthine-xanthine oxidase system as a source for $O_2^{\bullet-}$. SOD will compete for any $O_2^{\bullet-}$ generated and decrease the reduction rate of cytochrome *c*.

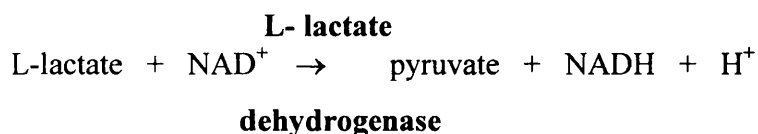
The reaction mixture (total volume 3 mL) containing solution A (2.9 ml) (Appendix X) and sample (50 μ L H_2O , SOD standards or unknowns) was equilibrated at 25°C prior to initiation of the reaction by admixing solution B (50 μ L). The absorbance change was monitored at 550 nm for 1 minute. To distinguish the mangano- or iron-type enzymes from the cupro-zinc type, 2 mM cyanide (10 μ L, 600 mM) was added to the assay medium to inhibit the latter, and the absorbance change was monitored at 550nm for a further minute.

One unit of SOD is defined as the amount of enzyme that inhibits the rate of cytochrome *c* reduction (under the conditions specified) by 50%. To be able to extrapolate accurately to this value of 50%, several dilutions (e.g. 5-8) of a commercial enzyme preparation should be used. Specific activity is expressed as units/mg protein.

2.3.7 Lactate dehydrogenase

The presence of the cytosolic enzyme, lactate dehydrogenase in the culture medium of hepatocytes or myocytes is a marker of irreversible damage to the cell membrane (Appendix XI). The activity of the enzyme in external medium was determined using a method modified from Bergmeyer (1965). During the assay the quantity of enzyme present in the medium (50 μ L) was estimated by measuring the concomitant decrease in the absorbance at 340 nm when NADH was oxidised to NAD^+ .

The procedure relies on the reversible reduction of pyruvate to lactate.



Cell supernatant (50 μL) was added to a cuvette (4.5 mL) containing phosphate buffer (2.71 mL), pyruvate (140 μL , 6.8 mM) and NADH (100 μL , 8.6 mM), the mixture inverted several times and the reaction followed at 340 nm for 1 minute. Values were expressed as $\mu\text{mol NAD}/\text{min}/\text{mg}$ protein.

2.3.8 Creatine kinase

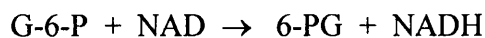
Intracellular levels of creatine kinase (CK) [EC 2.7.3.2] (an enzyme primarily located in skeletal muscle) were measured as a marker of irreversible damage to the plasma membrane of cultured myocytes. Leakage of the enzyme into culture medium could not be used as a reliable indicator of toxic insult, as the extracellular activity of CK declines rapidly (Harauchi and Hirata, 1993).

Intracellular activity of the enzyme was determined using a CK reagent (Sigma Diagnostics) and a procedure based on the method of Szasz et al. (1976). CK catalyses the reaction between creatine phosphate and adenosine diphosphate (ADP), forming creatine and adenosine triphosphate (ATP).



The ATP formed is used to phosphorylate glucose, producing glucose-6-phosphate (G-6-P) in the presence of hexokinase. G-6-P is subsequently oxidised to 6-phosphogluconate (6-PG) and the quantity of CK present in the medium estimated by the increase in absorbance at 340 nm associated with the reduction of NAD to NADH, during this oxidation reaction.

G-6-PDH



CK reagent (1.0 mL) was placed in a cuvette (4.5 mL) and allowed to equilibrate at 30°C. An aliquot of sample (20 µL) was added, mixed by inversion and incubated for 3 minutes. The increase in absorbance read at 340 nm was recorded for 2 minutes and values were expressed as µmol NADH/min/mg protein.

2.3.9 Preparation of rat muscle mitochondria

Skeletal muscle mitochondria were prepared essentially as described by Clark et al., (1997). Rats were sacrificed by cervical dislocation and muscle tissue from the hind limbs (a mixture of quadriceps and gastrocnemius muscles to give a yield of at least 10 g) was placed in high EDTA buffer (Appendix XII) in a pre-weighed beaker and weighed exactly. The muscle was finely chopped (1 mm cubes) with scissors, washed with more buffer, the fine muscle pieces allowed to settle under gravity and the supernatant decanted to remove blood and excess fat. This step was repeated several times until the supernatant was clear. The finely chopped muscle was re-suspended in high EDTA buffer (just enough medium to cover the sedimented tissue), and incubated for 30 minutes at 4°C with trypsin (type III) 0.5 mg/gram wet weight tissue.

The trypsin digestion was stopped by the addition of soybean trypsin inhibitor (3mg/mg trypsin). The digest was then diluted to 50 mL with high EDTA buffer and gently mixed to allow the trypsin and trypsin inhibitor to mix together.

The digested muscle was homogenised (in approximately 30 mL buffer) using an Ystral homogeniser at full speed for 15 seconds, and diluted to 50 mL in high EDTA isolation medium. The homogenate was centrifuged at 1500 g for 5 minutes; the resultant supernatant was decanted through muslin (to remove fat and connective tissue), and centrifuged at 7000 g for 10 minutes. The pellet was re-suspended in low EDTA buffer (Appendix XII) and homogenised in a loose (0.2 mm total clearance)

Potter-type (glass/teflon) homogeniser. The supernatant was made up to 50 mL with isolation medium and centrifuged at 1500 g for 5 minutes to remove any nuclear contamination. The supernatant was finally centrifuged at 7000 g for 10 minutes and the resultant supernatant discarded. The purified mitochondrial pellet was re-suspended in low EDTA isolation medium at approximately 10 mg/mL. The yield of mitochondria with this method was approximately 2-3 mg of mitochondrial protein (as measured using the Lowry method) per gram wet weight muscle.

2.3.10 Preparation of rat heart mitochondria

This was carried out essentially as described for muscle mitochondria, however, omitting the digestion step with trypsin. The yield of mitochondria was approximately 10 mg of mitochondrial protein per gram wet weight tissue.

2.3.11 Preparation of rat liver mitochondria

Rat liver mitochondria were prepared essentially as described by Bates et al. (1995). This method omits the digestion step with trypsin (described above) and the subsequent homogenisation step. Liver is a much softer tissue and requires gentle handling. Therefore once the tissue had been finely chopped it was hand homogenised in a very loose (0.5 mm total clearance) Potter-type (glass/glass) homogeniser and centrifuged as previously described. The yield of mitochondria was approximately 4 mg of mitochondrial protein per gram wet weight liver.

2.3.12 Bio-Rad DC protein assay

Mitochondrial protein content was assessed using the Bio-rad DC Protein Assay kit. The reaction is similar to the Lowry assay (Lowry et. al., 1951) but has been modified to save time. Mitochondria were diluted 1:20 in distilled water and a range of BSA standards were constructed (0.2-1.5 mg/mL in a final volume of 100 μ L) in duplicate.

Reagent A (500 μ L) was added to each tube and the mixture vortexed. Reagent B (4.0 mL) was then added to each tube and vortexed immediately. After 15 minutes the absorbance was measured at 750 nm.

2.3.13 Measuring respiratory control

The functional integrity of the isolated mitochondria was assessed by how tightly respiration was coupled to ATP synthesis. Oxygen uptake in the presence of the substrates glutamate (10 mM) and malate (10 mM) was measured before and after the addition of ADP (25 mM) and the respiratory control ratio (RCR) calculated.

After calibrating the electrode, freshly isolated mitochondria were diluted in the electrode chamber, with respiration medium (Appendix XIII) at 30°C to give 0.1 mg protein in a total of 250 μ L (i.e. 10 μ L of 10mg/mL stock). This was followed by additions of fat free BSA (2.5 μ L), glutamate (2.5 μ L) and malate (2.5 μ L). The collar and electrode were replaced (carefully avoiding air bubbles) and the suspension incubated for 2 minutes (endogenous or state-4 respiration). Using a Hamilton syringe, 3 μ L of ADP were added which stimulates state-3 respiration. This state-3/state-4 cycling was carried out 3 times. The RCR was calculated as the ratio of oxygen consumption in the presence (state-3) and absence (state- 4) of 25 mM ATP.

2.3.14 Measuring ATP synthesis

Assay tubes were set up as shown in Appendix XIV and incubated in a shaking water bath (90 cycles/minute) for 5 minutes at 30°C. Substrate (10 μ L, 1M succinate) was added at 15-second intervals and the incubation continued. The reaction was stopped after 10 minutes by transferring 200 μ L of each assay tube to an Eppendorf tube (1.5 mL) containing 10% TCA solution (200 μ L). The tubes were whirlimixed and centrifuged (14,000 rpm, 4°C) for 5 minutes.

Acid supernatant (100 μ L) was transferred to a test tube containing water (3 mL) and ammonium molybdate (300 μ L), and the mixture vortexed. ANSA reagent (200 μ L) was added and the tubes vortexed again. The absorbance was read at 750 nm after 10 minutes. The P_i content was calculated using a standard curve (0-0.8 mmol P_i) and expressed as nmol ATP/mg protein/min.

2.3.15 Mitochondrial Complex I assay

Mitochondrial Complex I [EC 1.6.99.3] catalyses the oxidation of NADH, electrons are then transferred through Complex I to ubiquinone (CoQ) which is reduced to ubiquinol. Complex I activity was measured as the rotenone sensitive rate of NADH oxidation (at 340 nm and 30°C) using a modification of the method of Ragan et al. (1987). The reaction mixture contained: 25 mM potassium phosphate pH 7.2, 0.2 mM NADH, 10 mM $MgCl_2$, 1 mM KCN, 2.5 mg fat-free BSA and approximately 20 μ g of mitochondrial protein in a final volume of 1 ml. The reaction was initiated by the addition of CoQ_1 (50 μ M final concentration) and read at 340 nm against a blank containing all the components except CoQ_1 . After five minutes, 10 μ L of 0.5 mM rotenone was added to the test cuvettes and the inhibited rate measured for a further 5 minutes.

2.3.16 Mitochondrial Complex II-III assay

Mitochondrial Complex II-III [EC 1.8.3.1] catalyses the dehydrogenation of succinate and the transfer of electrons from Complex II to Complex III and then to cytochrome *c*. Complex II-III activity was measured as the antimycin A-sensitive rate of cytochrome *c* reduction (at 550 nm and 30°C) using succinate as the substrate (King, 1967). The reaction mixture contained: 100 mM potassium phosphate pH 7.4, 0.3 mM potassium EDTA, 1 mM KCN, 100 μ M cytochrome *c* and approximately 20 μ g of mitochondrial protein in a final volume of 1 ml. The reaction was initiated by the addition of 20 μ L of 1.0 M succinate. After the assay had run for 5-7 minutes., 10 μ L of antimycin A

(2mg/mL) was added to the test cuvettes and the inhibited rate measured for a further 5 minutes.

2.3.17 Statistical analysis

All data is expressed as mean \pm SEM, unless otherwise indicated. Dunnett's test for multiple comparisons with a single control was used to determine significance between treatment and control groups.

CHAPTER 3

THE MORPHOLOGICAL AND BIOCHEMICAL EFFECTS OF A SINGLE DOSE OF TMPD *IN VIVO*

3.1 INTRODUCTION

TMPD and other members of the phenylene diamine family are established skeletal muscle toxicants (Munday et al., 1989, 1990; Harauchi and Hirata, 1993; Draper et al., 1994), but the mechanisms involved in this toxicity are still to be fully elucidated. Following on from these earlier studies we have therefore carried out a series of investigations, both *in vivo* and *in vitro*, in an attempt to determine the mechanistic basis of the toxicity of these agents to skeletal muscle in the rat.

Initial preliminary studies (data not shown) helped to evaluate the distribution and morphological effects of TMPD on a range of organ systems when given at varying dose levels in the male and female rat. Doses of TMPD used and the route of administration were based on the report of Munday et al. (1989, 1990) in which animals were given a subcutaneous injection of 30, 50 or 75 $\mu\text{mol kg}^{-1}$ TMPD, divided into two equal doses, 6 hours apart. In the present preliminary studies, toxicity was observed at a dose of 50 $\mu\text{mol kg}^{-1}$, and some animals given 75 $\mu\text{mol kg}^{-1}$ TMPD died prior to necropsy. However, this type of study design was found to pose two major problems. Firstly, the twice-daily dose regime made it difficult to relate the development of a histopathological lesion and the accompanying serum and/or tissue biochemical changes, which occurred, following TMPD treatment, to a particular dose level of the chemical. Secondly, it was difficult to identify the period of time over which these changes had occurred, that is, the time-point of exposure could not be clearly defined. Therefore subsequent experiments

were carried out using a modified experimental design where TMPD was administered in a single subcutaneous injection.

The effect of TMPD, administered at levels of up to 60 $\mu\text{mol kg}^{-1}$ as a single subcutaneous injection, was examined in a range of target organs to identify the sites of any tissue injury. It was found (results not shown) that histological lesions were almost exclusively myotoxic in nature, the only exception being a very specific toxic effect in the testis (at 50 and 60 $\mu\text{mol kg}^{-1}$), in the form of abnormal and degenerate spermatocytes in stage 14 tubules. There was no evidence of any histological changes to other major organs (liver, heart, kidney, lungs, brain, gastrointestinal tract etc). Serum chemistry results closely correlated with these histological findings (Blair, et al., 1997), and showed increases only in those parameters indicative of skeletal muscle (high levels of AST:ALT, LDH₁, CK-MM) and testicular (LDH₂) injury. As the biochemical basis of TMPD-induced myotoxicity was of the greatest importance in the overall objectives of the present project, later studies focused on the comparison of the effects of the compound on target (skeletal muscle) and non-target (liver) tissue.

Liver was chosen as a non-target comparative tissue for a number of reasons: 1), the liver is important as a first-pass organ for xenobiotics, and has a significant role in their detoxification (Kretzschmar and Klinger, 1990) and 2), liver and skeletal muscle contrast in their reported oxidant defence mechanisms (Grankvist et al., 1981), and 3), perhaps most importantly, the lack of any significant toxic effect related to TMPD treatment (Draper et al., 1994).

Munday (1990) hypothesised that the myotoxic nature of TMPD was inherently linked to the ability of the compound to autoxidize, and produce active oxygen species such as H₂O₂. The locus of this reaction was believed to be cytochrome *c* oxidase, a mitochondrial enzyme present in largest amounts in type I skeletal muscle fibres. It

therefore follows that type I muscle fibres should be those most damaged following the administration of TMPD. This proposal was therefore investigated in the present series of experiments by staining skeletal muscle from different sites with an antibody to fast myosin, which would allow the identification of the fibre population targeted by the amine.

The toxicity of a range of TMPD concentrations (with the compound administered as a single dose) was assessed in the first study (Study 1). The objective was to establish the most effective dose level of TMPD to be used in the second study (Study 2), which aimed to investigate the effect of the amine on tissue biochemistry parameters.

3.2 MATERIALS AND METHODS

3.2.1 Animals and compound administration

Male Wistar Hanover rats (GlaxoSmithKline), 250-300 g, were given a range of doses of TMPD by a single subcutaneous injection in the inter-scapular region. The dosing solution was made up immediately before injection in sterile phosphate buffered saline (PBS). The solution was administered at a volume of 4 mL kg⁻¹. The control group was given PBS alone.

During the experiments, animals were housed in individual metabolism cages (Techmate, Milton Keynes UK). Body weights, diet and water consumption were determined at appropriate times before and after TMPD treatment. Clinical signs were also recorded.

3.2.2 Fast myosin histochemistry

Tissue specimens from the diaphragm, soleus muscle, quadriceps muscle and gastrocnemius muscle were fixed in phosphate buffered formalin. Transverse serial sections (4 µm) were cut in a cryostat. Unstained sections were processed for fast myosin immunohistochemistry as described in Section 2.2.6.

3.2.3 Electron microscopy

Samples (1mm cubes) of liver, heart, diaphragm, soleus muscle and quadriceps muscle were fixed in 4% formaldehyde and 1% glutaraldehyde buffer (Appendix IV). Toluidine blue and ultrathin sections were processed and examined as described in Section 2.2.7.

To detect whether lesions resulting from TMPD treatment were related to the muscle fibre type, ultrastructural lesions were scored according to the fibre type in which they occurred. The following classification was used to define fibre type:

Type I: Smaller diameter than type II fibres; high mitochondrial numbers which are arranged interfibrillary in longitudinal rows, and closely packed in the subsarcolemmal region (Fig. 3.1). Mitochondria generally larger than in type II fibres. Sarcotubular system less well developed than in type II fibres. Z-lines thicker than in type II fibres (Fig. 3.1).

Type II: Large diameter; low mitochondrial numbers (Fig. 3.2); mitochondria usually arranged in pairs either side of the Z-line; more highly developed sarcotubular system than in type I fibres; thin Z-lines (Fig. 3.2).

3.2.4 Experimental design

Study 1: Investigation of skeletal muscle lesion development following a single dose of TMPD at 20 to 60 $\mu\text{mol kg}^{-1}$

After acclimatisation in metabolism cages for 2 days, rats were dosed at 0, 20, 30, 40, 50 and 60 $\mu\text{mol kg}^{-1}$ (n=4 per dose group) and sacrificed at 24 hours post dose by exsanguination under hypnorm/hypnovel anaesthesia. Serum was prepared, frozen and subsequently analysed for biochemical parameters. Liver, heart, quadriceps and gastrocnemius muscle, and diaphragm were fixed in phosphate buffered formalin for histological examination. Samples of diaphragm, soleus muscle, quadriceps muscle and gastrocnemius muscle were processed for fast myosin histochemistry.

Tissues taken for histopathology were embedded in paraffin, sectioned (4µm), and stained with haematoxylin and eosin; tissue sections were examined without reference to treatment group. Muscle lesions were scored using an arbitrary scale modified from Munday et al. (1989) as follows:

Table 3.1
Muscle lesion scoring system

0	No abnormality detected
1	Early degenerative changes (rounding up of fibres, disruption of intermyofibrillary network).
2	As 1, plus early necrosis in a few muscle fibres with presence of neutrophil polymorphs.
3	Early degenerative and necrotic changes; 20% of fibres affected.
4	As 3, but with 30% to 40% of fibres affected.
5	As 3, but more than 40% of fibres affected.

Study 2: Investigation in rats treated with TMPD to assess biochemical changes occurring prior to lesion development at 24 hours

Rats (n = 4) were sacrificed at 0, 0.5, 1, 2, 4, 8 and 24 hours after a single subcutaneous dose of TMPD (60 µmol kg⁻¹). Blood was taken as before for serum preparation. Samples of liver, diaphragm, soleus and quadriceps muscle were added to formalin for histological examination. Additional samples of each of these tissues (with the exception of soleus muscle) were rapidly freeze-clamped in liquid nitrogen for an assessment of tissue glutathione and ATP levels (0-8 hour groups only). To assess the ultrastructural changes associated with TMPD toxicity, 3 additional animals received a single subcutaneous injection of either 60 µmol kg⁻¹ TMPD (n = 2), or PBS (n = 1), 8 hours before sacrifice. Results are presented for biochemical changes at 0, 0.5, 1, 2, 4 and 8 hours, light microscopy at all time-points from 0-24 hours, serum biochemical changes at all time-points from 0-24 hours, and electron microscopy at 8 hours.

3.2.5 Statistical analysis

All data is expressed as mean \pm SEM. Dunnett's test for multiple comparisons with a single control was used to determine significance between treatment and control groups.

3.3 RESULTS

3.3.1 Study 1: Investigation of skeletal muscle lesion development following a single dose of TMPD at 20 to 60 $\mu\text{mol kg}^{-1}$

i) Clinical effects following TMPD administration

Animals dosed at 20 $\mu\text{mol kg}^{-1}$ TMPD showed no clinical evidence of toxicity. At levels of 30 $\mu\text{mol kg}^{-1}$ to 60 $\mu\text{mol kg}^{-1}$ TMPD, rats showed significant weight loss 24 hours post dosing (Fig. 3.3). At 40, 50 and 60 $\mu\text{mol kg}^{-1}$ TMPD, during the period 0-24 hours post dosing there was also decreased diet (Fig. 3.4) and water (Fig. 3.5) consumption. Animals that received 60 $\mu\text{mol kg}^{-1}$ developed oedema, weakness in their hind limbs and an abnormal gait 8 hours post treatment. However, at 24 hours post dosing a normal gait had returned in all affected animals.

ii) Serum biochemistry

Animals treated with 50 and 60 $\mu\text{mol kg}^{-1}$ TMPD had significantly lower mean serum ALP levels than the controls (Table 3.2). Levels of AST were raised at 50 and 60 $\mu\text{mol kg}^{-1}$, and ALT was increased at 60 $\mu\text{mol kg}^{-1}$. The AST:ALT ratio was very high at these dose levels, about 8:1; the control ratio was about 2.5:1. In the highest 2 dose levels there were significantly increased isoenzymes LDH₁ and LDH₂. Serum CK-MM was significantly raised after dosing with 60 $\mu\text{mol kg}^{-1}$. However, the other 2 CK isoforms, cardiac muscle (CK-MB) and brain (CK-BB), were also increased following doses of 40 and 60 $\mu\text{mol kg}^{-1}$ TMPD, respectively.

iii) Light microscopy

Quadriceps muscle and the diaphragm showed a general dose-related change in the severity of the lesion morphology (Table 3.1 and Table 3.3). At all dose levels except the 20 $\mu\text{mol kg}^{-1}$ group, pathological changes in the diaphragm were more severe than those of the quadriceps. Pathological changes characteristic of TMPD treatment are illustrated in Fig. 3.6a and 3.6b. Mild lesions (scores of 1 to 3) consisted of a few rounded and

swollen fibres that were more intensely stained, together with a small number of phagocytic cells (mainly neutrophil polymorphs) moving into the damaged areas. Moderate to severe lesions (scores of 4 to 5) consisted of ragged, disorganised and degenerating fibres with up to 40% of the fibres damaged. Tissue between the fibres was swollen and oedematous, and contained large numbers of neutrophil polymorphs.

Light microscopy did not reveal any abnormalities in the livers of control or TMPD-treated animals at any dose level. However, increased cytoplasmic basophilia, related to decreased glycogen storage, in the livers of the 30, 40, 50 and 60 $\mu\text{mol kg}^{-1}$ groups, was observed. With the exception of a single rat given 60 $\mu\text{mol kg}^{-1}$ of TMPD, which showed evidence of slight focal myocarditis, with myocardial necrosis and a small amount of oedema at the apex, no heart lesions were observed.

iv) *Fast myosin histochemistry*

In the muscle specimens of the control groups, no pathological changes could be observed and fibre typing was always possible with good identification of type I, type IIA, and type IIB fibres (Fig. 1.8).

The histopathological changes observed in the various muscles taken at necropsy (diaphragm, soleus, quadriceps, and gastrocnemius) were identical, but varied quite markedly in severity. In general, the most severely affected muscle specimens were (in decreasing order of severity): diaphragm (most severely affected), gastrocnemius, quadriceps and soleus. The extent of the inflammatory response seen in the 'red' parts of the gastrocnemius and quadriceps muscles was similar to that in the diaphragm, and these 'red' parts were more affected than the 'white' parts of the same muscles. In certain cases (particularly in the diaphragm) the area of muscle under examination was very damaged and this sometimes gave rise to false positive staining. Therefore, to obtain a more accurate picture of the fibre type(s) involved in TMPD toxicity, only those fields where the fibres were still largely intact were examined.

Comparison of the fast myosin staining pattern with serial haematoxylin and eosin-stained sections of each of the muscles, except the soleus, appeared to indicate that type IIA (or IIX) fibres were especially vulnerable to the effects of TMPD. These fibres showed more marked degenerative changes than either type I or type IIB fibres, in less severe areas of damage (Fig. 3.9a, 3.9b). Interestingly, none of the type IIA fibres, and only a very small number of the type I fibres, of the soleus muscle were damaged.

In summary, fast myosin staining demonstrated that all fibre types (with the exception of fibres in the soleus muscle) from the TMPD-treated animals were affected to some degree, i.e. TMPD was not selectively toxic to a specific fibre type. Furthermore, the greater the degree of the inflammatory response in the muscle tissue, the more generalised the effect of TMPD on the various fibre types became.

3.3.2 Study 2: Investigation in rats treated with TMPD to assess biochemical changes occurring prior to lesion development at 24 hours

i) Serum biochemistry

A single dose of TMPD ($60 \mu\text{mol kg}^{-1}$) significantly elevated the transaminase enzyme AST at 24 hours (Table 3.4); however, unlike Study I, this increase was not accompanied by a rise in serum ALT (data not shown). Total LDH, LDH₅ and serum CK levels were also significantly raised at 8 hours post dosing. This is in agreement with the early necrotic changes seen in the skeletal muscle samples taken at this time point. Although TMPD clearly caused myotoxicity, variation in the results from animals at all time points (except controls) meant that the increased levels of the muscle specific isoform CK-MM were not statistically significantly different from control values at any time point. Serum CK-MB was however, significantly elevated at 4 and 24 hours, and serum CK-BB was significantly raised at 4 hours. Nevertheless, as in the previous study, neither the CK-MB isoform nor the CK-BB isoform increased proportionally as much as CK-MM, which at the 4 hour time point was almost 170 times higher than control values, compared to increases of 12 (CK-MB) and 4 (CK-BB) times for the other two isoforms, at 4 hours post dose.

ii) *Light microscopy*

No pathological changes were evident in any of the tissue samples taken, with the exception of tissues at the 8 and 24 hours post dose groups. The muscle specimens of the 8-hour group showed early signs of necrosis, as described above. Pathological changes in the muscle samples of the 24-hour group were very similar to those reported in Study 1.

iii) *Electron microscopy*

Examination of skeletal muscle (diaphragm, soleus, and quadriceps) under the electron microscope revealed two types of morphological change responsible for the lesions seen at the light microscope level. The first change involved the mitochondria, and the second involved the sarcotubular system. In mild muscle lesions, the mitochondria showed reduced matrix density and reduced numbers of cristae (Fig. 3.7a). In more severe cases the mitochondria were markedly swollen, and, apart from sparse amounts of flocculent material, had a clear matrix giving them a vacuolar appearance (Fig. 3.7b). However, the mitochondrial lesion was not universal within a given fibre; only a small percentage within a field of view (magnification x13, 000) were affected, and many normal mitochondria were also present (Fig. 3.7a).

The lesion involving the sarcotubular system was such that it was not possible to distinguish whether the pronounced vacuoles evident were derived purely from the vacuolation of the sarcoplasmic reticulum, or the T tubule system, or both. These vacuoles consisted of a single membrane with clear contents (Fig. 3.8a). Very large vacuoles were also seen containing membranous material, thought to be the remnants of adjacent reticular or tubular membranes, which had fused to yield the larger vacuole (Fig. 3.8b). Muscle fibres from control animals showed only a small amount of sarcotubular dilation and mitochondrial change.

The simple classification of the muscle fibres by TEM into type I and type II subtypes showed that the mitochondrial changes were particularly pronounced in the type I fibres and that the swelling of the sarcotubular system was more evident in the type II fibres (Table 3.5). However, both types of morphological change sometimes occurred in the

same fibre, and also in both type I and type II fibres. The absence of a significant mitochondrial and sarcotubular change in the control samples from all three different muscle tissues (diaphragm, soleus and quadriceps), suggests that both these changes were related to TMPD treatment.

iv) Tissue glutathione

TMPD ($60 \mu\text{mol kg}^{-1}$) was administered to groups of rats ($n=4$ per group) that were sacrificed 0-8 hours post dosing. Samples of liver, diaphragm, and quadriceps muscle were rapidly removed and freeze-clamped into liquid nitrogen, and subsequently assayed for glutathione content.

TMPD treatment resulted in a reduction of liver glutathione (GSH) at 0.5 hours post dose (Fig. 3.10a). Despite the significance of the drop in liver GSH at 0.5 hours post dosing, the effect was quickly abolished by a recovery, and what appears to be a rebound synthesis of the peptide. As a result, liver GSH levels were not significantly different from control values as soon as 1 hour post dose. Diaphragm glutathione, was only significantly reduced at 4 hours after dosing with TMPD, however the data suggest that TMPD treatment has a more pronounced effect on the reduction of diaphragm GSH levels than that seen in liver; however diaphragm GSH levels returned to control values at 8 hours. Quadriceps GSH levels are not significantly affected by TMPD treatment (Fig. 3.10c), although this may be due to animal variation, as mean values at 1 and 2 hours post dose do show a moderate depletion of the tripeptide.

v) Tissue ATP

In TMPD-treated rats, liver ATP was significantly depleted compared with control levels at 0.5, 4, and 8 hours (Fig. 3.11a). Diaphragm levels of ATP were also significantly reduced, at 2 and 4 hours (Fig. 3.11b) after dosing with TMPD. Quadriceps ATP levels, however, were not significantly affected (Fig. 3.11c) at any time following TMPD administration.

3.4 DISCUSSION

Clinical signs of toxicity were evident in rats treated with levels as low as 30 $\mu\text{mol TMPD kg}^{-1}$; animals in this treatment group and above had significantly reduced food and water intakes, and reduced body weights compared to controls. In addition, the administration of a single dose of TMPD at levels from 20 to 60 $\mu\text{mol kg}^{-1}$ produced significant histological and biochemical evidence of skeletal muscle damage, particularly at dose levels of 50 and 60 $\mu\text{mol kg}^{-1}$.

The serum AST:ALT ratio (approximately 8:1) in rats treated with TMPD at 60 $\mu\text{mol kg}^{-1}$ (Table 3.2) is indicative of skeletal muscle damage. However, these enzymes are not exclusive to skeletal muscle, and are also found at high levels in the liver. Nevertheless, liver injury would normally result in an AST:ALT ratio much closer to unity (1:1 to 1:2). The much higher serum levels of the skeletal muscle-specific isoform of creatine kinase, CK-MM (Table 3.2) in rats treated with TMPD at 40-60 $\mu\text{mol kg}^{-1}$ tends to confirm the specific toxicity of TMPD towards muscle. These data are in accordance with those of Munday et al. (1990) and Draper et al. (1994). Decreased food consumption in rats has been linked to a reduction in serum ALP levels (York, personal communication). This would be a likely explanation for the significant reduction of serum ALP in Study 1 in rats treated with TMPD at 50 and 60 $\mu\text{mol kg}^{-1}$, in the light of the diet consumption data for these groups (Fig. 3.4).

Histopathological lesions resulting from TMPD treatment were always more severe in diaphragm > quadriceps > soleus muscle (Table 3.3, 3.5). These findings have not been previously reported and indeed somewhat contradict the hypothesis of TMPD toxicity put forward by Munday (1992). They proposed that the toxic nature of TMPD is associated with the ability of the compound to autoxidise, and that this reaction is catalysed *in vivo* by cytochrome-*c* oxidase. The greatest activity of cytochrome-*c* oxidase is found in type

I fibres such as occur in the soleus muscle, and therefore this muscle should be particularly vulnerable. However, when comparing the lesion scores presented in Table 3.3 and those of a preliminary study (data not shown), the soleus muscle appears to be least affected by TMPD treatment within the dose range used (20-60 $\mu\text{mol kg}^{-1}$).

The specificity of TMPD for particular muscle fibre types when examined at the ultrastructural level gave less than clear results (Table 3.5). This may be related to the small number of samples taken for analysis. The simple ultrastructural classification system used to discriminate between type I and type II fibres may have made any lesions of mitochondrial or sarcotubular origin appear more pronounced in type I and type II fibres, respectively.

To make a more accurate statement regarding the selectivity of TMPD to particular muscle fibre types, H&E sections were compared with serial sections stained with an antibody to fast myosin in all 4 muscles (diaphragm, gastrocnemius, quadriceps, and soleus). Using this method of analysis, it was found that those areas of muscle which were very damaged as a result of TMPD treatment often gave rise to false positive antibody staining. It is considered that this may be due to damage of surface antigens on the sarcolemma. Thus only those fields which consisted of predominantly intact muscle fibres were analysed. In these less damaged areas, and where fibre typing was always possible, the intermediate type IIA or IIX fibres showed greater degeneration than the other fibre types (type I, type IIB). The normal rat diaphragm has a truly mixed fibre-type population (Kanbara et al., 1997) but the other muscles (gastrocnemius, quadriceps) have regions which are historically referred to as 'red' (with a predominantly mixed fibre population, like the diaphragm) or 'white' (almost exclusively composed of type IIB fibres). The normal rat soleus however contrasts with the gastrocnemius and quadriceps muscles in that it is composed almost exclusively of type I fibres. In the present study the 'red' parts of both the gastrocnemius and the quadriceps muscles appeared to be more damaged by TMPD than the 'white' parts. The small number of fibres of the soleus

muscle that were damaged, were type I fibres.

Considering the results of the conventional light microscopy, immunohistochemistry and electron microscopy as a whole, the above findings appear somewhat conflicting. There are several possibilities for this. Firstly, the soleus muscle is a small discrete muscle consisting predominantly of a single fibre type, type I. The larger quadriceps and gastrocnemius muscles are much less uniform in their fibre type and their superficial portions are 'whiter' than their deeper layers. Therefore, this may account for the second possible explanation for the conflicting findings, in that depending on the tissue areas taken for light and electron microscopy, comparison between different tissue samples may not be valid, as the fibre composition may vary between different samples. However, the comparison of serially cut sections prepared for H&E and immunohistochemistry, allows a direct comparison. A third explanation may be that the number of tissue samples taken for electron microscopy were very small. Also, the ultrastructural classification of fibre types used is simpler than the classification system using immunohistochemistry techniques.

A final explanation for the conflicting results may be that the highly oxidative soleus muscle is reported to have greater antioxidant enzyme activity compared with muscle, such as the quadriceps, which has a much lower oxidative capacity (Laughlin et al., 1990; Powers et al., 1994). This may explain why the soleus muscle was consistently less affected by TMPD than the other skeletal muscle samples (all of lower oxidative activity) taken in Study 1. However, if muscle fibre type antioxidant capacity does play a large role in TMPD-induced toxicity, the order of muscle susceptibility to injury would be; quadriceps (most susceptible), gastrocnemius, diaphragm, and soleus muscle.

Thus, although it would at first appear that the results of the present studies conflict with the hypothesis of Munday and his co-workers (1992) regarding the toxic mechanism of

TMPD-induced muscle injury, the overall conclusions do fit in with the proposed mode of action of Munday (1992). The present findings show that those fibres with oxidative capacity i.e. types I, IIA and IIX do appear to be more susceptible to the effects of TMPD treatment than those fibres with a predominantly glycolytic activity i.e. type IIB. The reason for the very modest effect of TMPD on soleus muscle is, however, unclear.

The serum chemistry pattern of enzyme leakage in Study 2 (Table 3.4) is similar to that of Study 1, although not all the changes in the parameters in TMPD-dosed rats were statistically significant compared to controls. For example the increase in CK-MM with time, and AST. However, CK-MM levels were higher than control levels of the enzyme as early as 0.5 hours post dose, demonstrating a rapid toxic response to TMPD treatment at 60 $\mu\text{mol kg}^{-1}$. This early effect is further supported by raised levels of total LDH, at 0.5, 1 and 2 hours post dosing, which predominantly consisted of the muscle-specific isoform, LDH₅, and these increases reached significance at 8 hours. This 8-hour time-point was where early degenerative changes to the muscle fibres were seen.

In Study 2 liver GSH levels were significantly reduced 0.5 hours after dosing with TMPD (Fig. 3.10a). This effect may have been treatment related, or possibly a response to the stress of the injection because the level of GSH in the control animals also decreased slightly at this time. Normal levels of liver GSH (6-8mM) were rapidly regained, probably due to an increase in the synthesis of the tripeptide. The $t_{1/2}$ of the hepatic cytosolic GSH pool is approximately 2 hours (Meredith and Reed, 1982), and the pattern of the GSH content of the liver (Fig. 3.10a) post TMPD treatment, appears to correlate well with this reported time-frame. The pattern of GSH depletion from the diaphragm (Fig. 3.10b) is more consistent, and suggestive of oxidative stress within the tissue. Although the depletion is significantly different to control animals after 4 hours, both groups (TMPD-treated and control) show a large increase in cytosolic GSH, 8 hours post dose. This is surprising considering the much smaller cytosolic pool of the tripeptide within skeletal muscle, and the reportedly slow turnover rate of GSH in skeletal muscle

(116 hours; Potter and Tran, 1993). Quadriceps muscle does appear to have reduced levels of GSH at 1-2 hours post-dose (Fig. 3.10c), however, due to variation of the individual sample values, these decreases were not significantly different to the controls. Nor was the depletion as marked or as prolonged, as in the diaphragm. This may have been due to a number of reasons. Firstly, as previously discussed, the muscle lesion score data and the analysis of the fast myosin antibody-stained sections revealed a possible metabolic preference for a greater toxic effect in the diaphragm. Thus, oxidative fibres appear to be more susceptible than glycolytic fibres. Diaphragm (as a consequence of its own environment and function) contains many more oxidative fibres than quadriceps muscle (Baldwin and Tipton, 1972; Kanbara et al. 1997). Second, all muscle tissues show variation in their fibre-type uniformity depending on the region and depth of the muscle sampled. For example, histochemical studies of gastrocnemius muscle (Baldwin and Tipton, 1972) show marked variation in proportions of red, intermediate and white fibre content. The superficial layers of the gastrocnemius muscle are 100% white, the deepest layers 30% white, and 70% red. Quadriceps muscle has been reported to be 50 % 'white' (Baldwin and Tipton, 1972), although presumably this muscle also shows fibre-type variation, depending on the depth at which the tissue is sampled. Diaphragm muscle is a much thinner muscle than the quadriceps and therefore it is reasonable to expect the fibre pattern to be more uniform. Therefore, although at post-mortem examination in the present studies care was taken to ensure that similar sections of the muscle tissue, of each rat was sampled, the orientation and depth at which the sample was sectioned, as well as the thickness of the muscle tissue cut from the animal, would all probably influence both the biochemical character, and the fibre-type pattern of toxicity, of individual specimens.

TMPD treatment caused significant depletion of liver and diaphragm ATP (Fig. 3.11a and 3.11b) but not of quadriceps ATP (Fig. 3.11c). However, differences in the metabolic activity of the liver and the diaphragm suggest that the underlying mechanism for the depletion of these two tissues was not the same. Two of the most common causes of ATP depletion from the cell are interference with mitochondrial oxidative phosphorylation (either by uncoupling this process from electron transport, or via

inhibition of the electron transport chain itself), or depletion of NADH (Timbrell, 1992). Using electron microscopy, TMPD treatment was found to cause grossly swollen mitochondria, which would undoubtedly have caused loss of function of the affected organelles, in the damaged muscle fibres. Thus, depletion of ATP in the diaphragm was probably a result of irreversible damage to a large number of mitochondria in this tissue. No such ultrastructural changes to hepatic mitochondria were seen. ATP depletion would probably have been caused by the concomitant depletion of the cofactors NADH and NADPH, which play an important role in the maintenance of the reduced GSH levels of the cell. Hepatic levels of ATP remained depressed in TMPD-treated rats for at least 8 hours (Fig. 3.11a), suggesting that several rounds of oxidation/reduction of the redox cyclus took place before the chemical was successfully detoxified.

Table 3.2

Study 1; Serum biochemistry parameters in rats given a single dose of TMPD and sampled at 24 hours

Dose of TMPD ($\mu\text{mol kg}^{-1}$)	ALP (i.u.L^{-1})	AST (i.u.L^{-1})	ALT (i.u.L^{-1})	LDH ₁ (i.u.L^{-1})	LDH ₂ (i.u.L^{-1})	CK-MM (i.u.L^{-1})	CK-MB (i.u.L^{-1})	CK-BB (i.u.L^{-1})
0	453.2 (35.3)	65.4 (1.3)	26.2 (0.8)	11.5 (0.9)	3.5 (0.6)	35.2 (1.5)	41.8 (2.5)	211.5 (4.8)
20	427.0 (38.7)	109.5 (54.1)	32.3 (3.9)	14.8 (2.4)	6.0 (0.3)	34.7 (5.8)	36.0 (27.4)	212.8 (1.4)
30	465.0 (54.1)	209.4 (87.1)	43.4 (12.5)	26.0 (10.6)	17.0 (10.6)	52.8 (21.8)	39.3 (5.8)	172.5(21.8)
40	306.8 (44.2)	1212.0 (557.8)	106.2 (33.6)	95.5 (33.6)	126.0 (58.3)	538.8 (188.2)	101.0 (11.5)*	313.0 (24.5)
50	260.3 (19.2)*	1661.7 (420.5)*	157.7 (33.6)	224.7 (115.5)*	272.0 (144.5)*	510.7 (343.2)	54.3 (18.0)	298.0 (27.7)
60	280.8 (19.2)*	4601.0 (626.6)*	579.5 (144.5)*	270.8 (32.0)*	343.0 (58.3)*	1364.3 (682.3)*	90.5 (13.2)	378.0 (38.5)*

Values are means (SEM); n = 4. Results were statistically analysed using Dunnett's test for multiple comparisons using a single control, with the level of significance set at * $p < 0.05$. ALP (alkaline phosphatase); AST (aspartate aminotransferase); ALT (alanine aminotransferase); LDH_{1,2} (lactate dehydrogenase isoenzymes 1 and 2); CK-MM (creatine kinase muscle isoenzyme); CK-MB (creatine kinase heart isoenzyme); CK-BB (creatine kinase brain isoenzyme).

Table 3.3

Study 1; Muscle lesion scores of rats given a single dose of TMPD (20 to 60 $\mu\text{mol kg}^{-1}$) and sampled at 24 hours^a

Treatment ($\mu\text{mol kg}^{-1}$ TMPD)	0	20	30	40	50	60
Quadriceps	0.00	1.00	1.30	2.00	4.00	3.95
Diaphragm	0.00	0.65	2.25	4.00	4.75	4.50

^a Values are the mean of 4 rats

Table 3.4Study 2; Serum biochemistry parameters in rats given a single dose of TMPD (60 $\mu\text{mol kg}^{-1}$) and sampled at 0-24 hours

Time after injection (hours)	AST (iu.L ⁻¹)	LDH (iu.L ⁻¹)	LDH ₅ (iu.L ⁻¹)	CK (iu.L ⁻¹)	CK-MM (iu.L ⁻¹)	CK-MB (iu.L ⁻¹)	CK-BB (iu.L ⁻¹)
0	67.9 (10.5)	235.8 (34.2)	199.8 (268.1)	135.8 (17.6)	24.5 (10.8)	20.5 (8.6)	90.3 (15.4)
0.5	79.9 (136.0)	732.5 (67.3)	622.5 (67.6)	430.3 (37.9)	236.8 (38.2)	50.3 (47.1)	143.5 (17.0)
1.0	84.5 (21.4)	443.0 (54.8)	769.5 (185.1)	451.3 (60.4)	337.3 (52.4)	47.3 (19.2)	144.8 (25.3)
2.0	109.3 (14.3)	871.3 (82.4)	769.5 (86.2)	637.8 (59.4)	367.8 (47.4)	78.5 (25.2)	186.5 (25.4)
4.0	426.8 (93.8)	1163.3 (33.0)	768.3 (68.4)	4574.3 (353.4)	4057.3 (343.8)	235.3 (58.7)*	336.3 (37.8)*
8.0	502.0 (70.1)	3000.3 (184.6)*	1857.0 (157.3)*	799.8 (123.1)*	1274.0 (107.5)	48.7 (22.0)	186.0 (22.5)
24.0	2472.6 (130.4)*	1424.3 (62.4)	808.0 (74.5)	2036.5 (108.5)	1756.5 (114.6)	277.8 (27.6)*	224.0 (28.7)

Values are means (SEM); n = 4. Statistically analysed using Dunnett's test for multiple comparisons using a single control, with the level of significance set at * $p < 0.05$. AST (aspartate aminotransferase); LDH (total lactate dehydrogenase activity); LDH₅ (lactate dehydrogenase isoenzyme 5); CK (total creatine kinase activity); CK-MM (creatin kinase muscle isoenzyme); CK-MB (creatin kinase heart isoenzyme); CK-BB (creatin kinase brain isoenzyme).

Table 3.5

Study 2; Mitochondrial and sarcotubular changes in relation to fibre type at the ultrastructural level

Muscle type	Fibre type	Mitochondrial change	Sarcotubular change
Soleus	Type II	-	+
	Type I	+	-
Quadriceps	Type II	-	+
	Type I	+	-
Diaphragm	Type II	+	++
	Type I	+	+

- : No change, + : moderate lesion, ++: severe lesion

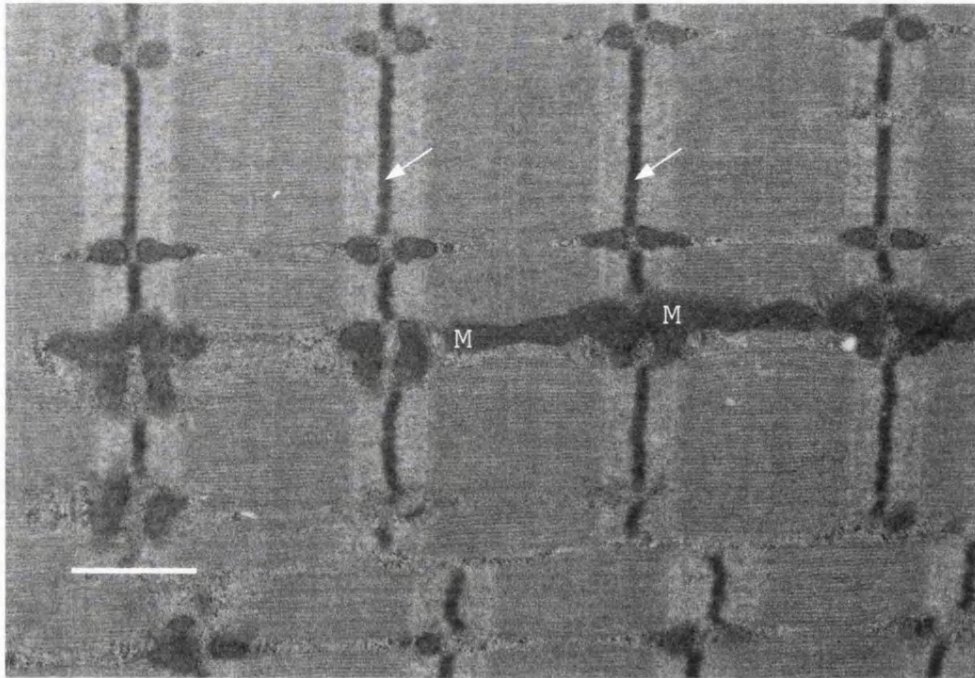


Figure 3.1. Electron micrograph of soleus (type I) muscle from a control rat showing many large mitochondria (M) and thick Z-lines (arrows). Bar = 1 μ m.

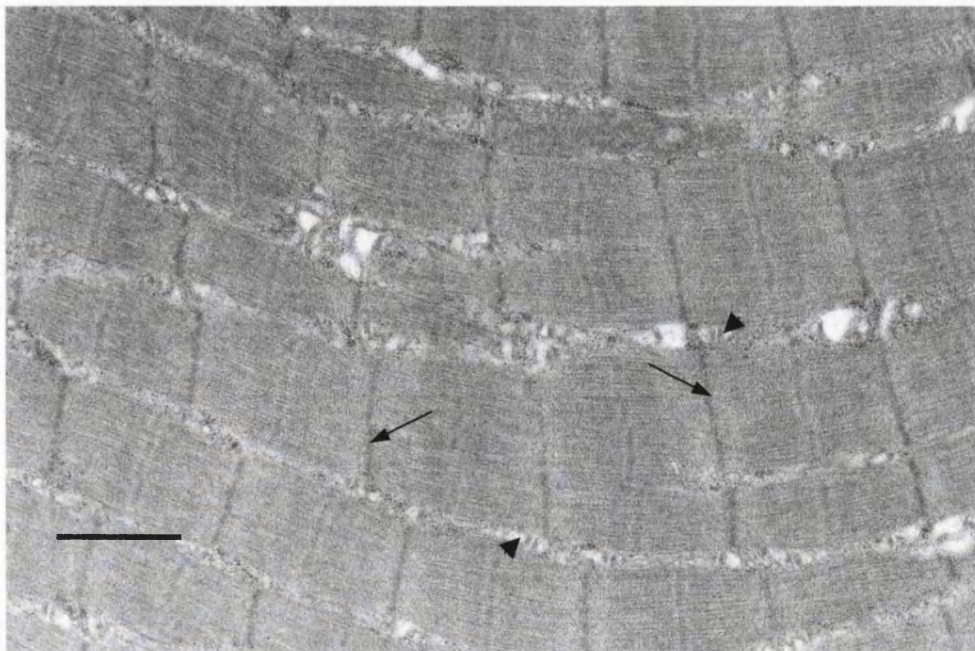


Figure 3.2. Electron micrograph of quadriceps (type II) muscle from a control rat showing a well-developed sarcotubular system (arrowheads) and thin Z-lines (arrows). Bar = 1 μ m.

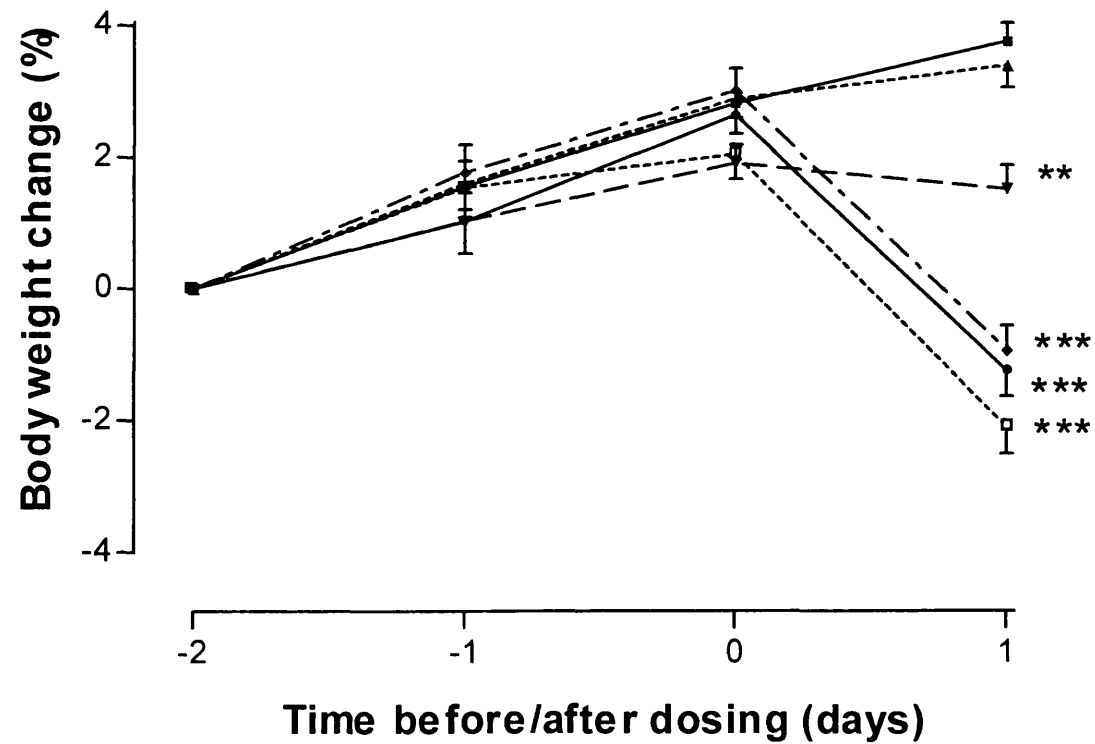


Figure 3.3. Effect of TMPD on body weight. Male rats were dosed with phosphate buffered saline (control) (■), 20 μM (▲), 30 μM (▼), 40 μM (◆), 50 μM (●), or 60 μM (□). Results are expressed as the mean ± SEM of 4 animals. ** ($P < 0.05$), or *** ($P < 0.01$), versus control group.

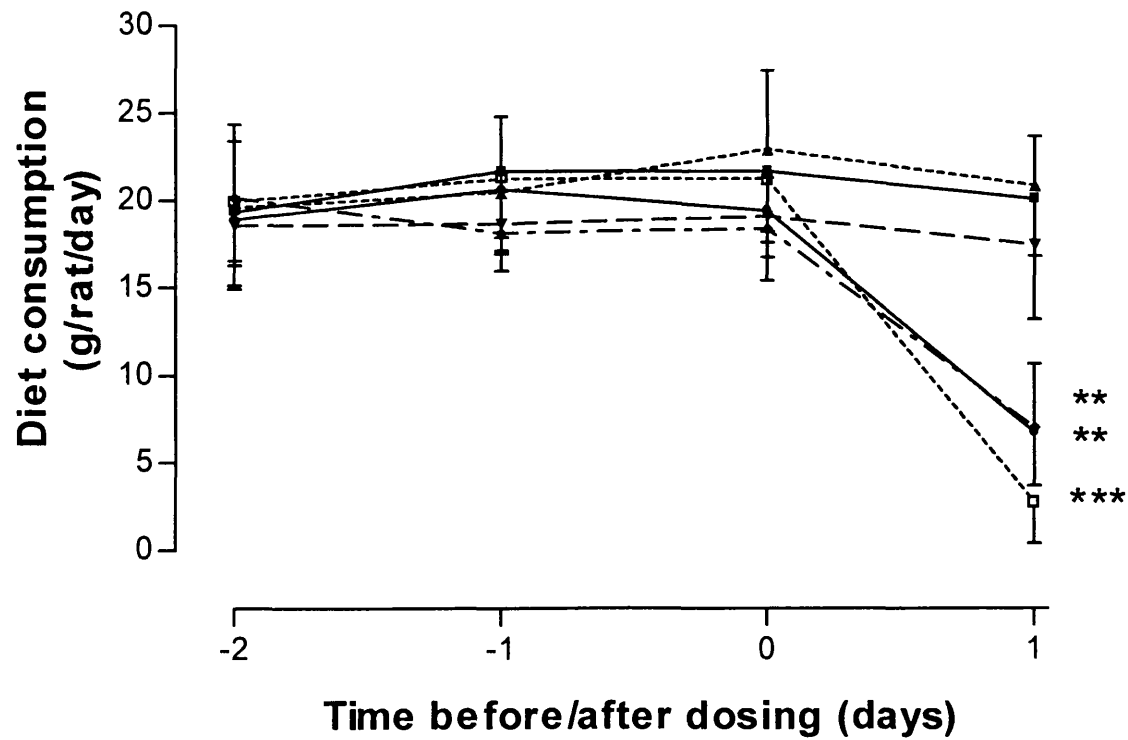


Figure 3.4. Effect of TMPD on diet consumption. Male rats were dosed with phosphate buffered saline (control) (■), 20 μM (▲), 30 μM (▼), 40 μM (◆), 50 μM (●), or 60 μM (□). Results are expressed as the mean ± SEM of 4 animals. ** ($P < 0.05$), or *** ($P < 0.01$), versus control group.

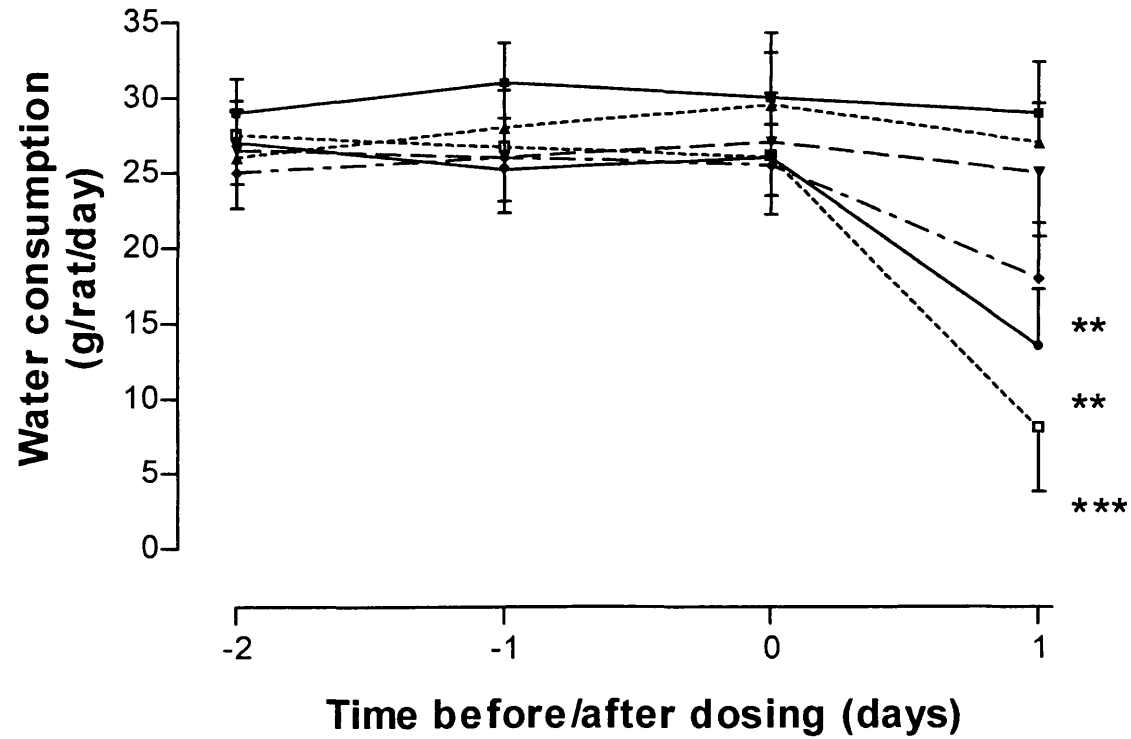


Figure 3.5. Effect of TMPD on water consumption. Male rats were dosed with phosphate buffered saline (control) (■), 20 μM (▲), 30 μM (▼), 40 μM (◆), 50 μM (●), or 60 μM (□). Results are expressed as the mean ± SEM of 4 animals. ** ($P < 0.05$), or *** ($P < 0.01$), versus control group.

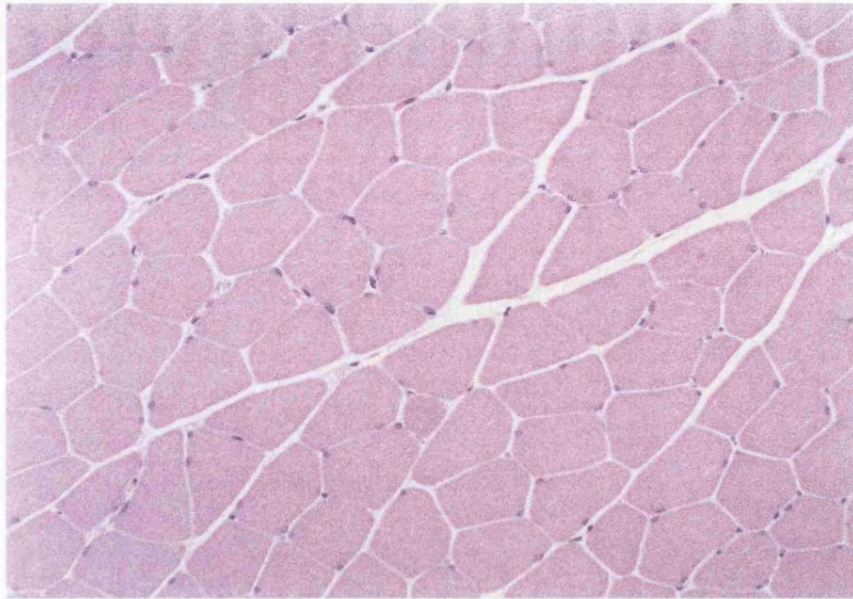


Figure 3.6. (a) Transverse section of normal gastrocnemius muscle showing a regular polygonal myofibre arrangement. H&E x 400.

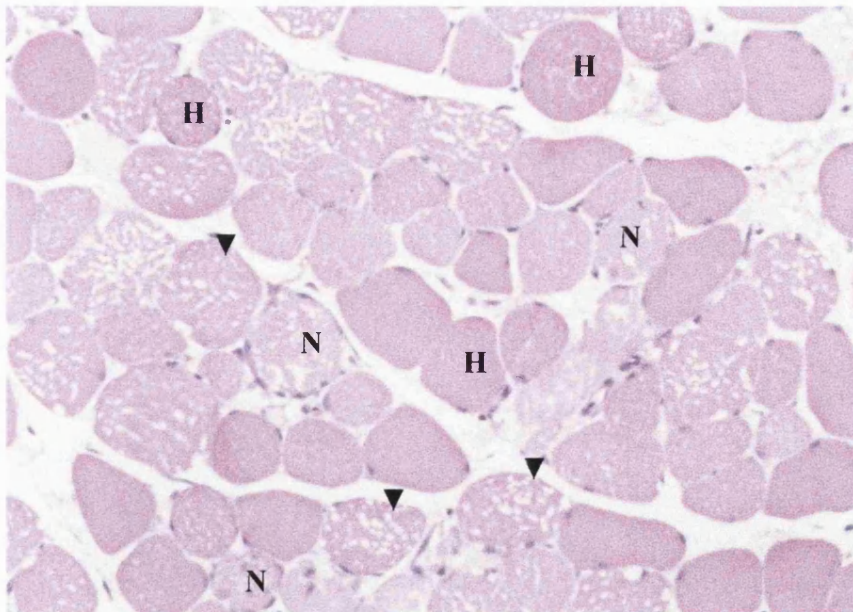


Figure 3.6. (b) Transverse section of gastrocnemius muscle taken 24 hours after dosing with TMPD ($60\mu\text{mol kg}^{-1}$). The muscle shows a moderate degree of necrosis (lesion score = 4), with rounded, hyaline fibres (H), necrotic fibres (N), and microvesicular fibres (arrowheads). H&E x 400.

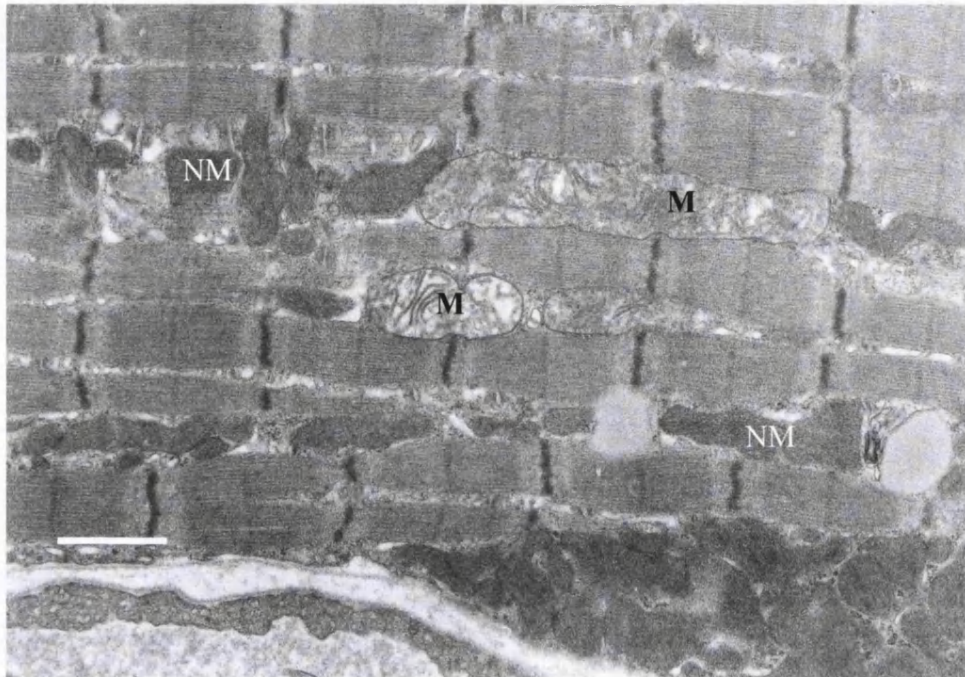


Figure 3.7. (a) Electron micrograph of soleus muscle taken 8 hours after dosing with TMPD ($60 \mu\text{mol kg}^{-1}$) showing slightly swollen mitochondria (M) with a reduced matrix density and reduced numbers of cristae. Many normal mitochondria (NM) are also present within the same myofibre. Bar = $1 \mu\text{m}$.



Figure 3.7. (b) Electron micrograph of soleus muscle taken 8 hours after dosing with TMPD ($60 \mu\text{mol kg}^{-1}$) showing markedly swollen mitochondria (arrows). Bar = $1 \mu\text{m}$.

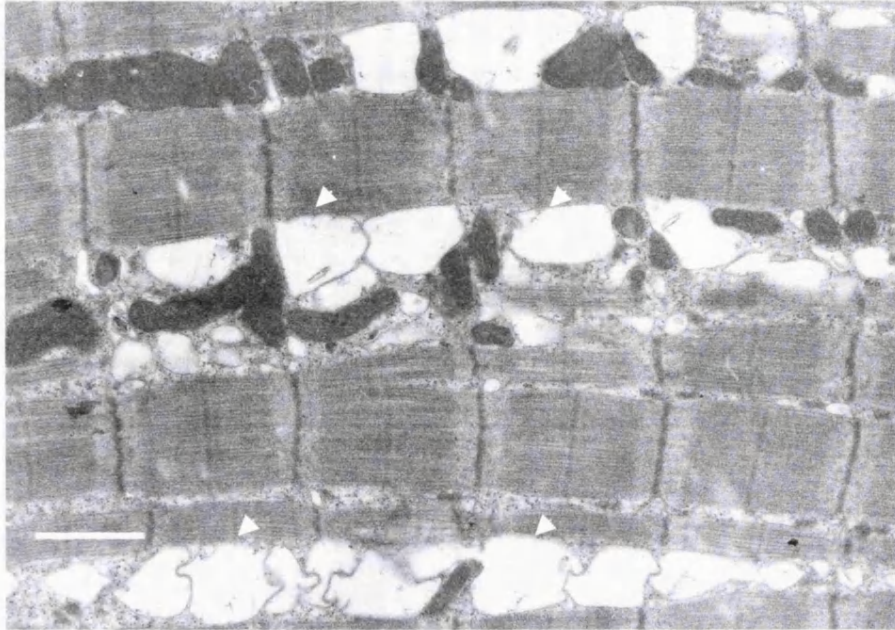


Figure 3.8a. Electron micrograph of diaphragm muscle taken 8 hours after dosing with TMPD ($60 \mu\text{mol kg}^{-1}$). Marked dilatation of the sarcotubular system is evident (arrowheads). Bar = $1 \mu\text{m}$.

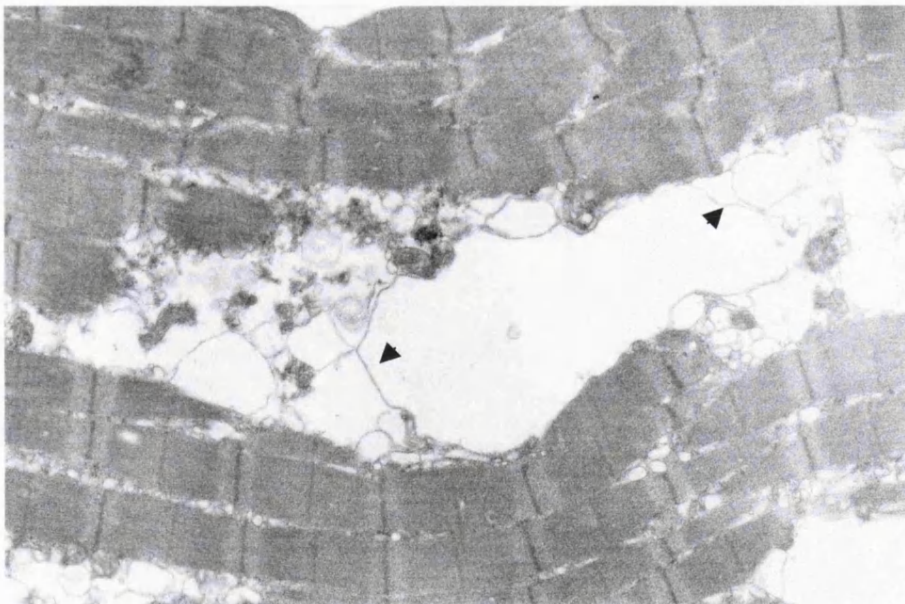


Figure 3.8. (b) Electron micrograph of soleus muscle taken 8 hours after dosing with TMPD ($60 \mu\text{mol kg}^{-1}$). Adjacent membranes of the sarcotubular system appear to have fused (arrowheads) to yield larger vacuoles. Bar = $1 \mu\text{m}$.

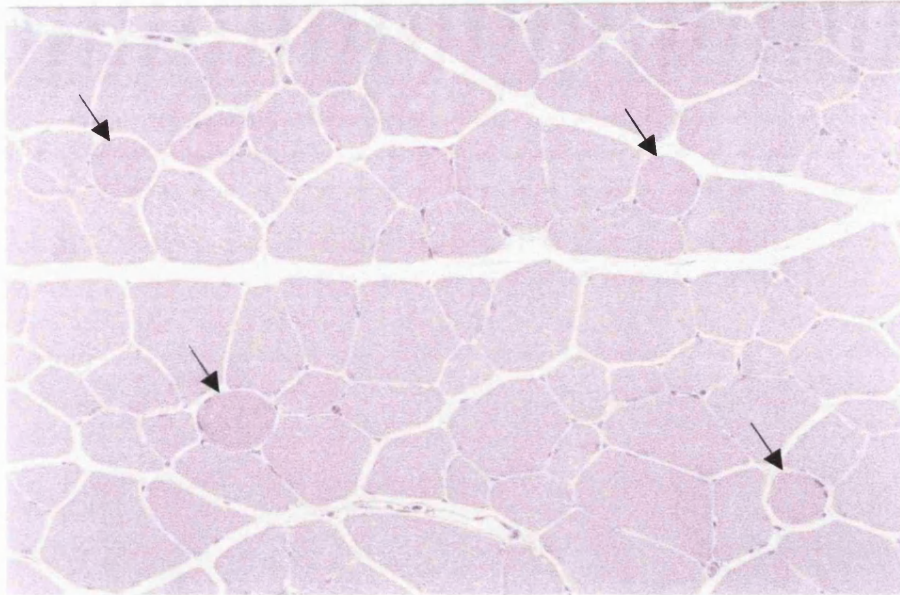


Figure 3.9. (a) Transverse section of quadriceps muscle taken from a rat at 24 hours after dosing with TMPD ($60\mu\text{mol kg}^{-1}$). Early signs of degeneration are evident with characteristic rounded hyaline fibres (arrows). H&E x 400.

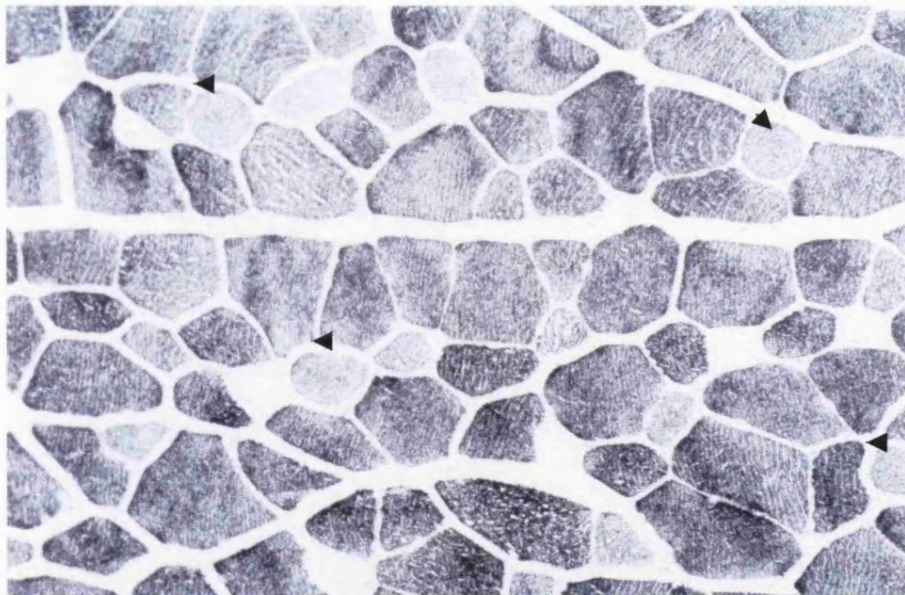


Figure 3.9. (b) Serial section of quadriceps muscle stained with fast myosin antibody. Early degeneration of some type IIA fibres (arrowheads) can be seen. x 400.

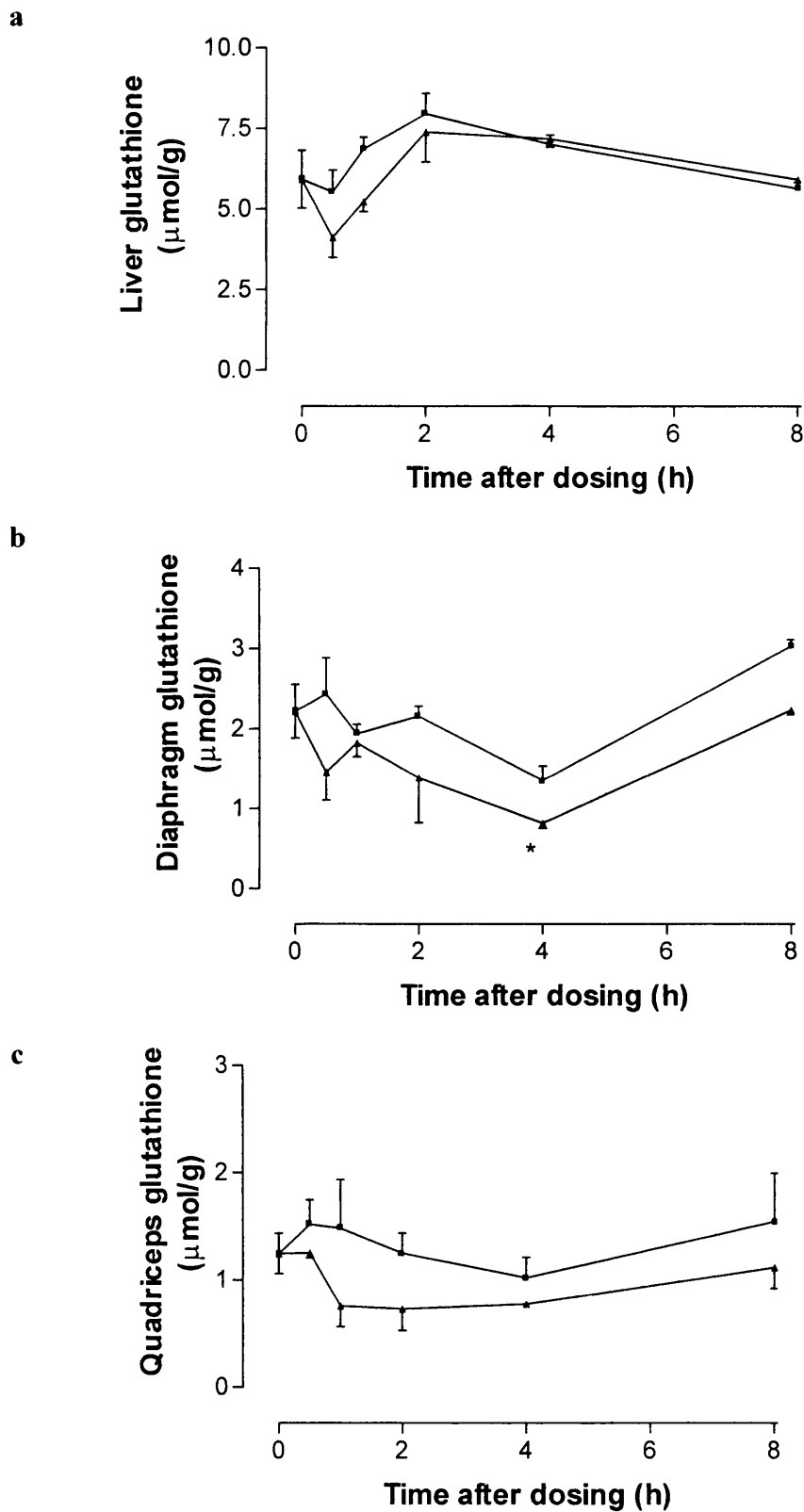


Figure 3.10. The time-dependant effect of TMPD on **a**) liver, **b**) diaphragm, and **c**) quadriceps glutathione at 0.5, 1, 2, 4, and 8 h. Male rats were dosed with phosphate buffered saline (control) (■), or $60\mu\text{mol kg}^{-1}$ TMPD (▲). Values are means \pm SEM; $n=4$ in each group except 0h and 8h control groups and 8h treated group where $n=3$; * ($P < 0.05$) versus control group.

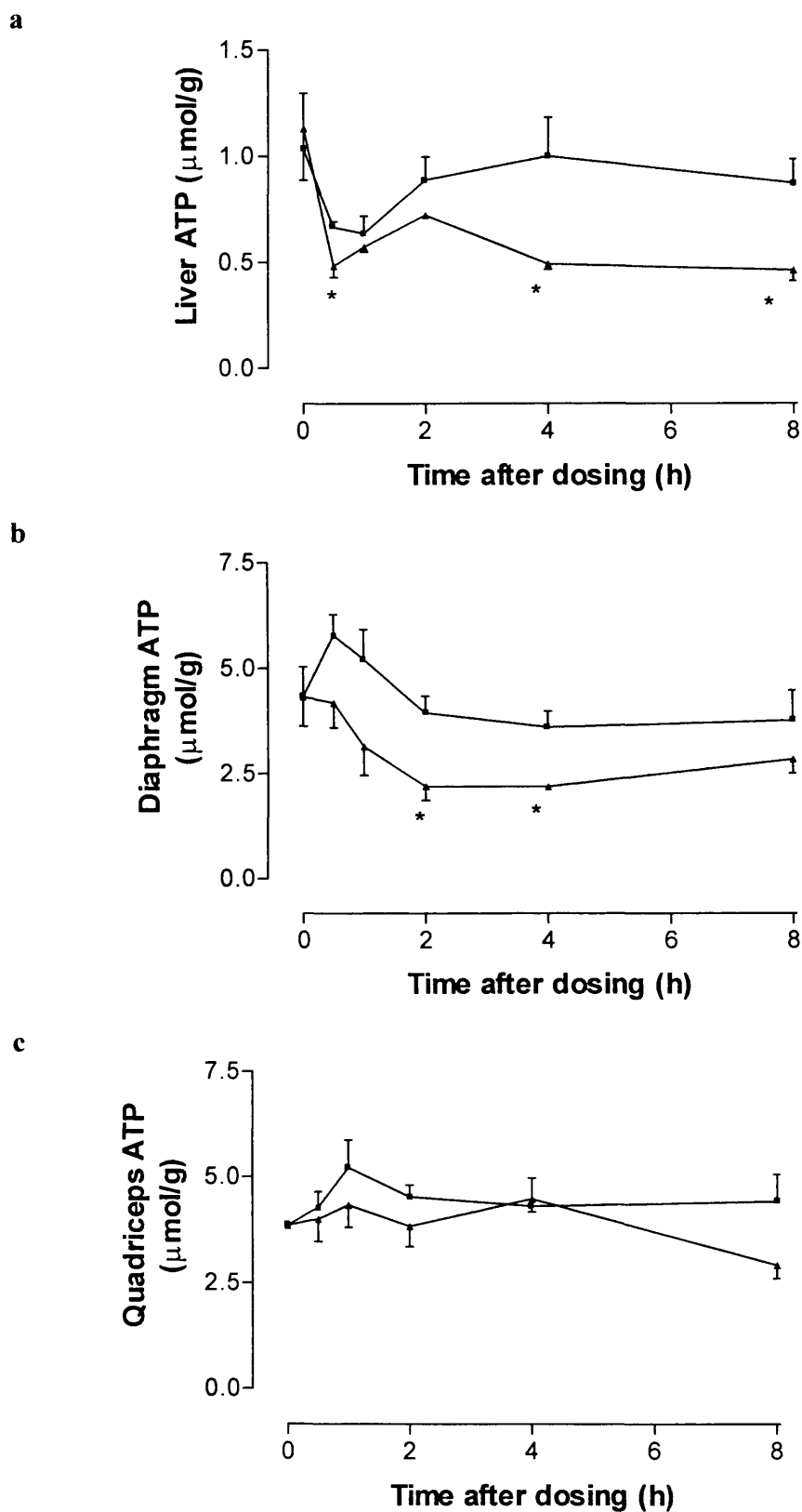


Figure 3.11. The time-dependant effect of TMPD on **a)** liver, **b)** diaphragm, and **c)** quadriceps ATP at 0.5, 1, 2, 4, and 8 hours. Male rats were dosed with phosphate buffered saline (control) (■), or $60\mu\text{mol kg}^{-1}$ TMPD (▲). Values are means \pm SEM; $n=4$ in each group except 0h and 8h control groups and 8h treated group where $n=3$; * ($P < 0.05$) versus control group.

CHAPTER 4

THE EFFECT OF TMPD ON LIVER AND SKELETAL MUSCLE ANTIOXIDANT ENZYME ACTIVITIES *IN VITRO AND IN VIVO*

4.1 INTRODUCTION

Muscle tissue is unique both in its requirements and ability to undertake very rapid and co-ordinated changes in energy supply and oxygen flux during contraction (Haycock et al., 1996). However, these characteristics have been suggested to render the tissue particularly prone to ROS-mediated damage as a result of increased electron influx and corresponding leakage from the mitochondrial respiratory chain (Jackson and O'Farrell, 1993). It has also been shown that the very high concentration of the haem-containing protein, myoglobin, found in skeletal muscle, confers greater sensitivity to free radical-induced damage, whereby H_2O_2 is converted to more reactive species via the Fenton reaction (Ostdal et al., 1997).

Ring-methylated TMPD is oxidised *in vitro* (Munday et al., 1990) to quinonedi-imine and H_2O_2 . These oxidation products can subsequently react with reduced pyridine nucleotides and glutathione which (as described in Chapter 1), rather than constituting an effective defence mechanism, may in fact lead to the uncontrolled generation of ROS.

The maintenance of the glutathione pool, together with the co-ordinated activities of the intracellular antioxidant enzymes, can be critical to cell viability (Griffith, 1999). Intracellular alterations in thiol status are thought to result in the oxidation of critical thiol

groups in ATP-dependant Ca^{2+} translocases leading to their inactivation, and with subsequent changes in Ca^{2+} homeostasis leading to cell death (Thor et al., 1982).

Skeletal muscle undergoes a number of pathological and biochemical changes as a result of TMPD treatment *in vivo*. This is in contrast to the liver, which shows only very minor and transient changes (Blair et al., 1997; Munday et al., 1990). These respective tissue sensitivities may reflect the differing GSH content, and the reported turnover rates of the peptide, in the two tissues (Potter and Tran, 1993). Antioxidant enzymes are an important line of defence for the cell when dealing with ROS-generating xenobiotics, and interestingly, levels of these enzymes are reportedly low in skeletal muscle in comparison with the liver (Grankvist et al., 1981).

To investigate the importance of glutathione status and the relative activities of the glutathione-dependant antioxidant enzymes, the toxicity of a range of TMPD concentrations was examined in cultured skeletal muscle myocytes and in isolated hepatocytes in Study 1, together with an assessment of the antioxidant capacity of each cell type and their response to TMPD treatment. In Study 2, antioxidant enzyme activity was assessed in liver and muscle (diaphragm) tissue samples excised from animals pre-treated with TMPD alone, or with TMPD and the thiol supplier N-acetylcysteine (NAC), which was given in an attempt to modulate the toxicity of the amine.

4.2 MATERIALS AND METHODS

4.2.1 Study 1: The effect of TMPD on antioxidant enzyme levels in isolated rat hepatocytes and cultured myocytes *in vitro*

Skeletal myocytes were isolated as described in Chapter 2 and allowed to grow and differentiate for 10 days prior to any treatment. Hepatocytes from adult male Han Wistar rats (200-250 g) were isolated by the collagenase perfusion method as described in Chapter 2. The cells were diluted with Williams Medium E and plated at a density of $1 \times 10^5 \text{ cm}^2$. The medium was changed 2 hours later to remove unattached cells and the remaining cells were allowed to recover overnight. Both cell types were then dosed with a range of TMPD concentrations and incubated (37°C, 95% O₂, 5% CO₂) for 24 hours.

4.2.1.1 Measurement of TMPD toxicity

TMPD toxicity was measured by the assessment of LDH leakage and assay of intracellular GSH, ATP and CK. Culture medium (1 mL) was removed for measurement of LDH leakage. Cells (myocytes and hepatocytes) were washed with ice-cold (4°C) PBS, then either lysed and re-suspended in 6.5% or 10% TCA (1 mL) for GSH, or ATP determination, respectively, or scraped into ice-cold PBS (1 mL) for cellular CK measurement.

4.2.1.2 Measurement of cell GRed, GST, GPx and SOD enzyme activities

Myocytes and hepatocytes were treated with various concentrations of TMPD as described above, scraped into 1 mL of serum-free culture medium and frozen at -80°C. On the day of analysis the samples were thawed, sonicated and centrifuged, and an aliquot of the supernatant taken for each enzyme assay (see Chapter 2 for details). The cell pellets were re suspended in NaOH (1M) for protein determination.

4.2.2 Study 2: TMPD toxicity and antioxidant enzyme activities of liver and skeletal muscle *in vivo*: effect of NAC

4.2.2.1 Animal husbandry

Male rats (250-350 g) were randomly allocated to treatment groups and housed 6 per cage. Food and water was given *ad libitum*. Prior to treatment the animals were acclimatised for 48 hours in a light and temperature controlled room.

4.2.2.2 Experimental design

Rats (n=6) received saline (controls), or 60 $\mu\text{mol kg}^{-1}$ (4 mL kg^{-1} solution) TMPD, sc., or 4 mmol kg^{-1} NAC (8 mL kg^{-1} solution, corrected to pH 7.4) ip., or both TMPD and NAC in group rotation, and were sacrificed 24 hours later. At autopsy, samples of liver and diaphragm muscle were excised and immediately frozen in liquid nitrogen for biochemical analysis of GSH and antioxidant enzyme activities. Blood was taken for serum preparation as previously described and analysed for biochemical parameters as set out in Chapter 3.

4.3 RESULTS

4.3.1 Study 1: The effect of TMPD on the antioxidant enzyme levels in isolated rat hepatocytes and cultured myocytes *in vitro*

4.3.1.1 Assessment of TMPD toxicity

TMPD-induced myocyte and hepatocyte toxicity was assessed by measuring intracellular GSH and ATP levels, LDH leakage, and intracellular CK activity (myocytes only). Depletion of GSH and ATP appeared to be dose-dependant in both cell types, (Fig. 4.1 and Fig. 4.2). However, control GSH levels of hepatocytes were more than 4 times greater than the control GSH levels of myocytes (Fig. 4.1); control ATP levels were similar for hepatocytes and myocytes (Fig. 4.2). The reduction in the levels of GSH and ATP was accompanied by a proportional increase in extracellular LDH (a marker of plasma membrane integrity), and loss of intracellular CK activity, from myocytes (also a marker of plasma membrane damage). Significant LDH leakage from myocytes (Fig. 4.3) occurred at a much lower concentration of TMPD (0.25 mM) than from hepatocytes (0.75 mM). CK loss from myocytes (Fig 4.4) was apparent at approximately the same concentration of TMPD at which GSH, ATP and LDH were lost from the cells (0.2-0.25 mM). Indeed, in those myocytes treated with levels of greater than 0.25 mM TMPD, very little CK activity was detectable (Fig. 4.4).

4.3.1.2 Cellular GRed, GST, GPx and SOD activities

Control levels of each antioxidant enzyme measured in the two cell types were markedly different (Table 4.1); only control and 0.2 mM TMPD-treated cell data are reported here, with the exception of those enzymes whose activity was significantly altered in response to TMPD-treatment, in which case data for each concentration of TMPD studied, are reported. Hepatocytes generally possessed higher enzyme activities than skeletal myocytes, with the exception of GPx (Table 4.1).

GRed activity in myocytes was significantly reduced following TMPD treatment, an effect not apparent in hepatocytes (Table 4.1, Fig. 4.5). GPx activity, although slightly reduced in myocytes, was not significantly different from controls. TMPD had no effect on hepatocyte GPx activity. GST levels were significantly increased by TMPD in both skeletal myocytes and hepatocytes (Table 4.1, Fig. 4.6), however, this increase (at concentrations from 0.125 mM TMPD in hepatocytes, and 0.15 mM TMPD in myocytes) as a percentage of control levels was much greater in myocytes (Table 4.1, Fig. 4.6). SOD activities (manganese and cupro-zinc isoforms) were not significantly affected by TMPD treatment (Table 4.1), with the exception of Cu-Zn SOD in TMPD-treated hepatocytes where activity was significantly higher in comparison to the control.

4.3.2 Study 2: TMPD toxicity and antioxidant enzyme activities of liver and skeletal muscle *in vivo*: effect of NAC

4.3.2.1 Skeletal muscle and liver GRed, GST, GPx and SOD activities

The administration of NAC alone to rats (4 mmol kg⁻¹), had no significant effect in the diaphragm or liver on the activities of any of the antioxidant enzymes measured when compared to control animals (Table 4.2). TMPD treatment alone significantly reduced GRed and GPx activities in the diaphragm, an effect not seen in the liver. GST activity was significantly raised in both the liver and the diaphragm, although this effect was more pronounced in the latter. SOD activity (both isoforms) in TMPD-treated animals was not significantly different from controls in either tissue.

Co-administration of NAC and TMPD (Table 4.2) did not appear to reduce the toxicity of the amine. In each case, and in both tissues, the pattern of activities was identical to treatment with TMPD alone.

Administration of NAC alone did not significantly affect any of the serum parameters measured when compared to control. The pattern of serum chemistry (Table 4.3) after administering a 60 µmol kg⁻¹ dose of TMPD is similar to that of the dose-response study, described in Chapter 3. Levels of ALT and AST were significantly increased. The high

AST: ALT ratio of approximately 7:1 in TMPD-treated rats is consistent with skeletal muscle injury. Serum levels of the lactate dehydrogenase enzyme isoforms were also increased upon TMPD treatment; however, these increases were not statistically significant. TMPD administration again significantly raised total CK activity, although this rise was predominantly due to a significant increase in the skeletal muscle isoform CK-MM rather than to any significant changes in either the heart or brain isoforms. When NAC was co-administered with TMPD, no protective effect was apparent, indeed those enzymes which showed increased activity following treatment with TMPD alone, showed a similar or greater increase in activity, for example the LDH isoforms 1-4.

4.4 DISCUSSION

The results obtained in this study clearly demonstrate the myotoxic nature of TMPD *in vitro*, and the dose-dependent loss of intracellular CK and concomitant increase in extracellular LDH are in accordance with the findings of Harauchi and Hirata (1993). However, in the present study, cytotoxic effects were found to occur both in skeletal myocytes and isolated hepatocytes.

Treatment with TMPD causes a significant depletion of intracellular GSH and ATP (Fig. 4.1 and Fig. 4.2), and the patterns of depletion were similar in both cell types, although it should be noted that myocytes have significantly lower control levels of GSH. Both types of cell appear to show a bi-phasic loss of GSH. The first drop, occurring between 0-0.25 mM TMPD, may correspond to loss of the cytosolic GSH pool. The second drop is less pronounced and occurs at concentrations > 0.25 mM TMPD. This pool of GSH appears to be more resistant to depletion; indeed skeletal myocyte GSH levels show an indication of a plateau at 0.25 mM. This may be an attempt by both types of cell to sequester GSH into their mitochondria (from which efflux of the peptide is slower), as described by Meredith and Reed (1982). This response in the mitochondria may be a mechanism to protect those proteins involved in the generation of ATP, a process that is pivotal in terms of cellular repair and survival. It is also possible (especially with regard to the pattern of myocyte GSH at doses > 0.25 mM TMPD) that those biochemical, and/or enzyme-catalysed reactions that take place to protect the cell against toxic insult (ROS generation in particular with respect to TMPD), are terminated either as a result of damage to the enzyme proteins themselves, or due to a more terminal endpoint, that is, the death of the cell.

ATP depletion is significant in both cell types upon exposure to ≥ 0.2 mM TMPD. There are a number of ways for toxic compounds to cause depletion of ATP (Timbrell, 1992). This phenomenon can be induced experimentally by inhibiting ATP synthesis *in vivo* e.g.

during ischaemia or in the presence of metabolic inhibitors or uncouplers such as dinitrophenol (Preece et al., 1990). Entrapment of the synthetic precursors of ATP will also reduce the cell's energy pool. For example inorganic phosphate can be trapped as fructose-1-phosphate during 2-deoxyglucose-treatment or in the presence of excess fructose or glucose (Farber, 1973). Depletion may also occur during the increased ATP utilisation that occurs as a result of oxidative stress and which can be attributed to the ATP requirements of *de novo* GSH synthesis (Meister and Anderson, 1983), or to the removal of oxidised GSSG from the cell. This mechanism of toxicity is thought to occur during chronic ethanol administration (Helzberg et al., 1987). However, since the depletion of ATP in the present study occurs at approximately the same TMPD concentration (0.2-0.25 mM) as GSH depletion from skeletal myocytes and hepatocytes, it seems unlikely that this was the only mechanism of toxicity involved. The most common cause of ATP depletion in a cell is interference with mitochondrial oxidative phosphorylation, which may result from damage to the mitochondria themselves (Timbrell, 1992). This hypothesis is likely to be applicable in the current study given the ROS-generating nature of the TMPD family of compounds (Munday et al., 1989; 1990), together with the ultrastructural evidence of TMPD-treated skeletal muscle injury from the *in vivo* study discussed in the previous chapter. Indeed, in an electron microscopical study to investigate the differential susceptibility of skeletal muscle proteins to free radicals (Haycock et al., 1996), mitochondria were identified as being particularly susceptible to ROS-induced oxidative injury.

Despite the similarities between changes in skeletal myocyte and hepatocyte ATP and GSH levels following TMPD treatment, the pattern of extracellular LDH leakage (Fig. 4.3) is distinctly different. Significant LDH leakage from skeletal myocytes occurs at much lower concentrations of TMPD (0.2 mM) than from hepatocytes (approximately 0.75 mM). Loss of this enzyme is a clear indication of severe cell damage (primarily, a loss of membrane integrity), and represents 'the point of no return' in the cascade of events leading up to cell death. Thus it would appear that although TMPD does produce toxic effects in isolated hepatocytes, they are less sensitive in comparison to skeletal

myocytes both *in vitro* and *in vivo*. Compromised membrane integrity of skeletal muscle cells (measured in the present study by LDH leakage), as a result of TMPD treatment is an observation further supported by the loss of intracellular CK at a similar dose level (Fig. 4.4). Total depletion of this enzyme occurred between 0.25-0.5 mM. Lower doses of the amine appear to induce CK activity and this may be a counter-response to the falling levels of ATP found in skeletal myocytes. One of the main functions of the CK/phosphocreatine (PCr) system is that of a 'temporal energy buffer' responsible for ATP regeneration (Wallimann et al., 1992). Glutathione reductase catalyses the reduction of GSSG to GSH (Carlberg and Mannervick, 1985), an essential reaction for the maintenance of glutathione levels. TMPD treatment of skeletal myocytes significantly decreased the reductase activity of these cells at a concentration of 0.2 mM (Table 4.1; Fig. 4.5). This loss of reduced GSH leaves other cellular components open to ROS-mediated attack. At the same concentration, glutathione reductase activity of hepatocytes is unchanged with respect to the controls (Table 4.1; Fig. 4.5), therefore the regenerated GSH may be able to offer the hepatocyte better protection against free radical damage at low levels (≤ 0.2 mM) of TMPD.

In response to TMPD treatment, both cell types showed a significant increase in GST activity (Table 4.1; Fig. 4.6). TMPD acts as an inducer of GST because of its chemical structure. It is a classic Michael acceptor in that it contains an unsaturated bond rendered electrophilic by conjugation with an electron-withdrawing group, NH_2 in this case. Electrophilic inducers like TMPD are expected to reduce the thiol content of the cell and promote a pro-oxidant state by 1), GST-mediated conjugation with GSH and 2), by non-enzymatic interaction with the sulphhydryl group of GSH (Daniel, 1993). These mechanisms are clearly at work in both types of cell.

Two enzymes are recognised to serve as primary defences against cytosolic H_2O_2 in eukaryotic cells, glutathione peroxidase (GPx) and catalase (Radi et al., 1991). GPx detoxifies the majority of H_2O_2 under normal conditions and peroxisomal catalase acts as

a significant scavenger of this oxidant when present at non-physiological concentrations (Chance et al., 1979). Unlike most organs, mammalian skeletal myocytes do not have peroxisomes and the catalase activity per g of tissue is approximately 2% that of liver (Nohl and Hegner, 1978). This may explain the lack of GPx induction in isolated hepatocytes, and it is plausible to assume that given the very low catalase activity of skeletal muscle, cellular GPx may have been overwhelmed by the amount of H₂O₂ formed.

Superoxide dismutase (SOD) works in concert with GPx in the detoxification of O²⁻ and H₂O₂ respectively. The mitochondrial electron transport chain, under normal physiological conditions, releases small amounts of these oxidants (Forman and Bovaris, 1982). When perturbed by inhibitors or uncouplers however, it may produce increased amounts of active oxygen, causing oxidative stress within the cell. The cytosolic form of SOD, Cu-Zn SOD is constitutively expressed, whereas its mitochondrial counterpart, Mn-SOD is a highly inducible enzyme. The lack of apparent change in Mn-SOD activity may simply reflect a low level of O²⁻ production in mitochondria, following treatment with TMPD. In hepatocytes, Cu-Zn SOD is significantly up regulated in response to TMPD treatment by more than 200% (Table 4.1) and even in cultured skeletal myocytes (although not significant) the cytosolic form of SOD is also elevated (> 40%). This may be due to a rapid efflux of O²⁻ (if formed) from mitochondria to cytosol, or as a result of increased O²⁻ formation within the cytosol relative to the mitochondria.

Study 2 involved the administration of 60 µmol TMPD kg⁻¹ to male rats, a dose known to induce significant toxic changes in skeletal muscle (Munday et al., 1990; Draper et al., 1994; Blair et al., 1997) *in vivo*, together with NAC. NAC is a GSH precursor that has been shown to rescue cellular GSH following depletion (Mitchell et al., 1973; Drew and Miners et al., 1984).

Antioxidant enzyme activities following TMPD treatment *in vivo* were remarkably similar to those seen *in vitro* (Study 1). Glutathione reductase activity was significantly

depressed in skeletal muscle upon TMPD treatment, and GST activity in both tissues was significantly elevated. However, none of the SOD isoforms (in either tissue) showed any apparent change in activity. This last result may suggest that superoxide formation is not a major factor in TMPD toxicity, and this would be in accordance with the findings of Munday et al. (1990) on the metabolism of the ring-methylated isomer.

NAC is an antioxidant (Malorni et al., 1995), which can increase intracellular GSH levels (Smilkstein et al., 1988; Burgunder et al., 1989). Depletion of GSH *in vivo* in rats treated with TMPD has been found to occur in skeletal muscle (Blair et al., 1997). Dose-dependent depletion of the peptide was also found to occur in cultured myocytes and isolated hepatocytes (Fig. 4.1). Cells of aerobic organisms are under constant threat to oxidative damage and maintenance of the cellular thiol pool is vital, particularly when the delicate oxidative balance is perturbed following exposure of the cell or tissue, to a redox cycling agent like TMPD. Both the nucleus and the mitochondrion are dependent upon the mechanisms enabling GSH exchange between themselves and the cytosol (whereby GSH is either synthesised *de novo*, or taken up from serum) in terms of their own and subsequently the survival of the cell *per se*. Co-administration of NAC and TMPD together had no effect on any of the antioxidant enzyme activities measured. Liver and diaphragm GSH levels were not significantly different to control values (data not shown) 24 hours after administering TMPD ($60 \mu\text{mol kg}^{-1}$) alone, or in conjunction with NAC (4 mmol kg^{-1}). Thus if NAC does indeed 'rescue' intracellular GSH, it appears unlikely that the major toxic mechanism of TMPD lies herein. The serum chemistry results are in accordance with this hypothesis. Treatment with TMPD ($60 \mu\text{mol kg}^{-1}$), with or without NAC, produced similar elevations in the activities of several serum enzymes and their isoforms; this is clear-cut evidence that significant tissue damage is taking/has taken place. This confirms that NAC in the present study conferred no protection against the toxic effects of TMPD.

Table 4.1

The effect of TMPD (0.0 and 0.2 mM) on the antioxidant enzyme activities of skeletal myocytes, and isolated hepatocytes

Myocytes	GR ^a	GPx ^b	GST ^c	Mn SOD ^d	Cu-Zn ^d SOD
Control (0.0 mM)	0.33 (0.04)	81.43 (17.73)	13.60 (0.00)	13.30 (6.44)	3.15 (0.44)
TMPD (0.2 mM)	0.12 (0.04)*	71.00 (34.13)	24.10 (0.00)*	14.90 (4.07)	4.42 (1.19)

Hepatocytes	GR ^a	GPx ^a	GST ^b	Mn SOD ^c	Cu-Zn ^c SOD
Control (0.0 mM)	1.26 (0.29)	31.57 (2.57)	291.4 (0.02)	32.09 (6.96)	7.95 (5.23)
TMPD (0.2 mM)	1.54 (0.45)	33.68 (4.85)	319.4 (0.05)*	37.72 (4.78)	17.68 (3.76)*

Antioxidant enzyme activities of skeletal muscle myocytes (10 DIV) and hepatocytes (1×10^5 cells) following a 24-hour incubation with TMPD (0.0-0.2 mM). Only data from controls and 0.2mM TMPD are given above. Values are means (SEM), n=4. * $P < 0.05$, Dunnett's test for multiple comparisons with a single control. GR, GPx, GST, Mn-SOD and Cu-Zn SOD indicate glutathione reductase, glutathione peroxidase, glutathione-s-transferase, mangano-superoxide dismutase and cupro-zinc superoxide dismutase, respectively. ^a nmol NADPH/min/mg protein, ^b nmol of conjugate/min/mg protein, ^c u/min/mg protein.

Table 4.2

The effect of co-administration of NAC on the antioxidant enzyme activities of skeletal muscle and liver in TMPD-treated animals.

Diaphragm	GR ^a	GPx ^b	GST ^c	Mn SOD ^d	Cu-Zn ^d SOD
Control	2.92 (0.15)	26.64 (1.07)	5.47 (0.22)	3.83 (0.14)	1.91 (0.08)
NAC	2.77 (0.11)	30.15 (3.21)	4.23 (0.18)	3.51 (0.17)	2.07 (0.07)
TMPD	1.17 (0.48)*	23.34 (1.14)*	8.53 (0.39)*	3.65 (0.15)	1.98 (0.08)
NAC + TMPD	1.05 (0.47)*	22.61 (0.91)*	7.48 (0.27)*	3.78 (0.16)	2.11 (0.10)

Liver	GR ^a	GPx ^a	GST ^b	Mn SOD ^c	Cu-Zn ^c SOD
Control	18.25 (0.73)	617.51 (26.40)	397.26 (16.89)	27.63 (1.15)	30.10 (1.31)
NAC	17.82 (1.83)	636.15 (29.61)	406.41 (17.15)	24.88 (1.04)	32.73 (2.16)
TMPD	19.37 (0.88)	624.93 (34.78)	447.57 (18.72)*	25.33 (1.82)	33.85 (1.94)
NAC + TMPD	18.73 (0.79)	631.82 (28.72)	439.63 (17.15)*	31.54 (3.67)	26.17 (1.78)

Antioxidant enzyme activities of skeletal muscle (diaphragm) and liver 24 hours following a single subcutaneous injection of TMPD (60 $\mu\text{mol kg}^{-1}$), a single intraperitoneal injection of N-acetylcysteine, NAC (4 mmol kg^{-1}) or both. Control animals were given phosphate buffered saline. Values are means (SD), n=4. * $P < 0.05$, Dunnett's test for multiple comparisons with a single control. GR, GPx, GST, Mn-SOD and Cu-Zn SOD indicate glutathione reductase, glutathione peroxidase, glutathione-s-transferase, mangano-superoxide dismutase and cupro-zinc superoxide dismutase, respectively. ^a nmol NADPH/min/mg protein, ^b nmol of conjugate/min/mg protein, ^c u/min/mg protein.

Table 4.3.

Effect of the administration of NAC (4 mmol kg⁻¹), TMPD (60 μmol kg⁻¹), and NAC + TMPD on serum enzyme levels in rats, with sampling at 24 hours post dosing

Group of animals	AST (iu.L ⁻¹)	ALT (iu.L ⁻¹)	LDH (iu.L ⁻¹)	LDH ₁ (iu.L ⁻¹)	LDH ₂ (iu.L ⁻¹)	LDH ₃ (iu.L ⁻¹)	LDH ₄ (iu.L ⁻¹)	CK (iu.L ⁻¹)	CK-MM (iu.L ⁻¹)
CONTROL	73.9 (2.4)	53.1 (2.8)	513.1 (117.8)	14.0 (1.1)	5.3 (0.5)	13.2 (1.4)	38.5 (12.7)	236.3 (33.8)	27.0 (3.3)
NAC	66.3 (3.1)	51.6 (2.8)	283.3 (73.8)	10.3 (2.8)	5.0 (0.7)	11.7 (2.5)	14.0 (3.1)	183.7 (41.8)	23.5 (3.8)
TMPD	3871.7 (1229.2)**	587.6 (172.0)**	1180.0 (191.4)	145.0 (16.7)	171.0 (28.0)	137.3 (68.7)	180.5 (19.6)	1577.3 (172.4)**	1352.8 (182.2)*
NAC + TMPD	3606.0 (1472.1)**	552.5 (1.8)**	1377.8 (351.1)*	180.3 (75.5)*	206.0 (90.4)*	166.5 (70.0)*	254.7 (111.5)*	1346.0 (556.4)*	1148.0 (567.7)*

Values are means (SEM); n = 6. Statistically analysed using Dunnett's test for multiple comparisons using a single control, with the level of significance set at * $p < 0.05$, ** $p < 0.01$. AST (aspartate aminotransferase); ALT (alanine aminotransferase); LDH (total lactate dehydrogenase activity); LDH_{1,2,3,4} (lactate dehydrogenase isoenzymes 1,2,3 and 4); CK (total creatine kinase activity); CK-MM (creatine kinase muscle isoenzyme).

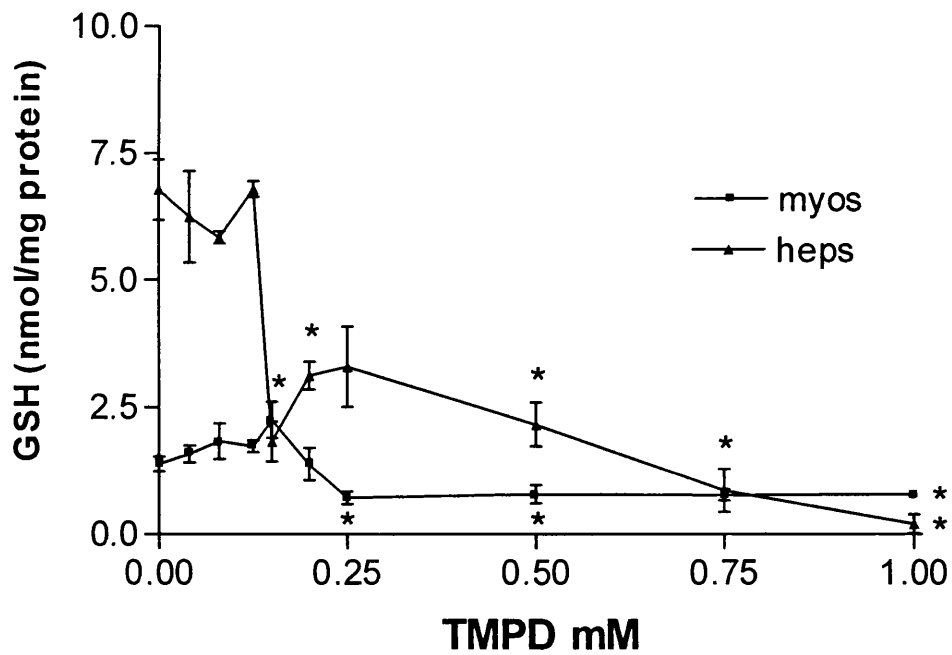


Figure 4.1. Intracellular rat myocyte (10 DIV) and hepatocyte (1×10^5 cells) GSH content following 24 hours exposure to TMPD. Values are means \pm SEM, $n = 4$. $*P < 0.05$ versus control.

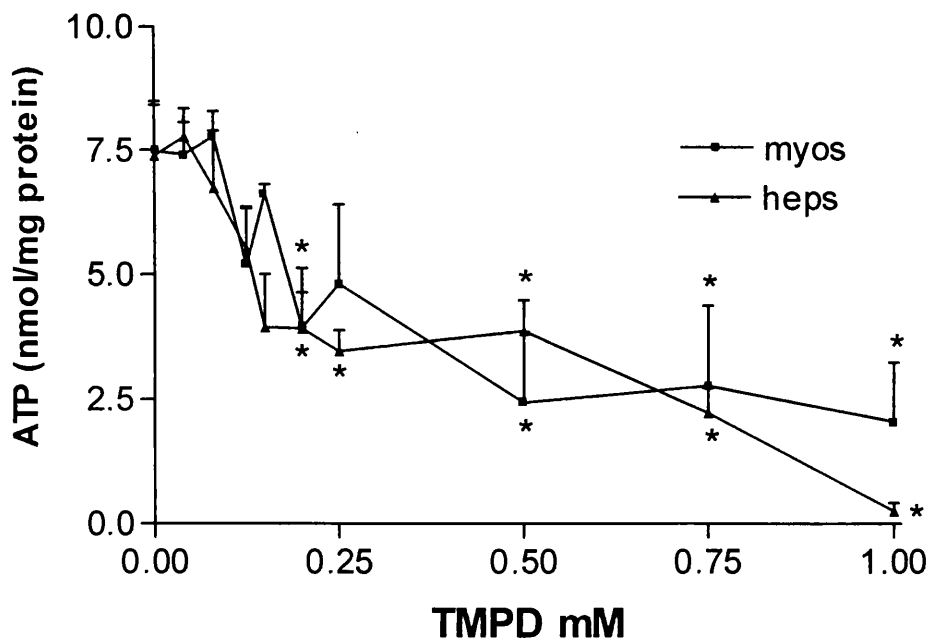


Figure 4.2. Intracellular rat myocyte (10 DIV) and hepatocyte (1×10^5 cells) ATP content following 24 hours exposure to TMPD. Values are means \pm SEM, $n = 4$. $*P < 0.05$ versus control.

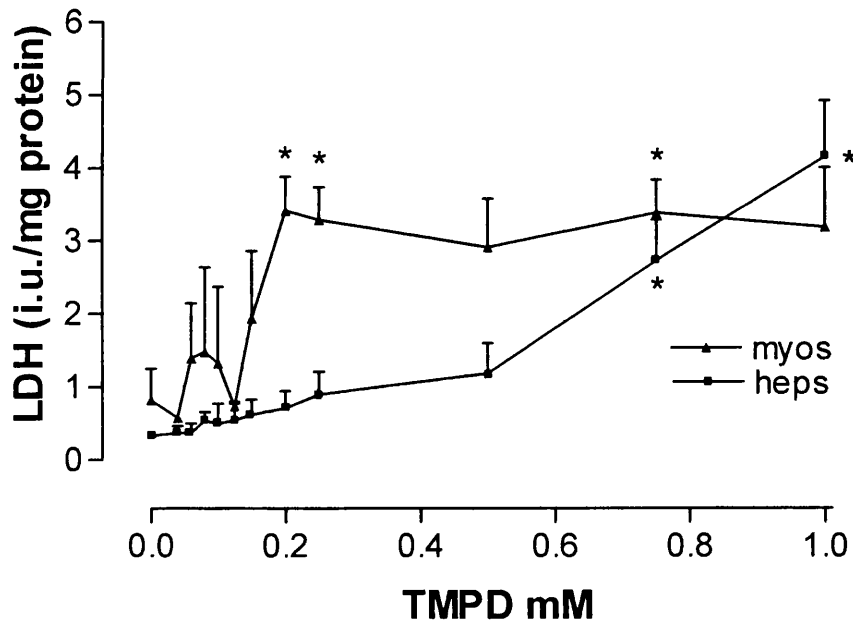


Figure 4.3. Extracellular rat myocyte (10 DIV) and hepatocyte (1×10^5 cells) LDH leakage following 24 hours exposure to TMPD. Values are means \pm SEM, $n = 4$. * $P < 0.05$ versus control.

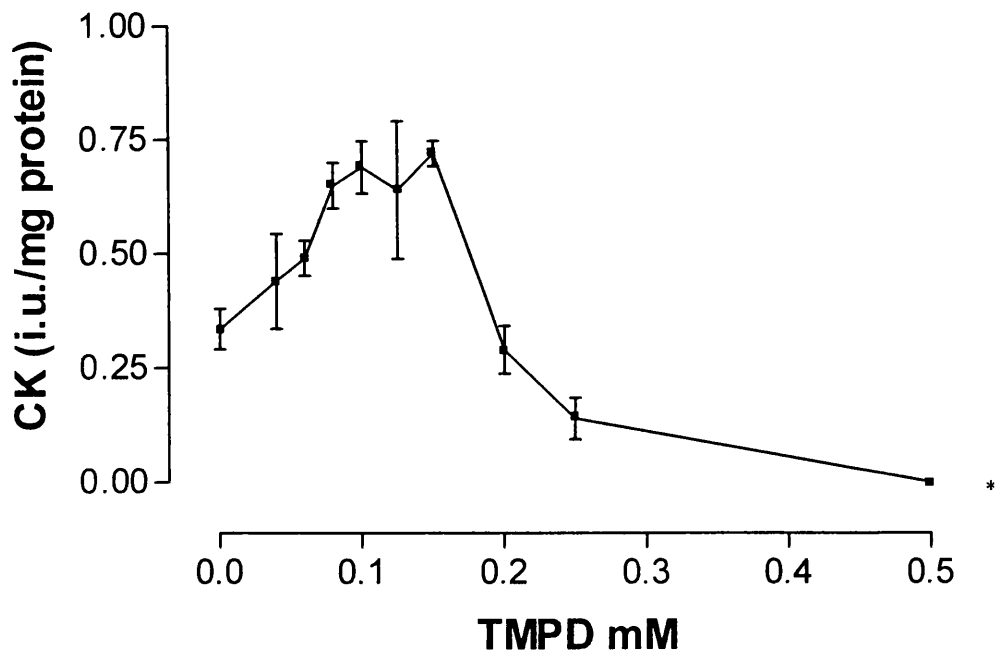


Figure 4.4. Intracellular rat myocyte (10 DIV) CK content following 24 hours exposure to TMPD. Values are means \pm SEM, $n = 4$. * $P < 0.05$ versus control.

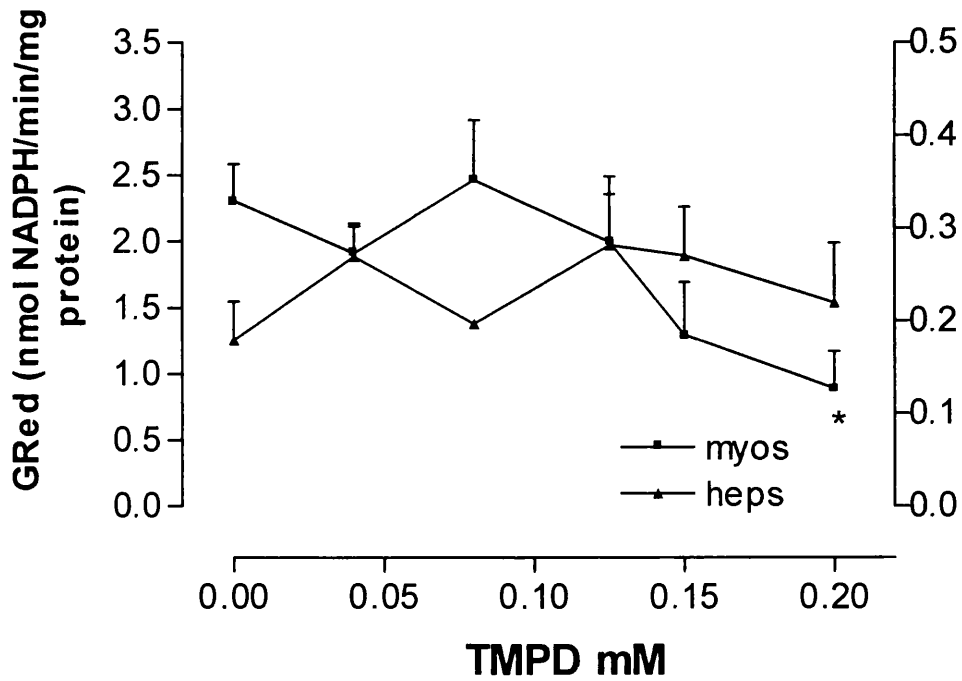


Figure 4.5. Intracellular rat myocyte (10 DIV; right-hand axis) and hepatocyte (1×10^5 cells; left-hand axis) glutathione reductase (GRed) activity following 24 hours exposure to TMPD. Values are means \pm SEM, $n = 4$. * $P < 0.05$ versus control.

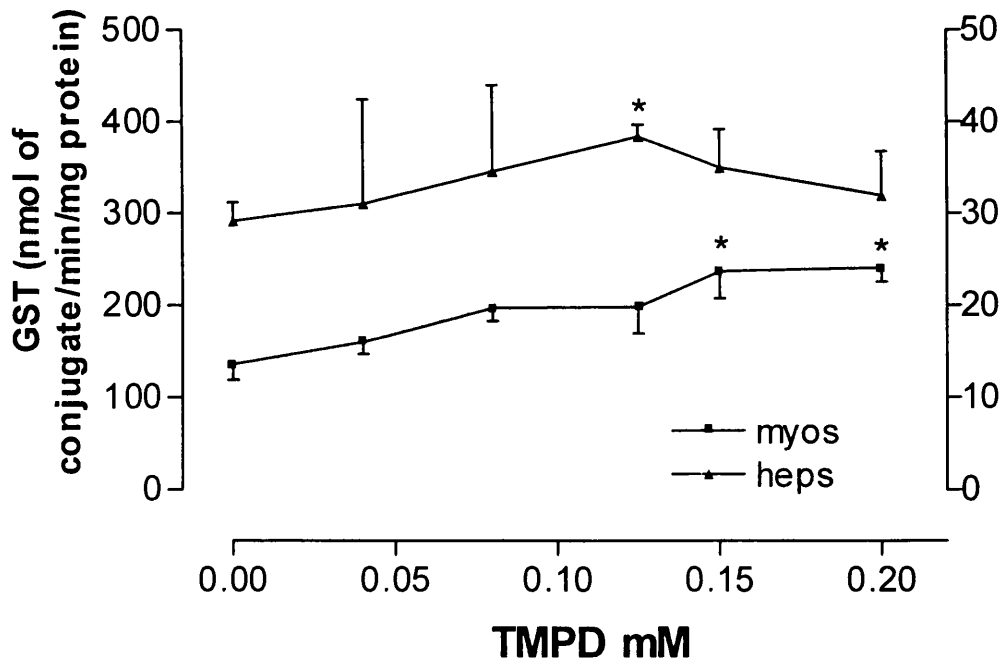


Figure 4.6. Intracellular rat myocyte (10 DIV; right-hand axis) and hepatocyte (1×10^5 cells; left-hand axis) glutathione-S- transferase (GST) activity following 24 hours exposure to TMPD. Values are means \pm SEM, $n = 4$. * $P < 0.05$ versus control.

CHAPTER 5

AN INVESTIGATION OF THE *IN VITRO* TOXICITY OF TMPD USING ISOLATED MITOCHONDRIA

5.1 INTRODUCTION

Ring-methylated TMPD causes severe skeletal muscle necrosis in rats (Munday et al., 1990, Draper et al., 1994). Although the mechanism remains to be fully elucidated, Munday et al. (1990) proposed that the cytotoxicity of this amine, and indeed all the members of the phenylene diamine family of compounds, could be attributed to reactive oxygen species generated upon metabolism *in vivo*. This hypothesis was based upon experimental findings, which showed a strong correlation between *in vitro* autoxidation rate (ease of oxidation) of the various phenylene diamines and the degree of *in vivo* tissue toxicity. Munday (1992) also reported that the target site of TMPD oxidation *in vivo* was likely to involve the mitochondrion, more specifically complex IV, cytochrome *c* oxidase, as a result of the discovery that isolated rat liver mitochondria catalysed a cyanide sensitive oxidation of TMPD to the di-imine metabolite. More recently, Sood, et al. (1997) confirmed that TMPD oxidation was prevented by cyanide, yet the complex II-III inhibitor antimycin A did not prevent oxidation of the amine; this indicates that complex IV is the site of TMPD oxidation *in vivo*.

Thus it would appear that the mitochondrion is responsible for initiating TMPD toxicity, and herein may lay the compound's mode of action. Therefore, a number of assays to test mitochondrial function were undertaken to determine the myotoxic mechanism of the ring-methylated isomer of TMPD.

5.2 MATERIALS AND METHODS

5.2.1 Animal husbandry

The animals used in these studies were adult Han Wistar (GlaxoSmithKline bred) rats of mixed sex (300-450 g). They were housed in communal cages in the animal house after arrival, and allowed food (rat and mouse No.1, Special Diet Services Ltd., Witham, Essex) and mains drinking water *ad libitum*. They were kept in a temperature-controlled room ($21^{\circ}\text{C} \pm 2^{\circ}\text{C}$) with a regular 12-hour light/dark cycle (lights on at 0700 hours).

To minimize damage to the mitochondria, the animals were culled by cervical dislocation and skeletal muscle (gastrocnemius and quadriceps), heart and liver were rapidly removed into ice-cold isolation buffer (Chapter 2; Appendix XII).

5.2.2 Isolation of mitochondria

Skeletal muscle mitochondria, heart, and liver mitochondria were isolated using the methods of Clark et al., (1997) and Bates et al., (1995), respectively (Chapter 2). Mitochondrial protein concentrations were measured using a modified method (Bio-Rad DC protein assay) of Lowry et al., (1951), with bovine serum albumin (BSA) used as a concentration standard.

5.2.3 The effect of TMPD on *in vitro* mitochondrial respiration.

Respiratory control of freshly isolated skeletal muscle, heart, and liver mitochondria (10 mg/mL protein) was measured in the presence and absence of TMPD (0.1-0.5 mM) using the oxygen electrode system described in Chapter 2.

5.2.4 The effect of TMPD on *in vitro* mitochondrial ATP synthesis

ATP synthesis of freshly isolated skeletal muscle, heart, and liver mitochondria was measured in the presence and absence of TMPD (0.1-0.5 mM) using the assay protocol described in Chapter 2.

5.2.5 The effect of TMPD on *in vitro* mitochondrial GSH concentration.

Freshly isolated skeletal muscle, heart, and liver mitochondria were incubated with and without TMPD (0.1-0.5 mM) as described in Chapter 2 (ATP synthesis protocol). At the end of the incubation period the mitochondrial suspensions were placed in Ependorph tubes, centrifuged (1500 rpm, 4°C, 5 min), and the supernatant discarded. TCA (0.5 mL, 6.5%) was added to the tubes, which were stored at -80°C until analysis.

5.2.6 The effect of TMPD on *in vitro* mitochondrial complex activities.

Complex activities following incubation with increasing concentrations of TMPD (0.1-0.5 mM) were measured as described in Chapter 2. At the end of the incubation period the mitochondrial suspensions were placed in Ependorph tubes, centrifuged (1500 rpm, 4°C, 5 min), and the supernatant discarded. The mitochondrial pellets were stored at -80°C. Prior to analysis of enzyme activity, the preparations were freeze-thawed 3 times and vortexed in between thawing cycles, ensuring complete mitochondrial lysis.

5.3 RESULTS

5.3.1 The effect of TMPD on *in vitro* mitochondrial respiration.

Respiration in skeletal muscle, heart, and liver mitochondria was stimulated upon addition of ADP (3 mM), an indication that the mitochondria were coupled (Table 5.1). Addition of carbonyl cyanide *m*-chloro-phenyl-hydrazone (CCCP), a well-known uncoupler of oxidative phosphorylation, caused a dramatic increase in respiration. ADP/O ratios of control mitochondria were close to the theoretical value of 3 (Table 5.1). TMPD caused a dose-dependant reduction in both RCR and ADP/O values in mitochondria from all 3 tissues. This decrease was generally significant at each dose level, and in all 3 mitochondrial types (Table 5.1)

5.3.2 The effect of TMPD on *in vitro* mitochondrial ATP synthesis.

The synthesis of ATP was significantly reduced by TMPD in skeletal muscle, heart, and liver mitochondria in a dose-related fashion. At the highest concentration of TMPD (0.5 mM), synthesis values were reduced to 52%, 54% and 43% of their respective controls (Fig. 5.1).

5.3.3 The effect of TMPD on *in vitro* mitochondrial GSH concentration.

Incubation of TMPD with skeletal muscle, heart, and liver mitochondria caused a marked depletion of GSH levels in a dose-dependant manner. This effect was significant at each TMPD concentration, and in all 3 tissues studied (Fig. 5.2).

5.3.4 The effect of TMPD on *in vitro* mitochondrial complex activities.

Complex I activity of liver mitochondria was not significantly affected by treatment with the amine (Fig. 5.3). TMPD treatment decreased the activity of Complex I in skeletal muscle mitochondria, and this effect was significant at the highest concentration of TMPD (0.5mM). However, heart values were reduced to 55% of controls at the highest concentration (0.5 mM), although due to sample variation this reduction was not statistically significant (Fig. 5.3).

Complex II-III activities showed a similar pattern to Complex I results following incubation with TMPD (Fig. 5.4). Liver activity, although depressed in comparison with controls (63% at 0.5 mM), was not significantly reduced. Skeletal muscle mitochondrial Complex II-III activities were markedly reduced by TMPD treatment. This effect was significant at each of the 3 TMPD concentrations studied. Complex II-III activity of heart mitochondria was also significantly reduced (66% with respect to controls) at the highest TMPD concentration level (Fig. 5.4).

5.4 DISCUSSION

The oxidation of TMPD, a reaction catalysed intracellularly by the mitochondrial protein cytochrome *c* oxidase (Complex IV) (Munday, 1992; Sood et al., 1997), requires the concomitant reduction of NAD^+ (Sood et al., 1997). NAD^+ is an important substrate required for ATP synthesis. Thus, unchecked oxidation of TMPD will compromise this synthetic pathway as the cellular pool of NAD^+ becomes depleted. Glutathione may react directly or indirectly with TMPD in an attempt to detoxify the amine. However, to ensure the continued protection of critical thiol groups present within the cell, from the oxidation products of TMPD metabolism, the pool of reduced glutathione (GSH) must be maintained. This is achieved by glutathione reductase, which catalyses the NAD(P)H dependent re-reduction of oxidised glutathione (GSSG). Although these events generally constitute a highly effective antioxidant defence mechanism, compounds such as TMPD which undergo redox cycling, could cause excessive glutathione oxidation and lead to pyrimidine nucleotide (e.g. NAD(P)H) depletion.

Previous investigations concerning the toxicity of ring-methylated TMPD have focused either on the mitochondrial metabolism of the amine and its effects on respiratory control, or on testing the hypothesis that the toxicity of TMPD is directly linked to its redox-cycling nature within the cell (Munday, 1992; Sood et al., 1997). The reason(s) for the deleterious effects of TMPD on mitochondrial function has received little attention by way of experimental study. Therefore, in the present studies, a number of assays were undertaken to determine the level of mitochondrial dysfunction and its importance in the overall mechanism of TMPD toxicity, were undertaken.

Investigations of mitochondrial respiration using isolated mitochondria incubated with TMPD in an oxygen electrode chamber resulted in a dramatic reduction of both respiratory control and ADP/O ratios, in skeletal muscle, heart, and liver mitochondria.

This effect was in accordance with the findings of Munday (1992) and was significant even at the lowest concentration of TMPD (0.1 mM).

Ring-methylated TMPD enters the respiratory chain at Complex IV, effectively bypassing 2 points of proton extrusion, namely, Complex I and Complex III. Thus, like its N-methylated isomer, ring-methylated TMPD could be described as a redox-slip inducer (Groen et al., 1990). This means that TMPD lowers the number of protons pumped per oxygen atom consumed from a maximum of 3 (possible with NAD-linked substrates) to just 1 proton. As one would expect, this translates into a reduction in the electrochemical gradient upon which the synthesis of ATP depends. Such an effect is reflected by the ATP synthesis data (Fig. 5.1), which shows significantly decreased synthesis in all 3 types of mitochondria and at each TMPD concentration with respect to controls.

Cells are normally protected against oxidative damage by multiple enzymatic mechanisms (discussed in Chapter 1), and by antioxidant molecules. Among the latter, glutathione is a key component and contributes to cellular defence in a number of guises: as a free radical scavenger, as a coenzyme for several antioxidant enzymes, in the maintenance of redox status, and in the detoxification of electrophilic xenobiotics via conjugation. However, redox cycling agents present something of a challenge in terms of the cell's ability to 1), halt the reaction and 2), detoxify and remove potentially harmful products. TMPD is believed to undergo futile redox cycling within the mitochondria (Sood et al., 1997) and if such a reaction occurs *in vivo*, the protection of this organelle against any pro-oxidants generated from the cytochrome-*c*-oxidase-catalysed oxidation of the ring-methylated amine, will largely depend upon local antioxidant defence systems. Skeletal muscle is reported to have low levels of catalase and superoxide dismutase (Grankvist et al., 1981), in comparison to other tissues, and therefore might be expected to rely on GSH-dependent reactions for the detoxification of reactive oxygen species.

Only a small fraction of cellular GSH (10-15%) resides in mitochondria, where it is concentrated (10 mM in the mitochondrion against 7 mM in the cytosol of hepatocytes) (Jocelyn, 1975). GSH is synthesized solely in the cytoplasm, in a translation-independent reaction from glutamine, glycine and cysteine (Griffith, 1999). The tripeptide is then transported into the mitochondria via an energy-dependent transporter (Meister et al., 1988). In the absence of applied stress (e.g. toxicant administration, radiation), very marked depletion of GSH, *in vivo*, was found to be necessary before skeletal muscle mitochondrial damage occurred (Martensson and Meister, 1989). Administration of TMPD caused a dramatic reduction of mitochondrial GSH levels (Fig. 5.2), and the lowest dose (0.1 mM) resulted in at least a 50% reduction of GSH in all 3 types of mitochondrial preparation. At the highest concentration of TMPD (0.5 mM), the reductions of mitochondrial GSH levels were even more pronounced, and were accompanied by a number of significant changes in mitochondrial function. These included, decreased ATP synthesis in skeletal muscle, heart and liver preparations, and decreased respiratory chain complex I, and complex II-III activities, of skeletal muscle and of skeletal muscle and heart, respectively.

Under normal physiological conditions, mitochondria are known to produce small but significant quantities of reactive oxygen species (Boveris and Chance, 1973) whereby an estimated 2-5% of the oxygen utilized by mitochondria is converted via superoxide dismutase to hydrogen peroxide. Normally the hydrogen peroxide is efficiently destroyed by glutathione peroxidase, but in conditions where free GSH is deficient (perhaps as a consequence of oxidative stress, or via experimental depletion, for example using buthionine sulphoximine, BSO) reactive oxygen species may accumulate leading to mitochondrial and other types of cell damage. A single dose of TMPD ($60\mu\text{mol kg}^{-1}$) administered subcutaneously to rats showed, at the level of the light microscope, myofibre necrosis and infiltration of neutrophil polymorphs (Fig. 3.6b). Electron microscopy showed evidence of mitochondrial swelling and vacuolization, with rupture of cristae and membrane damage (Fig. 3.7b). The mitochondrial changes were similar to those found after mitochondrial glutathione depletion by BSO treatment (Martensson and

Meister, 1989). Tissue levels of diaphragm glutathione were reduced following TMPD administration (Fig. 3.10b), although depletion was reversed at 8 hours post dose. Depletion of hepatic glutathione levels was much more transient, in that an effect concordant with rebound synthesis was observed at 1 hour post dose (Fig. 3.10a), suggesting that the liver can respond much more quickly to a shift in redox status *in vivo* than skeletal muscle. As discussed above, mitochondrial glutathione does not arise by intra-mitochondrial synthesis (Meister, 1995) but from the cytosol via a rapid exchange transport mechanism (Griffith and Meister, 1985). Thus in the absence of the cytosolic fraction of the cell, not only is *de novo* synthesis of GSH impossible, but repletion of mitochondrial GSH from the cytosolic pool is also prevented. This presumably accounts for the almost equal susceptibility *in vitro* of liver, heart and skeletal muscle mitochondria to the toxic effects of TMPD, namely its interference with mitochondrial energy metabolism and depletion of the mitochondrial GSH pool. Furthermore, if cardiac peroxisome activity plays an important role in the detoxification of TMPD in the heart, *in vivo*, the absence of the cell cytosol in the present experiments could explain the increased susceptibility of heart mitochondria, *in vitro*.

Redox cycling agents are particularly damaging to cells because attempts to 'neutralise' their ability to damage critical cellular proteins, will often lead to exhaustion of valuable cell substrates, many of which have functions other than detoxification and which will require re-synthesis if these additional functions can continue. NADH depletion has been reported to occur in hepatocyte cultures exposed to 2,3,5,6-TMPD (Sood et al., 1997). This would appear to be a consequence of TMPD oxidation by cytochrome-*c* oxidase and the subsequent regeneration of the parent compound by DT-diaphorase (NAD(P)H:quinone oxidoreductase, E.C.1.6.99.2). Inhibition of DT-diaphorase activity results in the accumulation of the di-imine metabolite and greatly reduces cell viability. Reduced glutathione also plays an important cytoprotective role, as prior removal of GSH, or inhibition of glutathione reductase, increases the toxicity of the amine (Sood et al., 1997). GSH regeneration by glutathione reductase requires NADPH as a cofactor. Successive rounds of oxidation and reduction of TMPD would ultimately lead to the

depletion of cellular NADPH, at which point glutathione reductase would be unable to reduce GSSG. Accumulation of GSSG often leads to the removal of the tripeptide from the cell, thereby decreasing the cellular thiol pool. NADPH can be regenerated via inter-conversion of NADH, thus facilitating glutathione reductase activity in the short-term but at the expense of the mitochondrion's requirements in terms of available substrate for ATP synthesis; this is the ultimate factor underlying cell death or repair. Additional support for pyrimidine nucleotide depletion, and the ensuing toxicity of TMPD, is provided by Sood et al. (1997). They demonstrated that glycolytic substrates, which increase cytosolic NADH levels such as pyruvate and lactate, delayed oxidised glutathione accumulation and were cytoprotective.

Thus, it would appear that the antioxidant defense systems of mitochondria can be effectively regenerated after or during oxidative stress as long as the mitochondria are in an energised state. Should the delicate balance between prooxidative/antioxidative activities be shifted, for example by a prooxidant like TMPD, antioxidant defense systems will become exhausted, and damage to the mitochondria will result. This will be manifested primarily by a loss of function (as demonstrated by the above experiments) followed by membrane injuries, oxidation and degradation of mitochondrial lipids and proteins leading finally to the total degradation of the mitochondria (Augustin et al., 1997).

Oxidative stress, in addition to glutathione depletion, may also lead to the accumulation of protein mixed disulphides. This process, also known as S-glutathiolation, is thought to be protective, whereby GSH prevents protein oxidation by conjugating with oxidised thiol groups to form protein mixed disulphides R-SSG. These molecules can then be re-reduced to protein and GSH by glutathione reductase, thioredoxin or protein disulphide isomerase (Jung and Thomas, 1996). However, whether or not such a reversible mechanism is at work in the toxicity of TMPD is unclear. In general, extensive oxidative modifications of proteins are related to a permanent loss of function (Berlett and

Stadtman, 1997). However a number of studies have revealed that certain proteins, including creatine kinase (Collison and Thomas, 1987), thioredoxin (Klatt and Lamas, 2000) and Ca²⁺-ATPase (Viner et al., 1999), are major targets for redox-dependent S-glutathiolation. In Chapter 4, TMPD was found to decrease glutathione reductase activity in myocyte cultures. This effect was also noted by Sood et al. (1997). However, bearing in mind the nature of the assay used to measure the enzyme's activity (NADPH used in the assay is in excess), the decrease in glutathione reductase activity cannot be attributed to lack of the cofactor NADPH, as Sood et al. (1997) suggest. Further work would be necessary to determine if the enzyme had been modified by S-glutathiolation.

Proteins of the mitochondrial electron transport chain are also reported to be targets of reactive oxygen species (Bolanos et al., 1996; Jha et al., 2000). Complex I (NADH ubiquinone oxido-reductase) is one of the largest and most important components of mitochondrial electron transport (Balijepalli et al., 1999), and contains several critical thiol groups which may be vulnerable to oxidative modification, resulting in loss of activity (Dupius et al., 1991). It has been hypothesized that inhibition of complex activity could lead to leakage of electrons, resulting in generation of oxidative stress leading to further inhibition of the enzyme (Balijepalli et al., 1999). A decrease in Complex I activity in skeletal muscle (Fig. 5.3) and in complex II-III activity in both heart and skeletal muscle (Fig. 5.4) following incubation of mitochondria with TMPD, suggests that these proteins are vulnerable to damage by reactive oxygen species *per se* or by depletion of reduced glutathione levels, both of which could lead to generation of reactive oxygen species (Ravindranath and Reed, 1990). Although the exact mechanism by which TMPD causes inactivation of these membrane proteins is unknown, it would appear from investigations by Sood et al. (1997) that if the process of S-glutathiolation does indeed occur in response to the oxidant challenge posed by TMPD, then the length of time afforded for protection would seem rather short. Sood and his co-workers found that NADH generators added after 60 minutes of TMPD-exposure to hepatocytes were not cytoprotective.

Table 5.1The effect of TMPD (0.1-0.5 mM) on *in vitro* mitochondrial respiration of skeletal muscle, heart, and liver

TMPD (mM)	RCR ^a			ADP/O ^b		
	Skeletal muscle	Heart	Liver	Skeletal muscle	Heart	Liver
0.00	4.75 (0.25)	6.67 (0.37)	4.67 (0.48)	2.94 (0.05)	2.82 (0.08)	2.87 (0.10)
0.10	2.05 (0.33)*	2.09 (0.51)*	2.24 (0.68)	1.54 (0.02)*	2.31 (0.10)*	1.48 (0.05)*
0.25	1.15 (0.28)*	1.34 (0.30)*	1.28 (0.11)*	1.25 (0.08)*	1.90 (0.05)*	1.31 (0.06)*
0.50	1.09 (0.17)*	1.14 (0.18)*	1.12 (0.23)*	1.13 (0.10)*	1.52 (0.15)*	1.18 (0.1)*

^a RCR represents respiratory control ratio, ^b ADP/O represents ADP/O ratio. Results are means (SEM) of 4 separate preparations. Statistically analysed using Dunnett's test for multiple comparisons using a single control, with the level of significance set at * $P < 0.05$.

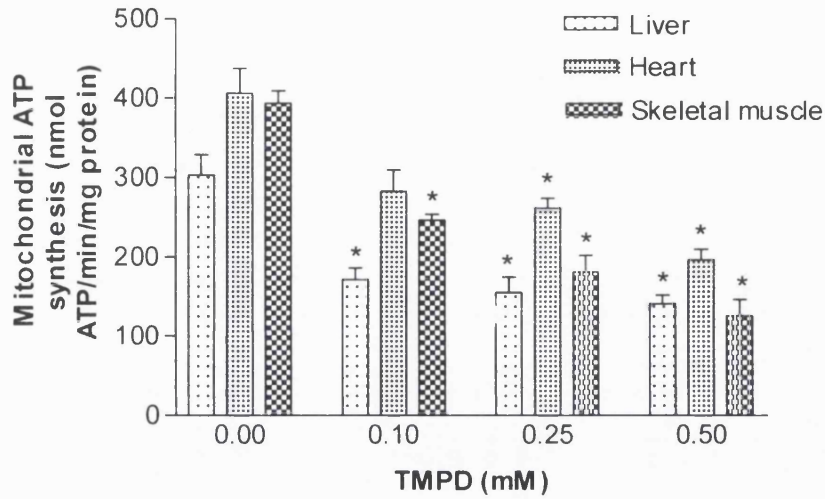


Figure 5.1 The effect of TMPD (0.1-0.5 mM) on ATP synthesis of freshly isolated rat liver, heart, and skeletal muscle mitochondria. Data are expressed as mean \pm SEM for 4 independent mitochondrial preparations. * $P < 0.05$, when compared to the appropriate control, one-way ANOVA and post hoc Dunnett test.

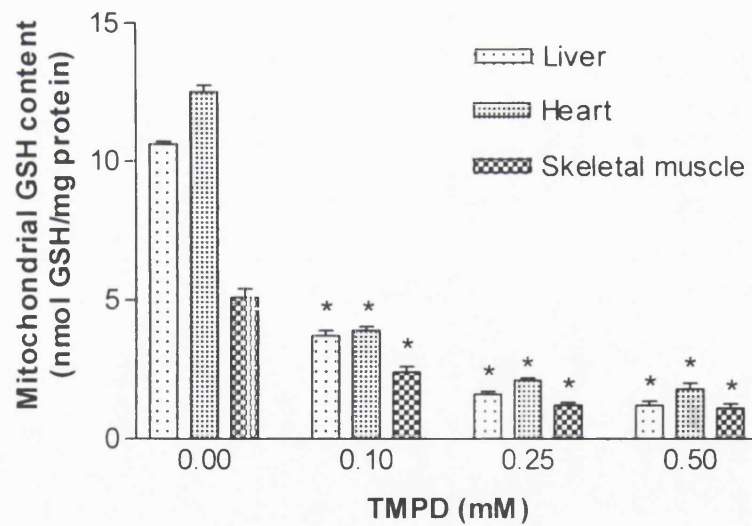


Figure 5.2 The effect of TMPD (0.1-0.5 mM) on GSH content of freshly isolated rat liver, heart, and skeletal muscle mitochondria. Data are expressed as mean \pm SEM for 4 independent mitochondrial preparations. * $P < 0.05$, when compared to the appropriate control, one-way ANOVA and post hoc Dunnett test.

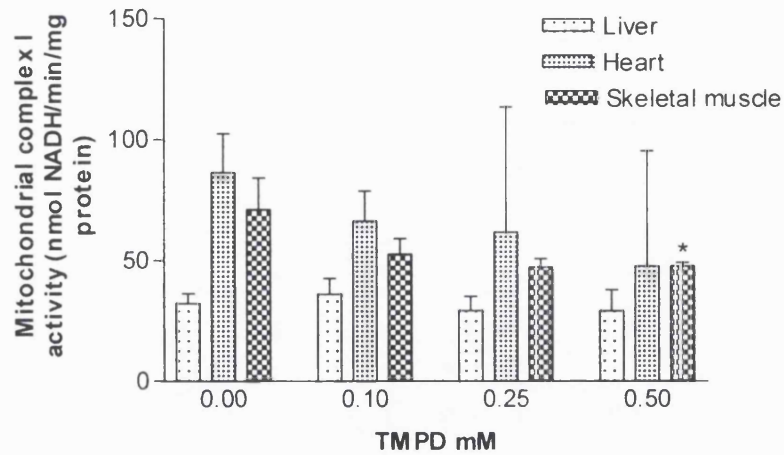


Figure 5.3 The effect of TMPD (0.1-0.5 mM) on Complex I activity of freshly isolated rat liver, heart, and skeletal muscle mitochondria. Data are expressed as mean \pm SEM for 4 independent mitochondrial preparations. * $p < 0.05$, when compared to the appropriate control, one-way ANOVA and post hoc Dunnett test.

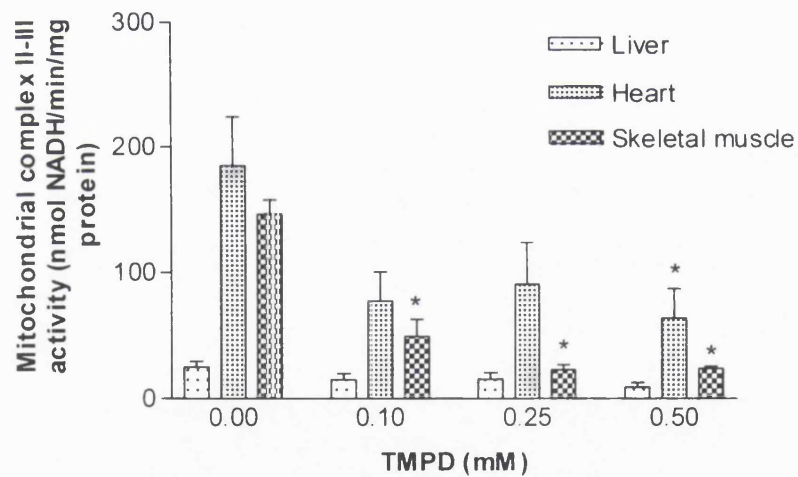


Figure 5.4 The effect of TMPD (0.1-0.5 mM) on Complex II-III activity of freshly isolated rat liver, heart and skeletal muscle mitochondria. Data are expressed as mean \pm SEM for 4 independent mitochondrial preparations. * $P < 0.05$, when compared to the appropriate control, one-way ANOVA and post hoc Dunnett test.

CHAPTER 6

FINAL DISCUSSION

6.1 THE ROLE OF THE MITOCHONDRION IN TMPD TOXICITY

2,3,5,6-TMPD is a highly selective toxic agent when administered *in vivo*. Its effects are almost exclusively myotoxic, with the exception of a discrete cytotoxic effect evident in the testis (Draper et al., 1994). Such specificity suggests that TMPD toxicity results from exposure to a metabolite of the parent compound rather than toxicity to TMPD *per se*.

At the start of the present project it was known that oxidation of 2,3,5,6-TMPD was effectively catalysed by cytochrome *c* oxidase (Packer and Mustafa, 1966) i.e. Complex IV of the mitochondrial respiratory chain. It had also been shown that mitochondria of skeletal muscle could facilitate the reaction more quickly than any other tissue studied, including the liver (Munday, 1992). Despite this knowledge and preliminary data to suggest that TMPD disrupts the normal respiratory function of isolated mitochondria, the mechanism of toxicity, and the reasons for the particular vulnerability of skeletal muscle, were not fully understood.

Studies of TMPD metabolism *in vitro* revealed that the amine will readily autoxidise to form the relatively stable Würster salt and quinone-dimine derivative. In the presence of NADH, NADPH or GSH, re-reduction of TMPD occurred (Munday et al., 1990), thus demonstrating the ability of the oxidised compound to accept electrons from a number of important cellular reducing agents. These findings are consistent with the establishment of a redox cycle between the amine and its oxidation products.

Interestingly, the cytotoxic effects of TMPD appear to be a consequence of the redox cycling *per se*, as opposed to a particular metabolite or indeed the amine itself, as demonstrated by Munday (1992) when equivalent deleterious effects of both the Würster salt and 2,3,5,6-TMPD upon oxidative phosphorylation were confirmed.

Depletion of cellular ATP following TMPD administration is clearly related to mitochondrial dysfunction. The amine causes a significant loss of the nucleotide *in vivo* (diaphragm), and *in vitro*, and interferes with the synthetic activity of isolated mitochondria. Electron micrographs of damaged skeletal muscle tissue reveal grossly swollen mitochondria (Fig. 3.7b) and sarcotubular systems (Fig. 3.8b). These structural changes are likely to arise as a result of compromised active transport into, out of, and within the cell, such that the concentrations of various ions (e.g. Na⁺ and K⁺) will change. Depletion of ATP would also lead to increased levels of intracellular Ca²⁺, presumably as a result of reduced activity of the Ca²⁺-transporting ATPases. Prolonged increases in cytosolic Ca²⁺ can stimulate the activity of Ca²⁺-dependant phospholipases and proteases. Under normal physiological conditions these enzymes are involved in the destruction of by-products of lipid peroxidation, and membrane remodelling, respectively. However, unchecked levels of cytosolic Ca²⁺ results in prolonged action of these enzymes, which in turn leads to the release of cytotoxic compounds, mediators of inflammation and destruction of the cell membrane. The infiltration of neutrophil polymorphs into damaged skeletal muscle tissue, in conjunction with raised levels of enzymes in the serum in TMPD-treated rats, and also the leakage of lactate dehydrogenase into the extracellular medium of cultured skeletal myocytes and loss of intracellular creatine kinase, all provide strong evidence to suggest that such secondary events do occur as a consequence of TMPD oxidation within the mitochondrion.

A recent study of TMPD cytotoxicity was carried out by Sood et al. (1997) using isolated hepatocytes. Despite an inhibitory effect of catalase on TMPD autoxidation reported by Munday et al. (1990) and the subsequent belief that the cytotoxic actions of TMPD were attributed to reactive oxygen species, Sood et al. (1997) found little detectable oxygen activation. Moreover, the absence of lipid peroxidation and lack of

cytoprotection by superoxide dismutase mimetics, and xanthine oxidase inhibitors, is in accordance with the findings of this project; skeletal muscle cells did not show any significant changes in the levels of superoxide dismutase activity *in vivo*, or *in vitro*. Sood and his co-workers (1997) proposed that the mechanism of TMPD toxicity was the result of a futile 2 electron redox cycle involving the oxidation of TMPD to its di-imine derivative by cytochrome *c* oxidase, and re-reduction by DT-diaphorase (NAD(P)H: quinone oxidoreductase). The reductive metabolism of quinones and their derivatives by DT-diaphorase produces stable hydroquinones that are removed by conjugation with glutathione or UDP-glucuronic acid (Radjendirane et al., 1997). The importance of DT-diaphorase in the detoxification of TMPD was demonstrated by Sood et al. (1997). They showed that TMPD cytotoxicity (as assessed by trypan blue exclusion) was markedly increased by inactivating this enzyme with dicumarol. A study of DT-diaphorase gene expression in several tissues of the mouse (Long and Jaiswal, 2000) revealed that the highest levels are found in heart, with slightly lower levels in liver. Mouse skeletal muscle tissue had an undetectable level of gene expression. It is also of interest that the testis was found to have undetectable levels (Long and Jaiswal, 2000). If the pattern of gene expression in the mouse, found a parallel in the rat, it would help to explain the particular susceptibility of skeletal muscle (and indeed the testis) to the toxic effects of TMPD.

6.2 THE ROLE OF THE GLUTATHIONE SYSTEM IN TMPD TOXICITY

Glutathione is the predominant non-protein, low molecular weight thiol in mammalian cells (Griffith, 1999), and plays a major role in the maintenance of cellular thiol-disulphide status. Many proteins, found within the cytosol or mitochondrion, including dehydrogenases, ATPases and transport proteins, contain essential sulphhydryl groups that must be in the reduced form to be active. Thus alterations in redox status with concomitant GSH oxidation will lead to loss of function (Smith et al., 1996).

Redox cycling of TMPD leads to the formation of glutathione disulphide (GSSG) (Sood et al., 1997). This species is reduced intracellularly to GSH by glutathione reductase in a NADPH-dependant reaction (Kehrer and Lund, 1994). At normal levels of oxidative stress, glutathione reductase activity and NADPH availability, are sufficient to maintain $[GSH]:[GSSG] > 100$ (Akerboom et al., 1982). However, the degree of stress evoked by TMPD is such that GSSG accumulates and is secreted from the cell (Sood et al., 1997). This shift in cell redox status is reported to evoke two consequences: 1), the activation of certain oxidant response transcriptional elements and 2), the GSSG secreted will be degraded extracellularly, as it cannot be taken up by intact cells (Griffith, 1999). The biochemical fate of oxidised glutathione will therefore increase the cellular requirement for *de novo* GSH synthesis.

Redox-sensitive regulatory molecules in the cell (e.g. NF K β) appear to detect oxidative stress-mediated events and react by triggering homeostatic responses to prevent cell injury (Schreck and Baeuerle, 1994). The increased glutathione-S-transferase (GST) activity observed *in vivo* and *in vitro*, both in liver and skeletal muscle cells, may be a direct effect of molecules such as NF K β activation and resultant gene transcription within the nucleus.

Glutathione reductase, the enzyme central to GSH regeneration, is inhibited by TMPD treatment. This effect is confined to skeletal muscle only, but occurs both *in vivo* and *in vitro*. Sood et al. (1997) reported a similar inhibitory effect of the amine and suggested that it was secondary to the exhaustion of cellular NADPH levels caused by redox cycling of TMPD. Glutathione reductase contains a number of cysteine residues that can be modified in response to oxidative stress. S-nitrosoglutathione (GSNO), an *in vivo* transport form of NO has been reported to oxidise the active site residue Cys 63 to a cysteine sulphenic acid (R-OH) (Becker et al., 1998). Quinones have also been reported to inactivate the enzyme and glutathione was found to protect against inactivation. This suggests that these compounds interact with a glutathione binding centre, probably Cys 2 (Bironaite et al., 1993). The reason for the loss in glutathione reductase activity is unknown at present. NADPH depletion and/or

cysteine residue modification are possible mechanisms that need to be further investigated.

Reduced activity of glutathione reductase and extrusion of the GSSG that accumulates as a result, will lead to the rapid depletion of the cellular thiol pool of skeletal muscle, a phenomenon observed to occur at certain time-points following TMPD administration *in vivo*, and more convincingly *in vitro*, in both cultured myocytes and isolated mitochondria exposed to the amine. This would render skeletal muscle vulnerable to the damaging effects associated with oxidative stress. When a tissue such as the liver has an increased requirement for glutathione, GSH is synthesized from its constituent amino acids by the sequential action of γ -glutamylcysteine synthetase (γ -GCS) and GSH-synthetase; the γ -GCS reaction is rate-limiting (Meister and Anderson, 1983). *De novo* GSH synthesis is thought to be regulated by at least 3 factors: 1), the level of γ -GCS present in the cell; 2), the availability of its substrates, particularly L-cysteine, and 3), feedback inhibition of GSH on γ -GCS (Griffith, 1999). There are major differences in GSH status between liver, heart and skeletal muscle. The liver is a major source of GSH synthesis, with a cytosolic GSH concentration of 7mM. Heart and skeletal muscle have a much smaller synthetic capacity, which is reflected by their modest [GSH] of 1.15 and 0.77 $\mu\text{mol g}^{-1}$, respectively (Meister, 1995). Moreover, low levels of γ -GCS activity have been found in heart (Mårtensson and Meister, 1989) although at 13.9 $\text{nmol h}^{-1} \text{mg}^{-1}$ protein, this activity is significantly higher than that present in skeletal muscle (5.5 $\text{nmol h}^{-1} \text{mg}^{-1}$ protein) (Mårtensson and Meister, 1989). In contrast, under comparable conditions, a liver γ -GCS activity of 83 $\text{nmol h}^{-1} \text{mg}^{-1}$ protein has been reported (Meister, 1995). γ -glutamyl transpeptidase activities (the enzyme responsible for cellular uptake of GSH precursor products), are in parallel with those of γ -GCS reported in liver, heart and skeletal muscle (Mårtensson and Meister, 1989). With such low inherent γ -GCS activity, skeletal muscle and heart will depend to a large extent upon the interorgan transport of extracellular glutathione. Turnover of the cellular thiol pool occurs very rapidly in liver ($t_{1/2} = 1$ hour), whereas GSH turnover in heart and skeletal muscle is much slower. Decline of GSH levels in mice treated with BSO is biphasic and reflects depletion of the cytosolic (fast component), and mitochondrial (slow component),

thiol fractions. With turnover rates of 5.5-460 hours and 16-120 hours in heart and skeletal muscle, respectively (Mårtensson and Meister, 1989), xenobiotic depletion of GSH from these tissues, particularly the mitochondrial fraction, is likely to result in the death of the affected cells. However, a number of biochemical characteristics of skeletal muscle appear to selectively predispose this tissue to the toxic effects of TMPD, including higher cytochrome *c* oxidase levels, negligible DT-diaphorase activity, and significantly less antioxidant capacity than either heart or liver.

Glutathione will react spontaneously with some electrophiles but most reactions require catalysis by GST. The initial products are chemically stable sulphides of GSH, but further metabolism removes the L-glutamate and glycine residues to form *S*-substituted L-cysteines. Subsequent formation of the easily excretable end product, mercapturic acid, results in the irreversible loss of L-cysteine, the amino acid most often limiting for GSH synthesis (Griffith, 1999). Glutathione replacement therapy whereby an L-cysteine precursor, typically N-acetyl-L-cysteine (NAC) is administered to increase the availability of this crucial amino acid (and to replace the L-cysteine irreversibly lost through the formation of GST products), is commonly used to treat acetaminophen overdose (Smilkstein et al., 1988). However, despite the similarities between acetaminophen and TMPD toxicity, NAC administration to TMPD-treated rats did not prevent the toxic effects of the amine. Ethanol ingestion has also been reported to decrease cytosolic and mitochondrial levels of reduced glutathione (Colell et al., 1997; Guidot and Brown, 2000). Alcohol exerts its effects by impairing the transport of GSH from the cytosol into the mitochondria (Colell et al., 1997). *S*-Adenosyl-L-methionine and procysteine supplementation of ethanol-fed rats restored mitochondrial glutathione levels but NAC did not (Colell et al., 1997; Guidot and Brown, 2000). Clearly the effects of NAC supplementation upon the GSH compartmentation in skeletal muscle of TMPD-treated rats, requires further investigation.

6.3 GENERAL CONCLUSIONS

- 1) The toxic effects of TMPD are exclusive to skeletal muscle with the exception of a discrete cytotoxic effect in the testis (at $> 40 \mu\text{mol kg}^{-1}$); the testicular lesion shows abnormal and degenerate spermatocytes in stage 14 tubules.
- 2) Type IIA/X muscle fibres appear to be more vulnerable to the toxic effects of TMPD than either type I or type IIB fibres. The large number of type IIA/X fibres in diaphragm may explain why lesions in this tissue were always more severe than those in the other muscles examined.
- 3) Depletion of cellular GSH in skeletal muscle occurs in parallel with the loss of cellular ATP. This is likely to be due to competition between the requirements of oxidative phosphorylation and those of GSH regeneration in an effort to maintain the viability of the muscle cell when exposed to TMPD.
- 4) The increased activity of GST in liver probably mediates the effective detoxification of TMPD in this organ. The increased GST activity of skeletal muscle is also likely to clear a significant portion of the amine, but at the expense of this tissue's much smaller thiol pool, together with the irreversible loss of L-cysteine, the rate-limiting amino acid of GSH synthesis.
- 5) Partial inactivation of GRed activity in skeletal muscle, as a consequence of TMPD treatment, will lead to the accumulation of GSSG and its removal from the cell, exacerbating the depletion of reduced glutathione.

- 6) Loss of mitochondrial glutathione is accompanied by a dramatic decrease in the activities of complex I and complex II-III enzymes. Under such circumstances the cell would be unable to maintain its ATP levels. Thus TMPD exerts its toxic effects by depleting the cell, or more specifically the mitochondrion, of GSH, with the concomitant loss of mitochondrial and other cellular functions.

REFERENCES

Akerboom, T. P., M. Bilzer, et al. (1982). The relationship of biliary glutathione disulfide efflux and intracellular glutathione disulfide content in perfused rat liver. *J Biol Chem* **257**: 4248-4252.

Alexandre, A. and A. L. Lehninger (1984). Bypasses of the antimycin a block of mitochondrial electron transport in relation to ubiquinone function. *Biochim Biophys Acta* **767**: 120-129.

Ames, B. N., J. McCann, et al. (1975). Proceedings: carcinogens are mutagens: a simple test system. *Mutat Res* **33**: 27-28.

Anthony, H. M. and G. M. Thomas (1970). Bladder tumours and smoking. *Int J Cancer* **5**(2): 266-272.

Argov, Z. and F. L. Mastaglia (1988). Drug-induced neuromuscular disorders in man. In: *Disorders of Voluntary Muscle*. Walton, J. N. (eds.) p 981, Churchill Livingstone, London.

Augustin, W., I. Wiswedel, et al. (1997). Role of endogenous and exogenous antioxidants in the defence against functional damage and lipid peroxidation in rat liver mitochondria. *Mol Cell Biochem* **174**: 199-205.

Baldwin, K. M. and C. M. Tipton (1972). Work and metabolic patterns of fast and slow twitch skeletal muscle contracting in situ. *Pflugers Arch* **334**: 345-356.

Balijepalli, S., J. Annepu, et al. (1999). Effect of thiol modification on brain mitochondrial complex I activity. *Neurosci Lett* **272**: 203-206.

Bates, T. E., A. Loesch, et al. (1995). Immunocytochemical evidence for a mitochondrially located nitric oxide synthase in brain and liver. *Biochem Biophys Res Commun* **213**: 896-900.

Becker, K., S. N. Savvides, et al. (1998). Enzyme inactivation through sulfhydryl oxidation by physiologic NO- carriers. *Nat Struct Biol* **5**: 267-271.

Berlett, B. S. and E. R. Stadtman (1997). Protein oxidation in aging, disease, and oxidative stress. *J Biol Chem* **272**: 20313-20316.

Bironaite, D. A., N. K. Chenas, et al. (1993). Inactivation of glutathione reductase by quinones and nitrosocarbamides. *Ukr Biokhim Zh* **65**: 97-100.

Blair, J.A., C.J. Waterfield, et al. (1997). The skeletal muscle-specific toxicity of 2,3,5,6-tetramethyl-*p*-phenylenediamine (TMPD): some preliminary studies. *Hum Exp Tox* **16**: 403.

Blair, J.A., C.J. Waterfield, et al. (1998). Comparative studies on the skeletal muscle toxicity of 2,3,5,6-tetramethyl-*p*-phenylenediamine *in vitro* using cultured myocytes, hepatocytes and isolated mitochondria. *Hum Exp Tox* **17**: 519.

Bolanos, J. P., S. J. Heales, et al. (1996). Nitric oxide-mediated mitochondrial damage: a potential neuroprotective role for glutathione. *Free Radic Biol Med* **21**: 995-1001.

Boveris, A. and B. Chance (1973). The mitochondrial generation of hydrogen peroxide. General properties and effect of hyperbaric oxygen. *Biochem J* **134**: 707-716.

O'Brien, P. J. (1988). Radical formation during the peroxidase catalyzed metabolism of carcinogens and xenobiotics: the reactivity of these radicals with GSH, DNA, and unsaturated lipid. *Free Radic Biol Med* **4**(3):169-183.

Brooke, M. H. and K. K. Kaiser (1970). Muscle fibre types: how many and what kind? *Arch Neurol (Chicago)* **23**: 369.

Burcham, P. C. and A. W. Harman (1991). Acetaminophen toxicity results in site-specific mitochondrial damage in isolated mouse hepatocytes. *J Biol Chem* **266**: 5049-5054.

Burgunder, J. M., A. Varriale, et al. (1989). Effect of N-acetylcysteine on plasma cysteine and glutathione following paracetamol administration. *Eur J Clin Pharmacol* **36**: 127-131.

Burnett, C. M. and E. I. Goldenthal (1988). Multigeneration reproduction and carcinogenicity studies in Sprague-Dawley rats exposed topically to oxidative hair-colouring formulations containing *p*-phenylenediamine and other aromatic amines. *Food Chem Toxicol* **26**: 467-474.

Burtis, C. B. and E. R. Ashwood (1995). *Tietz Fundamentals of Clinical Chemistry*. W. B. Saunders, New York.

Carbonera, D. and G. F. Azzone (1988). Permeability of inner mitochondrial membrane and oxidative stress. *Biochim Biophys Acta* **943**: 245-255.

Carlberg, I. and B. Mannervik (1985). Glutathione reductase. *Methods Enzymol* **113**: 484-90.

Chance, B. (1947). *Acta Chem Scand* **1**: 236.

Chance, B., H. Sies, et al. (1979). Hydroperoxide metabolism in mammalian organs. *Physiol Rev* **59**: 527-605.

Chaudière, J. (1994) Some chemical and biochemical constraints of oxidative stress in living cells. In: *Free Radical Damage and its Control*. Rice-Evans, C.A. and Burdon R.H. (eds.). pp. 25-66, Elsevier Science, London.

Clark, J. B., T. E. Bates et al. (1997) Investigation of mitochondrial defects in brain and skeletal muscle. In: *Neurochemistry – a practical approach* (2nd edition) Turner, A.J., and H. S. Bachelard (eds.) pp 151-174, Oxford University Press, Oxford.

Close, R. I. (1972). Dynamic properties of mammalian skeletal muscles. *Physiol Rev* **52**: 129.

Colell, A., C. Garcia-Ruiz, et al. (1997). Transport of reduced glutathione in hepatic mitochondria and mitoplasts from ethanol-treated rats: effect of membrane physical properties and S-adenosyl-L-methionine. *Hepatology* **26**: 699-708.

Collison, M. W. and J. A. Thomas (1987). S-thiolation of cytoplasmic cardiac creatine kinase in heart cells treated with diamide. *Biochim Biophys Acta* **928**: 121-129.

Combes, R. D. and R. B. Haveland-Smith (1982). A review of the genotoxicity of food, drug and cosmetic colours and other azo, triphenylmethane and xanthene dyes. *Mutat Res* **98**: 101-248.

Cooper, J. M., R. K. Petty, et al. (1988). An animal model of mitochondrial myopathy: a biochemical and physiological investigation of rats treated in vivo with the NAD-Cod reductase inhibitor diphenyleneiodonium. *J Neurol Sci* **83**: 335.

Crank, G. and Makin, M.I.H. (1984). Oxidations of aromatic amines by superoxide ion. *Aust J Chem* **37**: 845.

Crosbie, S. J., P. G. Blain, et al. (1997). An investigation into the role of rat skeletal muscle as a site for xenobiotic metabolism using microsomes and isolated cells. *Hum Exp Toxicol* **16**(3): 138-145.

Dalakas, M. C., I. Illa, et al. (1990). Mitochondrial myopathy caused by long-term zidovudine therapy. *N Engl J Med* **322**: 1098-1105.

Daniel, P. M. (1977). The metabolic homeostatic role of muscle and its function as a store of protein. *Lancet* **2**: 446-448.

Daniel, V. (1993). Glutathione S-transferases: gene structure and regulation of expression. *Crit Rev Biochem Mol Biol* **28**: 173-207.

Darley-USmar, V. M. and I. Ragan, et al. (1994). The proteins of the mitochondrial inner membrane and their role in oxidative phosphorylation. In: *Mitochondria: DNA, Proteins*

and Disease. Darley-Usmar, V. M. and A. H. V. Schapira (eds.) pp. 1-24, Portland Press, London.

Davis, J. E. (1946). Haemolytic anaemia as a manifestation of paraphenylenediamine toxicity. *J Pharmacol Exp Thera* **88**: 133-135.

Dawson, D. M. and F. C. A. Romanul (1964). Enzymes in muscle. II. Histochemical and quantitative studies. *Arch Neurol (Chicago)* **11**: 369.

De Duve, C. and P. Baudhuin (1966). Peroxisomes (microbodies and related particles). *Physiol Rev* **46**: 323-357.

De Master, E. G. and B. Redfern (1987). High performance liquid chromatography of hepatic thiols with electrochemical detection. In: Jakoby W. B. and Griffith O. W. (eds) *Methods in enzymology*, Vol **143**. pp 110-114, Academic Press, New York.

DiNardo, J. C., J. C. Picciano, et al. (1985). Teratological assessment of five oxidative hair dyes in the rat. *Toxicol Appl Pharmacol* **78**: 163-166.

Draper, R. P., C. J. Waterfield, et al. (1994). Studies on the muscle toxicant 2,3,5,6-tetramethyl p-phenylenediamine: effects on various biomarkers including urinary creatine and taurine. *Arch Toxicol* **69**: 111-117.

Drew, R. and J. O. Miners (1984). The effects of buthionine sulphoximine (BSO) on glutathione depletion and xenobiotic biotransformation. *Biochem Pharmacol* **33**: 2989-94.

Dubowitz, V. and A. G. Pearse (1960). A comparative histochemical study of oxidative enzyme and phosphorylase activity in skeletal muscle. *Histochemie* **2**: 105.

Dupuis, A., J. M. Skehel, et al. (1991). NADH:ubiquinone oxidoreductase from bovine mitochondria. cDNA sequence of a 19 kDa cysteine-rich subunit. *Biochem J* **277**: 11-15.

Ebashi, S. (1980). Regulation of muscle contraction. *Proc Royal Soc Lond B* **207**: 259.

Eklow, L., P. Moldeus, et al. (1984). Oxidation of glutathione during hydroperoxide metabolism. A study using isolated hepatocytes and the glutathione reductase inhibitor 1,3-bis(2-chloroethyl)-1-nitrosourea. *Eur J Biochem* **138**: 459-463.

Ellman, G. L. (1959). Tissue sulfydryl groups. *Arch Biochem Biophys* **82**: 70-77.

Engel, W. K. (1962). The essentiality of histo- and cytochemical studies of skeletal muscle in the investigation of neuromuscular disease. *Neurology (Minneapolis)* **12**: 778.

Evans, G. O. (1996). *Animal Clinical Chemistry – A Primer for Toxicologists*. Taylor and Francis, London.

Ferry, C. B. and M. J. Cullen (1991). Myopathic changes in indirectly stimulated mouse diaphragm after ecotiopate in vitro. *Int J Exp Pathol*. **72**(3):329-343.

Flohé, L and F. Ötting (1984). Superoxide dismutase assays. In: *Methods in enzymology*. **105**: 93-101. Academic Press, New York.

Flohé, L and W. A. Günzler (1984). Assays of glutathione peroxidase. In: *Methods in enzymology*. **105**:114-120. Academic Press, New York.

Farber, E. (1973). ATP and cell integrity. *Fed Proc* **32**: 1534-1539.

Forman, H. J. and Boveris. A. (1982) In: *Free Radicals in Biology*. Vol V, Pryor, W.A., (ed.). pp 14-20, Academic Press, New York.

Fridovich, I. (1986). Superoxide dismutases. *Adv Enzymol Relat Areas Mol Biol* **58**: 61-97.

Frieden, E. and H. S. Hsieh (1976). Ceruloplasmin: the copper transport protein with essential oxidase activity. *Adv Enzymol Relat Areas Mol Biol* **44**: 187-236.

Grankvist, K., S. L. Marklund, et al. (1981). CuZn-superoxide dismutase, Mn-superoxide dismutase, catalase and glutathione peroxidase in pancreatic islets and other tissues in the mouse. *Biochem J* **199**: 393-398.

Griffith, O. W. (1999). Biologic and pharmacologic regulation of mammalian glutathione synthesis. *Free Radic Biol Med* **27**: 922-935.

Griffith, O. W. and A. Meister (1985). Origin and turnover of mitochondrial glutathione. *Proc Natl Acad Sci U S A* **82**: 4668-4672.

Groen, B. H., J. A. Berden, et al. (1990). Differentiation between leaks and slips in oxidative phosphorylation. *Biochim Biophys Acta* **1019**: 121-127.

Guidot, D. M. and L. A. Brown (2000). Mitochondrial glutathione replacement restores surfactant synthesis and secretion in alveolar epithelial cells of ethanol-fed rats. *Alcohol Clin Exp Res* **24**: 1070-1076.

Harauchi, T. and M. Hirata (1993). Effects of p-phenylenediamines and adriamycin on primary culture of rat skeletal muscle cells. *Toxicol Lett* **66**: 35-46.

Harper, J. M., J. B. Soar, et al. (1987). Changes in protein metabolism of ovine primary muscle cultures on treatment with growth hormone, insulin, insulin-like growth factor I or epidermal growth factor. *J Endocrinol* **112**: 87-96.

Haycock, J. W., P. Jones, et al. (1996). Differential susceptibility of human skeletal muscle proteins to free radical induced oxidative damage: a histochemical, immunocytochemical and electron microscopical study in vitro. *Acta Neuropathol (Berlin)* **92**: 331-340.

Helzberg, J. H., M. S. Brown, et al. (1987). Metabolic state of the rat liver with ethanol: comparison of in vivo ³¹phosphorus nuclear magnetic resonance spectroscopy with freeze clamp assessment. *Hepatology* **7**: 83-88.

Hissin, P. J. and R. Hilf (1976). A fluorometric method for determination of oxidized and reduced glutathione in tissues. *Anal Biochem* **74**: 214-26.

Huxley, A. F. and R. Niedergerke (1954). Structural changes in muscle during contraction. *Nature* **173**: 971.

Huxley, H. E. and J. Hanson (1954). Changes in the cross-striations of muscle during contraction, stretch and their structural interpretation. *Nature* **173**: 973.

Ioannou, Y. M. and H. B. Matthews (1985). p-Phenylenediamine dihydrochloride: comparative disposition in male and female rats and mice. *J Toxicol Environ Health* **16**: 299-313.

Jacobs, E. E. (1960). Phosphorylation coupled to electron transport initiated by substituted phenylenediamines. *Biochem Biophys Res Comm* **3**: 536-539.

Jackson, M. J. and S. O'Farrell (1993). Free radicals and muscle damage. *Br Med Bull* **49**: 630-641.

Jasmin, G. (1961). Action Toxique de la Paraphenylenediamine chez le Rat et Quelques Autres Rongeurs. *Rev Can Biol* **20**: 37-46.

Jha, N., O. Jurma, et al. (2000). Glutathione depletion in PC12 results in selective inhibition of mitochondrial complex I activity. Implications for Parkinson's disease. *J Biol Chem* **275**: 26096-26101.

Jocelyn, P. C. (1975). Some properties of mitochondrial glutathione. *Biochim Biophys Acta* **396**: 427-436.

Jung, C. H. and J. A. Thomas (1996). S-glutathiolated hepatocyte proteins and insulin disulfides as substrates for reduction by glutaredoxin, thioredoxin, protein disulfide isomerase, and glutathione. *Arch Biochem Biophys* **335**: 61-72.

Junquiera, L. C., J. Carneiro, et al. (1986). *Basic Histology*. Appleton-Century-Crofts, East Norwalk,

Kakulas, B. A. and F. L. Mastaglia (1992). Drug-induced, toxic and nutritional myopathies. In: *Skeletal Muscle Pathology*. Landon, D. L. (ed.): pp. 511-540, Churchill Livingstone, Edinburgh.

Kalish, R. S. and J. A. Wood (1995). Sensitization of mice to paraphenylenediamine and structurally-related compounds: adjuvant effects of vitamin A supplementation. *Contact Dermatitis* **33**: 407-13.

Kanbara, K., A. Sakai, et al. (1997). Distribution of fiber types determined by in situ hybridization of myosin heavy chain mRNA and enzyme histochemistry in rat skeletal muscles. *Cell Mol Biol (Noisy-le-grand)* **43**: 319-327.

Kato, I., A. Harihara, et al. (1992). An in vitro model for assessing muscle irritation of antibiotics using rat primary cultured skeletal muscle fibers. *Toxicol Appl Pharmacol* **117**: 194-199.

Kehrer, J. P. and L. G. Lund (1994). Cellular reducing equivalents and oxidative stress. *Free Radic Biol Med* **17**: 65-75.

Keilin, D. and E. F. Hartree (1938). Cytochrome oxidase. *Proc Roy Soc. London, Ser. B* **125**: 171-186.

Kerr, J. F. (1971). Shrinkage necrosis: a distinct mode of cellular death. *J Pathol* **105**: 13-20.

Kerr, J. F. (1972). Shrinkage necrosis of adrenal cortical cells. *J Pathol* **107**: 217-219.

King, T. S. (1967). Preparation of succinate cytochrome c reductase, and the cytochrome b-c₁ particle, and reconstitution of succinate cytochrome c reductase. *Methods Enzymol* **10**: 217-235.

Klatt, P. and S. Lamas (2000). Regulation of protein function by S-glutathiolation in response to oxidative and nitrosative stress. *Eur J Biochem* **267**: 4928-4944.

Kosower, N. S. and E. M. Kosower (1978). The glutathione status of cells. *Int Rev Cytol* **54**: 109-160.

Kretzschmar, M. and W. Klinger (1990). The hepatic glutathione system--influences of xenobiotics. *Exp Pathol* **38**: 145-164.

Kuhne, W. (1865). Farbstoff der Muskeln. *Archiv fur Pathol Anat Physiol* **33**: 79.

Landon, D. N. (1992). *Skeletal Muscle Pathology*. Churchill Livingstone, Edinburgh.

Laughlin, M. H., T. Simpson, et al. (1990). Skeletal muscle oxidative capacity, antioxidant enzymes, and exercise training. *J Appl Physiol* **68**: 2337-2343.

- Lawrie, R. A. (1952). The activity of the cytochrome system in muscle and its relation to myoglobin. *Biochem J* **55**: 298.
- Lawrie, R. A. (1953). The relation of energy-rich phosphate in muscle to myoglobin and to cytochrome-oxidase activity. *Biochem J* **55**: 305.
- Layer, R. W. (1978). Amines, aromatic (Phenylenediamines). *Othmer Encyclopaedia of Chemical Technology*.2: pp 348-354, Wiley, New York.
- Layer, R. W. (1966). *Rubber Chem Technol* **39**: 1584.
- Liden, C. and A. Boman (1988). Contact allergy to colour developing agents in the guinea pig. *Contact Dermatitis* **19**: 290-295.
- Lightfoot, R. (1998). The Muskuloskeletal system. In: *Target Organ Pathology. A Basic Text*. Turton, J. and J. Hooson, (eds.). pp. 239-253, Taylor and Francis Ltd, London.
- Long, D. J., and A. K. Jaiswal (2000). Mouse NRH:quinone oxidoreductase (NQO2): cloning of cDNA and gene- and tissue-specific expression. *Gene* **252**: 107-117.
- Lowry, O.H., Roseborough, N.J. et al. (1951). Protein measurement with the Folin reagent. *J Biol Chem* **193**: 265-275.
- LuValle, J.E., D.B. Glass, et al. (1948). Oxidation processes. XXI. The autoxidation of the p-phenylenediamines. *J Am Chem Soc* **70**: 2223.
- Malaisse, W. J., F. Malaisse-Lagae, et al. (1982). Determinants of the selective toxicity of alloxan to the pancreatic B cell. *Proc Natl Acad Sci U S A* **79**: 927-930.
- Malorni, W., R. Rivabene, et al. (1995). The antioxidant N-acetyl-cysteine protects cultured epithelial cells from menadione-induced cytopathology. *Chem Biol Interact* **96**: 113-123.
- Martensson, J. and A. Meister (1989). Mitochondrial damage in muscle occurs after marked depletion of glutathione and is prevented by giving glutathione monoester. *Proc Natl Acad Sci U S A* **86**: 471-475.
- Mastaglia, F. L. (1982). Adverse effects of drugs on muscle. *Drugs* **24**:304-321.
- Mastaglia, F. L., J. M. Papadimitriou, et al. (1977). Vacuolar myopathy associated with chloroquine, lupus erythematosus and thymoma. Report of a case with unusual mitochondrial changes and lipid accumulation in muscle. *J Neurol Sci* **34**: 315-28.
- Mayer, R. L. (1954). Group sensitization to compounds of quinone and its biochemical basis; role of these substances in cancer. *Progr Allergy* **4**: 79.

McCord, J. M. and I. Fridovich (1969). The utility of superoxide dismutase in studying free radical reactions. I. Radicals generated by the interaction of sulfite, dimethyl sulfoxide, and oxygen. *J Biol Chem* **244**: 6056-6063.

Meister, A. (1995). Mitochondrial changes associated with glutathione deficiency. *Biochim Biophys Acta* **1271**: 35-42.

Meister, A. and M. E. Anderson (1983). Glutathione. *Annu Rev Biochem* **52**: 711-60.

Meister, R., J. Comte, et al. (1988). Cyclic GMP, cyclic AMP, glucose at birth, and maturation of rat liver mitochondria. *Biochim Biophys Acta* **936**: 67-73.

Meredith, M. J. and D. J. Reed (1982). Status of the mitochondrial pool of glutathione in the isolated hepatocyte. *J Biol Chem* **257**: 3747-53.

Michaelis, L., Schubert, M.P. et al. (1939). *J Chem Soc* **61**: 1981-1992

Mitchell, P. (1979). Keilin's respiratory chain concept and its chemiosmotic consequences. *Science* **206**(4423): 1148-1159.

Mitchell, J. R., D. J. Jollow, et al. (1973). Acetaminophen-induced hepatic necrosis. IV. Protective role of glutathione. *J Pharmacol Exp Ther* **187**: 211-217.

Miners, J. O., R. Drew, et al. (1984). Mechanism of action of paracetamol protective agents in mice in vivo. *Biochem Pharmacol* **33**: 2995-3000.

Moldeus, P., J. Hogberg and S. Orrenius (1978). *Methods in Enzymology*. Fleisher, S. and L. Packer (eds.), Vol. 52, pp. 60-71, Academic Press, New York.

Munday, R. (1986). Generation of superoxide radical and hydrogen peroxide by 1,2,4-triaminobenzene, a mutagenic and myotoxic aromatic amine. *Chem Biol Interact* **60**: 171-181.

Munday, R. (1987). Oxidation of glutathione and reduced pyridine nucleotides by the myotoxic and mutagenic aromatic amine, 1,2,4-triaminobenzene. *Chem Biol Interact* **62**: 131-41.

Munday, R. (1988). Generation of superoxide radical, hydrogen peroxide and hydroxyl radical during the autoxidation of N,N,N',N'-tetramethyl-p-phenylenediamine. *Chem Biol Interact* **65**: 133-43.

Munday, R. (1992). Mitochondrial oxidation of p-phenylenediamine derivatives in vitro: structure-activity relationships and correlation with myotoxic activity in vivo. *Chem Biol Interact* **82**: 165-179.

- Munday, R., E. Manns, et al. (1989). Muscle necrosis by N-methylated p-phenylenediamines in rats: structure- activity relationships and correlation with free-radical production in vitro. *Toxicology* **57**(3): 303-14.
- Munday, R., E. Manns, et al. (1990). Structure-activity relationships in the myotoxicity of ring-methylated p-phenylenediamines in rats and correlation with autoxidation rates in vitro. *Chem Biol Interact* **76**: 31-45.
- Nachmias, V. T. and H. A. Padykula (1958). A histological study of normal and denervated red and white muscles of the rat. *J Biophys Biochem Cytol* **4**: 47.
- Ngaha, E. O., M. A. Akanji, et al. (1989). Studies on correlations between chloroquine-induced tissue damage and serum enzyme changes in the rat. *Experientia* **45**: 143-146.
- Nohl, H. and D. Hegner (1978). Evidence for the existence of catalase in the matrix space of rat-heart mitochondria. *FEBS Lett* **89**: 126-130.
- Nohl, H. and W. Jordan (1980). The metabolic fate of mitochondrial hydrogen peroxide. *Eur J Biochem* **111**: 203-210.
- O'Brien, J. and R. Walker (1988). Toxicological effects of dietary Maillard reaction products in the rat. *Food Chem Toxicol* **26**: 775-783.
- Ostdal, H., L. H. Skibsted, et al. (1997). Formation of long-lived protein radicals in the reaction between H₂O₂-activated metmyoglobin and other proteins. *Free Radic Biol Med* **23**: 754-761.
- Packer, L. and M. G. Mustafa (1966). Pathways of electron flow established by tetramethylphenylenediamine in mitochondria and ascites tumor cells. *Biochim Biophys Acta* **113**: 1-12.
- Panegyres, P. K., J. M. Papadimitriou, et al. (1990). Vesicular changes in the myopathies of AIDS: ultrastructural observations and their relationship to zidovudine treatment. *J Neurol, Neurosurg and Psychi* **53**: 649.
- Paul, H. S. and S. A. Abidi (1979). Paradoxical effects of clofibrate on liver and muscle metabolism in rats. *J Clin Inv* **64**: 405.
- Pember, S. O., R. Shapira, et al. (1983). Multiple forms of myeloperoxidase from human neutrophilic granulocytes: evidence for differences in compartmentalization, enzymatic activity, and subunit structure. *Arch Biochem Biophys* **221**: 391-403.
- Pette, D. and R. S. Staron (1988). Molecular basis of the phenotypic characteristics of mammalian muscle fibres. *Plasticity of the neuromuscular system*. pp. 22, Wiley, Chichester.

- Polinger, I. S. (1970). Separation of cell types in embryonic heart cell cultures. *Exp Cell Res* **63**: 78-82.
- Potter, D. W. and T. B. Tran (1993). Apparent rates of glutathione turnover in rat tissues. *Toxicol Appl Pharmacol* **120**: 186-192.
- Powers, S. K., D. Criswell, et al. (1994). Influence of exercise and fiber type on antioxidant enzyme activity in rat skeletal muscle. *Am J Physiol* **266**: R375-380.
- Preece, N. E., S. Ghatineh, et al. (1990). Course of ATP depletion in hydrazine hepatotoxicity. *Arch Toxicol* **64**: 49-53.
- Preedy, V. R. and T. J. Peters (1990). Changes in protein, RNA and DNA and rates of protein synthesis in muscle-containing tissues of the mature rat in response to ethanol feeding: a comparative study of heart, small intestine and gastrocnemius muscle. *Alcohol* **25**: 489-498.
- Radi, R., J. F. Turrens, et al. (1991). Detection of catalase in rat heart mitochondria. *J Biol Chem* **266**: 22028-22034.
- Ragan, C. I., M. T. Wilson, et al. (1987). Subfractionation of mitochondria, and isolation of the proteins of oxidative phosphorylation. In: *Mitochondria – a practical approach*. Darley-Usmar, V. M. and D. Rickwood et al. (eds.) pp. 1-33, IRL press, Oxford.
- Radjendirane, V., P. Joseph and A. K. Jaiswal (1997). In: Cadenas, E., Forman, H. J. (Eds.), *Oxidative stress and signal transduction*. Chapman and Hall, New York, pp. 441-469.
- Rajka, G. (1952) On hypersensitive to 'para group'. *Acta allergol* **5**: 11.
- Ravindranath, V. and D. J. Reed (1990). Glutathione depletion and formation of glutathione-protein mixed disulfide following exposure of brain mitochondria to oxidative stress. *Biochem Biophys Res Commun* **169**: 1075-1079.
- Reed, D. J. (1986). Regulation of reductive processes by glutathione. *Biochem Pharmacol* **35**: 7-13.
- Reichel, K., C. Rehfeldt, et al. (1993). [Effect of a beta-agonist and a beta-agonist/beta-antagonist combination on muscle growth, body composition and protein metabolism in rats]. *Arch Tierernahr* **45**: 211-225.
- Rickwood, D. and M. T. Wilson et al. (1987). Isolation characteristics of intact mitochondria. In: *Mitochondria – a practical approach*. Darley-Usmar, V. M. and D. Rickwood et al. (eds.) pp. 1-33, IRL press, Oxford.

Rojanapo, W., P. Kupradinun, et al. (1986). Carcinogenicity of an oxidation product of p-phenylenediamine. *Carcinogenesis* **7**: 1997-2002.

Ross, M. H., L. J. Romrell, et al. (1995). *Histology - A Text and Atlas*. Williams and Wilkins, Baltimore.

Sarti, P., G. Antonini, et al. (1994). Lonidamine-mediated respiratory changes in rat heart myocytes: a re-examination of the functional response of mitochondrial cytochrome c oxidase. *Biochem Pharmacol* **47**: 2221-2225.

Schmalbruch, H. (1980). The early changes in experimental myopathy induced by chloroquine and chlorphentermine. *J Neuropathol Exp Neurol* **39**: 65.

Schreck, R. and P. A. Baeuerle (1994). Assessing oxygen radicals as mediators in activation of inducible eukaryotic transcription factor NF-kappa B. *Methods Enzymol* **234**: 151-163.

Smilkstein, M. J., G. L. Knapp, et al. (1988). Efficacy of oral N-acetylcysteine in the treatment of acetaminophen overdose. Analysis of the national multicenter study (1976 to 1985). *N Engl J Med* **319**: 1557-1562.

Smith, C. V., D. P. Jones, et al. (1996). Compartmentation of glutathione: implications for the study of toxicity and disease. *Toxicol Appl Pharmacol* **140**: 1-12.

Smith, H. K., M. J. Plyley, et al. (1999). Expression of developmental myosin and morphological characteristics in adult rat skeletal muscle following exercise-induced injury. *Eur J Appl Physiol Occup Physiol* **80**: 84-91.

Sontag, J. M. (1981). Carcinogenicity of substituted-benzenediamines (phenylenediamines) in rats and mice. *J Natl Cancer Inst* **66**: 591-602.

Sood, C., S. Khan, et al. (1997). Phenylenediamine induced hepatocyte cytotoxicity redox. Cycling mediated oxidative stress without oxygen activation. *Biochim Biophys Acta* **1335**: 343-352.

Szasz, G., W. Gruber, et al. (1976). Creatine kinase in serum: 1. Determination of optimum reaction conditions. *Clin Chem* **22**: 650-656.

Stanley, P. E. and S. G. Williams (1969). Use of the liquid scintillation spectrometer for determining adenosine triphosphate by the luciferase enzyme. *Anal Biochem* **29**: 381-92.

Steiness, E., F. Rasmussen, et al. (1977). A comparative study of serum creatine phosphokinase (CPK) activity in rabbits, pigs and humans after intramuscular injection of local damaging drugs. *Acta Pharmacol et Toxicol* **42**: 357.

Stryer, L. (1988) *Biochemistry*. 3rd edition. W.H. Freeman, New York.

Subrahmanyam, V. V. and P. J. O'Brien (1985). Peroxidase catalysed oxygen activation by arylamine carcinogens and phenol. *Chem Biol Interact* **56**: 185-199.

Tainter, M. L. and P. J. Hanzlik (1924). The mechanism of oedema production by paraphenylenediamine. *J Pharmacol Exp Therap* **24**: 179.

Thor, H., M. T. Smith, et al. (1982). The metabolism of menadione (2-methyl-1,4-naphthoquinone) by isolated hepatocytes. A study of the implications of oxidative stress in intact cells. *J Biol Chem* **257**: 12419-12425.

Tietz, N. W. (1995). *Clinical Guide to Laboratory Tests*. W. B. Saunders, New York.

Timbrell, J.A. (1992) *Principles of Biochemical Toxicology*. 2nd edition. Taylor and Francis, London.

Van der Ouderaa, F. J., M. Buytenhek, et al. (1977). Purification and characterisation of prostaglandin endoperoxide synthetase from sheep vesicular glands. *Biochim Biophys Acta* **487**: 315-331.

Van Vleet, J. F., V. J. Ferrans, et al. (1991). Cardiovascular and Skeletal Muscle Systems. In: *Handbook of Toxicologic Pathology*. W. M. Haschek and C. G. Rousseaux (eds.):pp. 539-624, Academic Press, Inc, New York.

Vater, R., M. J. Cullen, et al. (1992). The fate of desmin and titin during the degeneration and regeneration of the soleus muscle of the rat. *Acta Neuropathol (Berlin)* **84**: 278-88.

Venitt, S. and C. E. Searle (1976). Mutagenicity and possible carcinogenicity of hair colourants and constituents. *IARC Sci Publ* **13**: 263-271.

Viner, R. I., T. D. Williams, et al. (1999). Peroxynitrite modification of protein thiols: oxidation, nitrosylation, and S-glutathiolation of functionally important cysteine residue(s) in the sarcoplasmic reticulum Ca-ATPase. *Biochemistry* **38**: 12408-12415.

Walker, R. (1970). Myotoxicity of amine metabolites from brown FK. *Food Chem Toxicol* **8**: 539-542.

Wallimann, T., M. Wyss, et al. (1992). Intracellular compartmentation, structure and function of creatine kinase isoenzymes in tissues with high and fluctuating energy demands: the 'phosphocreatine circuit' for cellular energy homeostasis. *Biochem J* **281**: 21-40.

Warholm, M., C. Guthenberg, et al. (1985). Glutathione transferases from human liver. *Methods Enzymol* **113**: 499-504.

Watanabe, T., T. Hirayama, et al. (1990). The mutagenic modulating effect of p-phenylenediamine on the oxidation of o- or m-phenylenediamine with hydrogen peroxide in the Salmonella test. *Mutat Res* **245**: 15-22.

Williams, G. R., R. Lemberg, et al. (1968). The oxidized forms of cytochrome oxidase. *Can J Biochem* **46**: 1371-1379.

Williams, J. N. and S. L. Thorp (1969). Re-evaluation of cytochrome c concentrations in rat organs using a new method for cytochrome c. *Biochim Biophys Acta* **189**: 25-28.

Wolfe, S. I. (1972). *Biology of the Cell*. Wadsworth Publishing Company, Inc., Belmont, USA.

Wu, C. M., T. Matsuoka, et al. (1992). An experimental model of mitochondrial myopathy: germanium-induced myopathy and coenzyme Q10 administration. *Muscle Nerve* **15**: 1258-1264.

Wynder, E.L., Onderdonk, J. et al. (1963). An epidemiological investigation of cancer of the bladder. *Cancer* **16**: 1388-1407.

APPENDICES

APPENDIX I **Determination of reduced glutathione (Spectrophotometric method)**

Sample preparation:

At autopsy, approximately 0.5 g of liver was homogenised in a preweighed tube containing sulphosalicylic acid (2 mL, 4% w/v). The tube was re-weighed and immediately frozen at -80°C. On the day of analysis the samples were thawed and centrifuged (2000rpm, 5 minutes) to pellet the precipitated protein. Supernatant (0.5 mL) was then removed for assay of reduced glutathione (total non-protein sulphhydryls).

APPENDIX II **Determination of reduced glutathione (Fluorometric method)**

Sample preparation:

Diaphragm, heart and quadriceps muscle: a sample of each tissue (< 0.5 g) was homogenised as quickly as possible into pre-weighed tubes containing 2 mL of ice-cold TCA (10% w/v). The tubes were re-weighed and immediately frozen at -80°C. On the day of assay the samples were thawed and centrifuged (2000 rpm, 5minutes) and the supernatants diluted (5x, 5x, and 10x, respectively) with 10% TCA.

Hepatocytes and myocytes: the cultured cells were washed 2x with ice-cold PBS. TCA (0.5 mL, 6.5%) was added to each culture well, and the plate allowed to sit on ice for 10 minutes, to stabilise released GSH and to precipitate the cellular protein. The TCA extract was removed and stored at -80°C until the day of analysis (within 2 weeks).

APPENDIX III Determination of ATP (Luciferase method)

Reagents:

ATP Buffer:

80 mM MgSO₄.7H₂O 9.86 g/500 mL

10 mM KH₂PO₄ 0.68 g/500 mL

100 mM Na₂AsO₄.7H₂O 15.6 g/500 mL

On the day of the assay, these solutions were mixed 1:1:1 and the pH adjusted to 7.4.

Luciferase-Firefly lantern extract was resuspended in deionised water (5 mL) and centrifuged (5 minutes, 1000rpm). The resultant supernatant (light and heat labile) was stored in a dark container on ice throughout the assay.

Sample Preparation:

Liver, diaphragm, and quadriceps muscle: at autopsy, 0.2-0.5 g of tissue was homogenised into pre-weighed tubes containing 2 mL of ice-cold TCA (10% w/v). The tubes were re-weighed and immediately frozen at -80°C. On the day of analysis, the samples were thawed, centrifuged and the supernatant diluted (5x, 10x and 10x, respectively) with 10% TCA to ensure that the counts did not exceed that of the top standard.

Hepatocytes and myocytes: the cultured cells were washed 2x with ice-cold PBS. TCA (0.5 mL, 10%) was added to each culture well, and the plate allowed to sit on ice for 10 minutes, to stabilise released ATP and to precipitate the cellular protein. The TCA extract was removed and stored at -80°C until the day of analysis (within 5 days).

APPENDIX IV Preparation of formaldehyde/glutaraldehyde fixative

Reagents:

For 100 mL:

NaH₂PO₄·2H₂O 1.16 g

NaOH 0.27 g

40% formaldehyde 10 mL

25% glutaraldehyde 4 mL

Make up with 100 mL distilled water so that the final concentration is 4% formaldehyde/1% glutaraldehyde.

The fixative may be stored at 4°C for up to 3 months.

APPENDIX V Isolation of rat hepatocytes

Reagents:

A. Krebs-Henseleit (K+H) buffer (x2 stock):

100 mL 16.09% NaCl	80.45 g /500 mL
75 mL 1.1% KCl	5.50 g/500 mL
12.5 mL 0.22M KH ₂ PO ₄	7.49 g/500 mL
25 mL 2.74% MgSO ₄ ·7H ₂ O	6.85 g/250 mL
50 mL 0.12M CaCl ₂ ·2H ₂ O	8.82 g/500 mL
392.5 mL UHQ water	
500 mL 0.97% NaHCO ₃	4.85 g/500 mL

These solutions were mixed and gassed with carbogen (95% O₂/5% CO₂) for 10 minutes, with the exception of NaHCO₃ which was added at the end to prevent precipitation of CaCO₃.

Working K+ H buffer (solutions made fresh on day of use):

150 mL K+H x2 stock
150 mL UHQ water
0.9 g HEPES (final concentration 12.6 mM)

The HEPES was dissolved and the solution gassed with carbogen for 2-3 minutes.

K+H Alb buffer:

1 g albumin was dissolved in 100 mL of working K+H

Hanks balanced salt solution (x10 stock):

80 g NaCl

3 g KCl

2 g MgSO₄·7H₂O

0.6 g Na₂HPO₄·2H₂O

0.6 g KH₂PO₄

Made up to 1 L with UHQ water.

Working Hanks (solution was prepared on the day of use):

50 mL Hanks x10 stock

450 mL UHQ water

1.5 g HEPES (final concentration 12.6 mM)

1.05 g NaHCO₃ (final concentration 25 mM)

Mixed together and gassed with carbogen for 2-3 minutes.

This solution was then divided as follows:

Hanks I: 300 mL working Hanks; 68.4 mg EGTA; 2 g albumin.

Hanks II: 200 mL working Hanks; 2 mL 5.88% CaCl₂. Collagenase (50 mg) was weighed and kept at -20°C until added to 100 mL Hanks II immediately prior to use.

The above solutions were adjusted to pH 7.4 with 1 M NaOH.

APPENDIX VI Tissue culture media

Growth medium

DMEM 500mL
10% Foetal Calf Serum
2% Chick Embryo Extract
1% Gentamycin (10mg/mL)

Differentiation medium

DMEM 500 mL
5% Foetal calf serum
1% Chick embryo extract
1% Gentamycin (10 mg/mL)

Hepatocyte culture medium

Williams' medium E
5% Foetal calf serum
5 mL Hydrocortisone (4.8 mg/mL in sterile water)
5 mL Insulin (0.574 mg/mL in sterile water)
5 mL Glutamine (200 mM stock)
3 mL Gentamycin (10 mg/mL stock)

APPENDIX VII Determination of glutathione reductase

Reagents:

0.2 mM KH ₂ PO ₄	13.7 g/500 mL
2 mM EDTA.2H ₂ O	0.41 g/500 mL
2 mM NADPH in	42 mg/25 mL
10 mM TRIS-HCl	0.61 mg/500 mL (pH 7.0)
20 mM GSSG	6.12 g/500 mL

APPENDIX VIII Determination of glutathione peroxidase

Reagents:

0.1 M KH_2PO_4 6.85 g/500 mL (pH 7.0)

1 mM $\text{EDTA}\cdot 2\text{H}_2\text{O}$ 0.21 g/500mL

2.4 u/mL GRed

10 mM GSH 1.53 g/500 mL

1.5 mM NADPH in 31.5 mg/25mL

0.1% NaHCO_3 0.84 g/100 mL

1.5 mM H_2O_2 (from 30% stock)

APPENDIX IX Determination of glutathione-S-transferase

Reagents:

0.1 M KH_2PO_4 6.85 g/500 mL (pH 6.5)

1 mM $\text{EDTA}\cdot 2\text{H}_2\text{O}$ 0.21 g/500mL

20 mM GSH in 61 mg/10 mL

de-ionised H_2O

20 mM CDNB in 41 mg/10 mL

95% ethanol

APPENDIX X Determination of superoxide dismutase

Reagents:

Solution A:

5 μ mol xanthine	0.76 mg
in 1 mM NaOH	
2 μ mol cytochrome <i>c</i>	24.8 mg
both added to 100 mL	
50 mM KH ₂ PO ₄	3.4 g/500 mL
0.1 mM EDTA	0.185 g/500 mL

The solution is stable for 3 days at 4°C.

Solution B

Freshly prepared solution of:

Xanthine oxidase	~ 0.2 u/mL
In 0.1 mM EDTA	0.021 g/500 mL

The activity of xanthine oxidase may vary, therefore one must use sufficient enzyme to produce a rate of cytochrome *c* reduction of 0.025 absorbance units/minute in the absence of SOD.

APPENDIX XI Determination of lactate dehydrogenase activity

Reagents:

Pyruvate/phosphate buffer – 3.75 mg pyruvate was dissolved in 100 mL of 0.05 M phosphate buffer (6.8 g $\text{KH}_2\text{PO}_4/\text{L}$, pH 7.5)

Sample Preparation:

For extracellular LDH activity, the cell culture medium (0.5 mL) was removed 24 hours post treatment with TMPD and stored on ice. The samples were spun (14 000 rpm, 4°C) to remove any cell debris. The supernatant was retained for LDH estimation.

APPENDIX XII Isolation of mitochondria

Reagents:

High EDTA buffer

210 mM mannitol 38.26 g/L

70 mM sucrose 23.96 g/L

50 mM TRIS 6.06 g/L

10 mM K⁺EDTA 4.04 g/L

pH 7.4 at 4°C

Low EDTA buffer

225 mM mannitol 41.0 g/L

75 mM sucrose 25.7 g/L

100 μM K⁺EDTA 41 mg/L

10 mM TRIS 1.2 g/L

pH 7.2 at 4°C

APPENDIX XIII Respiration buffer for O₂ electrode

Reagents:

100 mM KCl	7.455 g/L
75 mM mannitol	13.66 g/L
25 mM sucrose	8.557 g/L
10 mM TRIS	1.211 g/L
50 μM EDTA	500μL/L (from stock solution of 0.1M EDTA, 4.0447 g/100 mL).

pH 7.4 (using TRIS crystals) at 30°C.

THE SKELETAL MUSCLE-SPECIFIC TOXICITY OF 2,3,5,6-TETRAMETHYL-P-PHENYLENEDIAMINE (TMPD): SOME PRELIMINARY STUDIES

J.A.Blair¹, C.J.Waterfield¹, R.M.Lightfoot², A.Rowlands², M.J.York² & J.A.Turton¹, ¹School of Pharmacy, University of London, Department of Toxicology, 29/39, Brunswick Square, London WC1N 1AX and ²GlaxoWellcome Research and Development, Park Road, Ware, Hertfordshire SG12 0DP.

The aromatic amine 2,3,5,6-tetramethyl-*p*-phenylenediamine (TMPD) evokes a specific toxic response in skeletal muscle *in vivo*¹. In addition we have reported histopathological changes in stage 14 tubules of the testis². Rapid autoxidation of TMPD *in vitro* suggests that free-radical species generated through intracellular oxidation could be involved in the toxic effects of this compound¹. Inadequacies in the antioxidant capacity of muscle may result in the selective toxicity. The purpose of these studies were to investigate this.

Rats (male, Han Wistar, 250-300g, 4 group⁻¹), were given TMPD (20- 60µmol kg⁻¹day⁻¹HCl, s.c.) or saline (controls). Post-dose (24 h), animals were sacrificed, blood taken for serum preparation, and tissues removed for histological examination and lesion scoring. In a second study animals were given TMPD (60µmol kg⁻¹day⁻¹HCl, s.c.), sacrificed 8h post-dose and tissues removed for biochemical analysis.

Table. Serum enzymes, histological assessment and glutathione measurement in tissues from animals treated with TMPD.

Dose TMPD (µmol kg ⁻¹ day ⁻¹)	AST(i.u.)	ALT(i.u.)	CK-MM(i.u.)	Lesion scoring (0-5)			GSH (µmol/g)	
				Diaphragm	Quadriceps	Liver	Diaphragm	Quadriceps
0	65.4 (1.3)	26.2 (0.8)	35.2 (1.5)	0.00	0.00	9.8 (0.9)	1.8 (1.3)	1.5(0.6)
20	109.5 (54.1)	32.3 (3.9)	34.7 (5.8)	0.65	1.00	-	-	-
30	209.4 (87.1)	43.4 (12.5)	52.8 (21.8)	2.25	1.30	-	-	-
40	1212.0 (557.8)	106.2 (33.6)	538.8 (188.2)	4.00	2.00	-	-	-
50	1661.7 (420.5)	157.7 (343.2)	510.7 (343.2)	4.75	4.00	-	-	-
60	4601.0 (626.6)*	579.5 (144.5)*	1364.3 (682.3)*	4.50	3.95	7.0 (1.8)	0.0	0.0

Values are means ± s.e.m. * p<0.05, Dunnett's test for multiple comparisons with a single control.

TMPD caused a dose-dependent increase in serum AST, ALT and CK-MM, (the creatine kinase muscle-specific isoenzyme), all of which were significantly higher at the top dose level (Table). These parameters correlated well with histopathological findings whereby lesion severity and frequency in both diaphragm and quadriceps muscle were also increased in a dose dependant manner.

Skeletal muscle has low levels of reduced glutathione and antioxidant enzymes e.g. superoxide dimutase, catalase, and glutathione peroxidase, in comparison with other organs³. Thus oxidation of TMPD would generate reactive oxygen species, and an organ such as the liver which has higher levels of reduced glutathione in comparison with skeletal muscle (Table), would be better protected. The highest dose of TMPD was observed to greatly reduce GSH in both quadriceps and diaphragm muscle, both of which had very low initial GSH levels. This TMPD-induced reduction may be indicative of oxidative stress, which is consistent with the earlier-stated hypothesis for the possible mechanism of TMPD toxicity.

1. Munday, R. (1992) Chem. Biol. Inter. 82: 165-179.
2. Draper R.P., Waterfield C.J., York, M.J. & Timbrell, J.A. (1994) Arch. Toxicol. 69: 111-117.
3. Grankvist, K., Marklund, S.L. & Taljedal, I. (1981) Biochem. J. 199: 393-398.

COMPARATIVE STUDIES ON THE SKELETAL MUSCLE TOXICITY OF 2,3,5,6-TETRAMETHYLPHENYLENEDIAMINE *IN VITRO* USING CULTURED MYOCYTES, HEPATOCYTES AND ISOLATED MITOCHONDRIA.

J.A. Blair¹, C.J. Waterfield¹, T.E. Bates², R.M. Lightfoot³, A. Rowlands³ & J.A. Turton¹, ¹Centre of Toxicology, School of Pharmacy, University of London, 29/39, Brunswick Square, London WC1N 1AX, ²Department of Neurochemistry, Institute of Neurology, Queen's Square, WC1N 3BG and ³Glaxo-Wellcome Research and Development, Park Road, Ware, Hertfordshire SG12 0DP.

The aromatic amine 2,3,5,6-tetramethyl-*p*-phenylenediamine (TMPD) evokes a specific toxic response in skeletal muscle *in vivo*^{1,2}. The mitochondrion is believed to be the locus of TMPD's rapid oxidation, and *in vitro* studies suggest that free-radical species generated through intracellular oxidation could play a role in the toxic mechanism of this compound *in vivo*¹. Detoxification of reactive oxygen species requires adequate tissue levels of superoxide dismutase (SOD), glutathione peroxidase (GPx), glutathione-*s*-transferase (GST) and glutathione reductase (GR). To gain more information about the mitochondrion's role in the toxicity of TMPD, and of the defense capacity of skeletal muscle versus liver, respiratory control ratios (RCR), using isolated mitochondria, glutathione (GSH) content, and SOD and GSH-dependent enzyme activities using 2 primary culture systems: hepatocyte monolayers, isolated from adult rats, and cultured myocytes, isolated from the hindlimbs of neonatal rats, were measured in the present study.

The RCR of isolated skeletal muscle and liver mitochondria were measured following incubation with increasing dose levels of TMPD. Only results taken from incubations in 0.0 and 0.1mM TMPD are reported here. Antioxidant enzyme activity, as well as GSH levels were measured in hepatocytes and myocytes in both control (culture medium only) and treated (24 hour incubation with TMPD, over a dose range, 37°C, 5% CO₂) cells. Only results taken from incubations in 0.0 and 0.2mM TMPD are reported here.

Table 1. SOD, GSH, GSH-related enzymes and RCR measured in cultured rat hepatocytes, myocytes and mitochondria respectively, treated with TMPD.

Myos	GR ^a	GPx ^b	GST ^c	SOD	RCR muscle ^f	Heps	GR ^a	GPx ^b	GST ^c	SOD	RCR liver ^f		
Control (0.0mM)	0.33 (0.04)	81.43 (17.73)	13.60 (0.00)	13.30 ^{d1} (6.44)	3.15 ^{d2} (0.44)	4.75 (0.25)	Control (0.0mM)	1.26 (0.29)	31.57 (2.57)	291.4 (0.02)	32.09 ^{d1} (6.96)	7.95 ^{d2} (5.23)	4.67 (0.48)
Treated (0.2mM)	0.12* (0.04)	71.00 (34.13)	24.10* (0.00)	14.90 ^{d1} (4.07)	4.42 ^{d2} (1.19)	2.05 (0.33)	Treated (0.2mM)	1.54 (0.45)	33.68 (4.85)	319.4* (0.05)	37.72 ^{d1} (4.78)	17.68 ^{d2*} (3.76)	2.24 (0.68)
GSH ^e (control)	6.18 (1.68)	-	-	-	-	-	GSH ^e (control)	9.53 (1.75)	-	-	-	-	-

Values are means (s.d.) *p<0.05, Dunnett's test for multiple comparisons with a single control. ^anmol of NADPH/min/mg protein, ^bNADPH/min/mg protein, ^cnmol of conjugate/min/mg protein, ^{d1}MnSOD: u/min/mg protein, ^{d2}Cu/ZnSOD: u/min/mg protein, ^enmol/mg protein, ^fwhen incubated with 0.1mM TMPD.

Mitochondrial RCR were similar in the 2 tissues. Increasing levels of TMPD caused a dose dependant reduction in RCR. The uncoupling effect of TMPD is probably due to its ability to induce a permeability transition of the inner mitochondrial membrane. Hepatocytes had higher SOD and GSH-dependant enzyme levels than did myocytes (except for GPx) which are associated with a higher GSH content in hepatocytes. In response to TMPD treatment, both cell types showed significantly elevated GST levels. Hepatocyte CuZnSOD was also significantly elevated. In contrast GR levels of myocytes were significantly decreased following incubation with TMPD, a response not observed in hepatocytes.

It is concluded that myocytes are less well adapted in comparison with hepatocytes to deal with the events of oxidative stress, as reflected by their poor antioxidant status. In addition, the inability to react to such conditions e.g. by increased enzyme activity or indeed, glutathione synthesis itself, would render skeletal muscle more susceptible to the effects of redox cycling agents than the liver.

J.A.B is grateful to Glaxo-Wellcome for financial support.

¹ Munday, R. (1992) Chem. Biol. Inter. 82: 165-179.

² Blair, J.A., Waterfield, C.W., Lightfoot, R.M., York, M. and Turton, J.A. (1997) Hum. Exp. Tox. 16: 403.

Elucidating the Mechanism of the Skeletal Muscle Toxicant 2,3,5,6-tetramethylphenylenediamine: Studies Using Isolated Mitochondria

J.A.Blair¹, T.E.Bates², C.J.Waterfield³, R.M.Lightfoot³, A.Rowlands³ and J.A.Turton¹.

¹Centre for Toxicology, School of Pharmacy, University of London, 29/39, Brunswick Square, London WC1N 1AX, ²Department of Neurochemistry, Institute of Neurology, Queen's Square, WC1N 3BG and ³GlaxoSmithKline Research and Development, Park Road, Ware, Hertfordshire SG12 0DP.

The aromatic amine, 2,3,5,6-tetramethyl-*p*-phenylenediamine (TMPD) causes necrosis of skeletal muscle in a highly specific manner when administered to rats: Blair *et al.* (1997). The mitochondrial respiratory chain protein, cytochrome c-oxidase (complex IV) catalyses the oxidation of the amine: Munday (1992), and is believed to initiate TMPD toxicity *in vivo*. Investigations concerning the toxicity of TMPD *in vitro* have largely focused on the metabolism of the amine and its effects on mitochondrial respiratory control. However, the biochemical mechanism which underlies the deleterious effects of TMPD on mitochondrial function has received little attention. Therefore a number of assays to determine the level of mitochondrial dysfunction and its importance in the overall mechanism of TMPD toxicity were undertaken.

The ADP/O ratio, GSH content and respiratory chain enzyme activities of isolated rat skeletal muscle and liver mitochondria were measured following incubation with increasing concentrations of TMPD (0.1-0.5mM).

Table ADP/O, GSH, and respiratory chain enzyme activities measured in isolated skeletal muscle and liver mitochondria, treated with TMPD

TMPD mM	Skeletal muscle				Liver			
	ADP/O ^a	GSH ^b	Complex I ^c	Complex II-III ^c	ADP/O ^a	GSH ^b	Complex I ^c	Complex II-III ^c
0.00	2.94(0.05)	5.10(0.30)	146.34(11.61)	71.22(12.92)	2.87(0.10)	10.60(0.10)	25.27(4.51)	32.24(4.08)
0.10	1.54(0.02)*	2.40(0.20)*	49.37(13.58)	52.70(6.49)	1.48(0.05)*	3.70(0.20)*	15.09(5.01)	36.02(6.50)
0.25	1.25(0.08)*	1.20(0.10)*	23.04(4.18)	47.23(3.64)	1.31(0.06)*	1.60(0.10)*	15.69(5.42)	29.18(6.01)
0.50	1.13(0.10)*	1.10(0.15)*	24.05(1.85)*	47.72(1.57)*	1.18(0.10)*	1.20(0.15)*	9.41(3.74)	29.06(8.81)

Values are means (sem); * p<0.05, Dunnett's test for multiple comparisons with a single control. ^anmol O/min/0.1mg protein, ^bnmol/mg protein, ^cnmol NADH/min/mg protein.

Mitochondrial ADP/O values were similar in the 2 tissues (Table); increasing concentrations of TMPD caused a dose-dependant reduction in ADP/O. Mitochondrial GSH is markedly decreased upon TMPD treatment in both tissues, at each concentration. The loss of mitochondrial GSH in skeletal muscle was accompanied by a significant reduction in respiratory chain complex I and complex II-III activities. Liver respiratory chain enzyme activities were not significantly affected by TMPD treatment.

The impairment of mitochondrial respiration coincides with a dramatic reduction in both skeletal muscle and liver mitochondrial GSH, and a reduction in skeletal muscle mitochondrial complex I and complex II-III activities. Complex I is an important component of the electron transport chain and contains several critical thiol groups which may be vulnerable to oxidative modification, resulting in loss of activity. Liver is much less susceptible to the toxic effects of TMPD *in vivo*: Blair *et al.* (1997). However, *in vitro*, in the absence of the cytosolic fraction of the cell, not only is *de novo* synthesis of GSH impossible, repletion of mitochondrial GSH from the cytosolic pool is also prevented. This may explain the almost equal susceptibility, *in vitro*, of isolated skeletal muscle and liver mitochondria to the toxic effects of TMPD.

J.A.B is grateful to GlaxoSmithKline for financial support.

Blair, J.A., Waterfield, C.J., Lightfoot, R.M., York, M and Turton, J.A. 1997 Hum. Exp. Tox. 16, 403.
Munday, R. 1992 Chem. Biol. Inter. 82, 165-179.